D2.4 System characterization and operational parameters

Authors: Athanasios Nesiadis (CERTH), Georgios Zisopoulos (CERTH), Konstantinos Atsonios (CERTH), Nikolaos Nikolopoulos (CERTH), Alberto Belda González (CARTIF), Konrad Zdun (Enetech)

This project has received funding from the European Union´s Horizon 2020 research and innovation programme under the grant agreement No 869821

D2.4 – System characterization and operational parameters

Summary

The scope of Deliverable D2.4 is to summarize the findings of Deliverables 2.1, 2.2 and 2.3 and provide a link between them and the system specifications as defined in the framework of technical WPs 2, 3, 4 and 5. First a comprehensive review of available thermal energy storage technologies is presented, followed by a comparison of MiniStor with competing technologies. MiniStor, despite its current low maturity, presents significant advantages such as very high energy storage density, high exergetic efficiency and ability to provide heating and cooling using renewable energy inputs. This analysis is combined with calculations of peak heating and cooling demand of representative dwellings in several European countries. A comparison with MiniStor demo site loads, shows that the latter are well within the load intervals of corresponding dwelling types of relatively new construction.

Furthermore, renewable energy systems (RES systems) suitable for integration with MiniStor are identified. Photovolatic thermal panels (PVTs) in combination with solarthermal collectors and conventional photovoltaic panels (PVs) integrated with Heat Pumps (HPs) are characterized by the significant advantage of presenting zero emissions, while offering the possibility of electricity generation and storage as well. Biomass boilers, although lacking the abilities of the latter, can also be a feasible option as their operation is independent from the intermittent nature of solar irradiance. The choice of the appropriate energy source should also take into consideration the individual RES availability and penetration throughout Europe, supported by a thorough analysis of relevant data as included in this deliverable. In addition, MiniStor operation modes are conceptually defined and the detailed steps involved in each of the four basic modes are described. Data about the system operating conditions in each case are also presented. Finally, the document includes thermal load estimations for Santiago de Compostela demo site, as this information was not possible to be included in D2.2, due to the late admission of University of Santiago de Compostela (USC) into the MiniStor consortium.

Deliverable Number	Work Package
D2.4	WP.2
Lead Beneficiary	**Deliverable Author(s)**
Centre of Research and Technology Hellas (CERTH)	Athanasios Nesiadis (CERTH), Georgios Zisopoulos (CERTH), Konstantinos Atsonios (CERTH), Nikolaos Nikolopoulos (CERTH), Alberto Belda González (CARTIF), Konrad Zdun (Enetech)
Beneficiaries	**Deliverable Co-author (s)**
EndeF University of Santiago de Compostela (USC)	Adriana Coca-Ortegon (EndeF) Juan Enrique Arias Rodríguez (USC)
Beneficiaries	**Deliverable Reviewer (s)**
IERC CARTIF	Carlos Ochoa (IERC), María López (IERC) Manuel Andrés Chicote (CARTIF)
Planned Delivery Date	**Actual Delivery Date**
30/04/2021	27/05/2021

Type of deliverable	R	Report	X
Dissemination Level	CO	Confidential, only for members of the consortium (including the Commission)	
	PU	Public	X

Index

Index 3
List of Tables 5
List of Images 7
List of Abbreviations and Nomenclature 9
1 Introduction 11
1.1 Scope and objective of the deliverable 11
1.2 Deliverable structure and connections 11
2 Context description, Stakeholder and User Characterisation 12
2.1 Review of energy storage technologies 12
2.1.1 Sensible Heat Storage Systems 13
2.1.2 Latent Heat Storage 14
2.1.3 Thermochemical Storage 16
2.1.4 Strengths and Weaknesses for each competing technology 18
2.2 Estimations of peak heating & cooling loads for various residential buildings throughout Europe 19
2.2.1 Methodology for determining the heating and cooling loads 20
2.2.2 Heating and Cooling Demand calculation 22
2.2.3 Methodology for determining the domestic hot water requirements 30
2.2.4 Relevance to the energy needs of MiniStor project demo sites 32
3 Methods to integrate MiniStor with RES systems 34
3.1 Identification of RES suitable for integration with MiniStor system 34
3.1.1 Integration of hybrid photovoltaic thermal panels and solar thermal collectors 34
3.1.2 Integration of photovoltaic panels combined with heat pump 37
3.1.3 Integration of biomass boilers 39
3.1.4 Strengths and weaknesses for each RES technologies 39
3.2 Exploration of compatible with MiniStor RES utilisation throughout Europe 40
3.2.1 Solar Energy 42
3.2.2 Heat Pumps 45
3.2.3 Biomass 46
3.2.4 Geothermal potential 46
4 Assessment of application barriers on MiniStor installation 48
5 MiniStor specifications and operation modes 50
5.1 Definition of the conceptual operation modes of MiniStor system 50
5.1.1 Introduction to operation modes definition 50
5.1.2 Main thermal operation modes 51
5.1.3 Operation mode: TCM charge 53
5.1.4 Operation mode: TCM discharge 55
5.1.5 Operation mode: Direct supply from solar 58
5.1.6 Operation mode: Demand covered by PCM units only 59
5.2 Overview of system operating conditions and system main specifications 60
5.2.1 Factors shaping the system operating conditions 60
5.2.2 Operating conditions in the defined main operating modes 61
5.2.3 System main specifications 65
6 Current and future thermal loads estimations for Santiago de Compostela demo site 66
6.1 Demo site description 66
6.2 The Heating and Cooling Degree Days methodology 67
6.3 Estimations of the demo site current heat load 68

6.3.1 Approximation of annual heating demand based on fuel consumption data 68
6.3.2 Approximation of heat load based on the EN 12831:2017 Standard 69
6.3.3 Estimation of load profiles for thermodynamic simulations 70
6.4 Estimations of the demo site future loads 72
6.4.1 Calculation of future Heating and Cooling Degree Days 72
6.4.2 Estimation of future heating and cooling loads 74
7 Conclusions 77
References 79
Annex 84

List of Tables

Table 1: Classification of thermal Energy Storage Systems (Sarbu & Sebarchievici, 2018) 13

Table 2: Main characteristics of organic and inorganic materials (adapted from (Cabeza et al., 2011)) 15

Table 3: Main advantages and disadvantages of the open and closed reactor TCM systems (Scapino et al., 2017) 16

Table 4: Summary of prototype open and closed TCM systems developed 17

Table 5: Summary of prototype open and closed TCM systems developed 18

Table 6: Base temperature selection for each country 21

Table 7: Analysis index 22

Table 8: Representative cities and corresponding TMY files for each region and country considered 22

Table 9: Area, Heat Loss Coefficient, Peak Heating and Peak Cooling load of the typical detached dwellings in the four climatic zones in Greece 23

Table 10: Area, Heat Loss Coefficient, Peak Heating and Peak Cooling load of the typical flats in the four climatic zones in Greece 23

Table 11: Area, Heat Loss Coefficient, Peak Heating and Peak Cooling load of the typical detached houses and flats in Hungary 24

Table 12: Heat Loss Coefficient for the detached, semi-detached and multifamily dwellings in Germany 25

Table 13: Peak Heating and Peak Cooling Load of the detached dwellings in Germany 25

Table 14: Peak Heating and Peak Cooling Load of the semi-detached dwellings in Germany .. 26

Table 15: Peak Heating and Peak Cooling Load of the typical flats in Germany 26

Table 16: Area and Heat Loss Coefficient of the typical detached dwellings, semi-detached dwellings and flats in France 27

Table 17: Peak Heating and Peak Cooling Load of the typical detached dwellings in France ... 27

Table 18: Peak Heating and Peak Cooling Load of the typical semi-detached dwellings in France 28

Table 19: Peak Heating and Peak Cooling Load of the typical flats in France 28

Table 20: Heat Loss Coefficient, Peak Heating and Peak Cooling load for the typical detached dwellings, semi-detached dwellings and flats in Italy 29

Table 21: Heat Loss Coefficient, Peak Heating and Peak Cooling load for the typical detached dwellings, semi-detached dwellings and flats in Spain 29

Table 22: Monthly Energy Demand for DWH for Greece 30

Table 23: Monthly Energy Demand for DWH for Hungary 31

Table 24: Monthly Energy Demand for DWH for Germany 31

Table 25: Monthly Energy Demand for DWH for France 32

Table 26: Monthly Energy Demand for DWH for Italy 32

Table 27: Monthly Energy Demand for DWH for Spain 32

Table 28: Total area of PVTs and FPCs foreseen to be installed in MiniStor demo sites 37

Table 29: Main technologies of solar PV cells (adapted from (Shubbak, 2019)) 37

Table 30: Main strengths and weaknesses of the RES systems suitable for integration with MiniStor 40

Table 31: Total number of heat pumps in operation in 2019 in European Union (EurObserv'ER, 2020) 45

Table 32: MiniStor subsystems by functional typology 50

Table 33: Characteristic temperatures of the storage subsystems 60

Table 34: Main interactions between MiniStor subsystems and the environment 61

Table 35: Estimations of consumed diesel energy content per month (USC demo site) 68

Table 36: Estimations of annual heat demand (space heating and DHW) of RUBN building 68

Table 37: Average monthly heat demand (space heating and DHW) of RUBN building and apartment B 69

Table 38: Characteristics of the used EURO-CORDEX simulations for future temperature estimations 73

Table 39: Average and maximum daily degree day values for USC location 74

Table 40: Estimated heating and cooling loads in reference year, 2030 and 2050 for USC demo site 74

Table 41: Estimated average and maximum daily heating loads in reference year, 2030 and 2050 for USC demo site 76

Table 42: Estimated average and maximum daily cooling loads in reference year, 2030 and 2050 for USC demo site 76

Table 43: Total annual heating requirements of the most common building types in Greece 84

Table 44: Total annual cooling requirements of the most common building types in Greece 84

Table 45: Average monthly ground temperature at 0.5m in Greece 84

Table 46: Total annual heating and cooling requirements of the most common building types in Hungary 85

Table 47: Average monthly ground temperature at 0.5m in Hungary 85

Table 48: Total annual heating and cooling requirements of the typical detached dwellings in Germany 85

Table 49: Total annual heating and cooling requirements of the typical semi-detached dwellings in Germany 86

Table 50: Total annual heating and cooling requirements of the typical flats in Germany 87

Table 51: Average monthly ground temperature at 0.5m in Germany 87

Table 52: Total annual heating requirements of the most common building types in France 88

Table 53: Total annual cooling requirements of the most common building types in France 89

Table 54: Average monthly ground temperature at 0.5m in France 89

Table 55: Total annual heating and cooling requirements of the most common building types in Italy 90

Table 56: Average monthly ground temperature at 0.5m in Italy 90

Table 57: Total annual heating and cooling requirements of the most common building types in Spain 90

Table 58: Average monthly ground temperature at 0.5m in Spain 90

List of Images

Figure 1: Deliverable structure and connections 12

Figure 2: Maturity level of various thermal and electricity storage technologies (adapted from (IEA, 2014)) 13

Figure 3: Simplified diagram of the estimation procedure. 21

Figure 4: Peak heating loads in all examined building types and countries 33

Figure 5: Peak cooling loads in all examined building types and countries 33

Figure 6: Main types of solar thermal collectors and PVTs (adapted from (Tyagi et al., 2012)) . 36

Figure 7: Share of energy from renewable sources in EU + UK for electricity and heating and cooling purposes (2019). Source: (Eurostat, 2019) 41

Figure 8: Structure of RES used in gross electricity production in EU countries in 2019 (excluding biofuels). Source: (Eurostat, 2019) 42

Figure 9: Structure of RES used in heat and cool production in EU countries in 2019. Source: (Eurostat, 2019) 42

Figure 10: PV capacity installed in European Union (adapted from (IEA, 2020)) 43

Figure 11: Historical and forecasted PV capacity net add-ons in Germany (adapted from (IEA, 2020)) 44

Figure 12: Historical and forecasted PV capacity net add-ons in Italy (adapted from (IEA, 2020)) 44

Figure 13: Historical and forecasted PV capacity net add-ons in France (adapted from (IEA, 2020)) 44

Figure 14: Historical and forecasted PV capacity net add-ons in United Kingdom (adapted from (IEA, 2020)) 45

Figure 15: Share of energy generated in residential biomass installations in total amount of biomass heat generation in each country. Source: (Eurostat, 2019) 46

Figure 16: Geothermal resources in Europe (adapted from (Große et al., 2017)) 47

Figure 17: Energy (electricity and heat) generation from geothermal resources throughout Europe. Source: (Eurostat, 2019) 47

Figure 18: Overall configuration of the MiniStor system components 48

Figure 19: Main subsystems within the MiniStor system 50

Figure 20: Electrical energy flow representation for the Operation mode 2. 51

Figure 21: Basic diagram of the MiniStor thermal system, including main interactions among main sub-systems 52

Figure 22: Detailed layout of the MiniStor thermal system 52

Figure 23: Main operation modes of the MiniStor thermal system 53

Figure 24: Operation mode “TCM charge”. Basic diagram 54

Figure 25: Operation mode “TCM charge”. Detailed diagram 54

Figure 26: Operation mode “TCM discharge”. Basic diagram 55

Figure 27: Operation mode “TCM discharge”. Detailed diagram 56

Figure 28: Operation mode “TCM discharge - Very cold periods”. Basic diagram 57

Figure 29: First phase of the operation mode “TCM discharge - Very cold periods”. Detailed diagram 57

Figure 30: Operation mode “Direct supply from solar”. Basic diagram 58
Figure 31: Operation mode “Direct supply from solar”. Detailed diagram..... 59
Figure 32: Operation mode “Demand covered by PCM units only”. Basic diagram 60
Figure 33: Operation mode “Demand covered by PCM units only”. Detailed diagram 60
Figure 34: Boundaries of operating temperatures in winter TCM charge mode 62
Figure 35: Boundaries of operating temperatures in summer TCM charge mode..... 62
Figure 36: Boundaries of operating temperatures in winter TCM discharge mode 63
Figure 37: Boundaries of operating temperatures in TCM discharge mode during very cold periods 64
Figure 38: Boundaries of operating temperatures in summer TCM discharge mode 64
Figure 39: Boundaries of operating temperatures in direct supply form solar mode 65
Figure 40: Aerial view of the Burgo de Las Naciones University Residence. The west wing where the demo apartment is located is marked with the red circle. 66
Figure 41: Sketch of the demo Apartment B 67
Figure 42: Hourly temperature variation of the extreme and average winter scenarios in Santiago de Compostela 71
Figure 43: Variation of the hourly radiation on horizontal surface for the extreme and average winter scenarios in Santiago de Compostela 71
Figure 44: Heating system operation schedule..... 72
Figure 45: Extreme and Average heating load in Santiago de Compostela demo site 72
Figure 46: Estimation of the Heating Degree Days in 2030 and 2050 in comparison to the reference year (2005) 74
Figure 47: Estimated monthly heating loads in reference year, 2030 and 2050 for USC demo site 75
Figure 48: Estimated monthly cooling loads in reference year, 2030 and 2050 for USC demo site 75

List of Abbreviations and Nomenclature

Abbreviation	Definition
CDD	Cooling Degree Days
CDH	Cooling Degree Hours
COP	Coefficient of performance
D	Detached dwelling
DHW	Domestic Hot Water
DR	Demand Response
DSSC	Dye-sensitized solar cell
ETC	Evacuated tube collector
F	Flat (dwelling typology)
FPC	Flat plate collector
GHG	Green-house gases
GCM	Global Climate Model
HDD	Heating Degree Days
HDH	Heating Degree Hours
HIT	Heterojunction with intrinsic thin layer
HLC	Heat Loss Coefficient
HP	Heat Pump
HT	High temperature
HtF	Heat-transfer fluid
LFR	Linear Fresnel reflector
LSA	Indicator of the difference of the daily HDD and total solar radiation values from the corresponding daily average values
LSE	Indicator of the difference of the daily HDD and total solar radiation values from the corresponding daily extreme values
NZEB	Nearly Zero Energy Building
PCM	Phase Change Material
PDR	Parabolic dish reflector
PTC	Parabolic through collector
PV	Photovoltaic panel
PVT	Photovoltaic thermal panel
RCM	Regional Climatic Model
RCP	Representative Concentration Pathway scenario
RES	Renewable Energy Sources
RUBN	Burgo De Las Naciones University Residence
SAHP	Solar-assisted Heat Pump
SD	Semi-detached dwelling
SHS	Sensible Heat Storage
TCM	Thermochemical Material
TES	Thermal Energy Storage
TMY	Typical Meteorological Year
USC	University of Santiago de Compostela
VHT	Very high temperature

Symbol	Definition
c_p	Specific heat capacity (kJ/(Kg·K))
G_h	Total solar radiation on horizontal surface (W/m^2)
H_r	Hour (h)
N_h	Number of hours of a day
N_d	Number of days of a month

Q	Energy demand (kWh)
T	Temperature (°C)
V	Volume (L)
ρ	Density (kg/m^3)
Subscript	**Definition**
ave	average daily value
b	base
daily	value over a whole day period
des	desorption
dhw	domestic hot water
ext	external (outdoor)
ht	heating
i	refers to the ith hour of the day
ind	indoor
j	refers to the jth day of the year
m	refers to the mth month of the year
max	maximum daily value
mean	mean daily value
min	minimum daily value
sorp	sorption
ws	refers to water supply to the building

1 Introduction

1.1 Scope and objective of the deliverable

This document presents the main outcomes of the activities carried out in the framework of Task 2.4 "Characterization of an interoperable and adaptable storage solution, easily integrated with PVT and other local RES". The main scope of this deliverable is to capitalize on the main outcomes of Deliverables 2.1, 2.2 and 2.3 and translate them into a set of operational specifications of MiniStor main components.

More specifically, D2.2 defined the general context in which MiniStor energy storage system will be applied, by conducting a first research about climatic conditions, building typologies (in relation to type, age, area and type of heating system of dwellings) and user profiles throughout Europe. Based on these findings, D2.1 included a preliminary estimation of MiniStor market size by identifying competing technologies and examining the dwelling types and the energy sources used for space heating in European countries. The current report completes this research by proving information about the heating and cooling needs of residential buildings of different type and age in several European countries, while also including a thorough review of thermal energy storage technologies. It also aims to link the basic findings of D2.3 regarding the limitations imposed by the use of ammonia as a refrigerant by MiniStor, with the characteristics of the common residential building types in Europe.

Furthermore, the current document includes an investigation of the possible ways to integrate MiniStor with RES systems. This investigation is accompanied by a thorough research of RES utilization for energy generation throughout Europe and is of particular importance, since MiniStor aims to offer sustainable production and storage of heating, cooling and electricity by using renewable energy inputs. The basic operating modes of the system are also discussed and analysed in a conceptual but comprehensive manner.

Concluding, the aim of D2.4 is to summarize all the necessary information that a potential user of MiniStor would like to have in order to explore the possibility of using it. Thus, this "user manual" covers the following topics, providing a full insight of MiniStor operation and characteristics:

- Description of MiniStor pros and cons compared to other thermal energy storage technologies.
- Estimation of the buildings thermal and cooling demand.
- Identification of methods for harvesting renewable energy that will feed MiniStor.
- Information about the most popular RES systems in European countries.
- Restrictions that should be taken into account and which are imposed by the usage of ammonia.
- Summary of MiniStor operation modes.
- Overview of MiniStor operating conditions.

Finally, D2.4 includes estimations of current and future thermal loads of University of Santiago de Compostela (USC) demo site. The corresponding information for the other demo sites of MiniStor was included in D2.2. However, due to the late admission of USC into the consortium and the early due date of D2.2, it was not possible to include these data in the latter document.

1.2 Deliverable structure and connections

This report is divided in five main sections, each one corresponding to a specific chapter and focusing on one of the main topics addressed by the document:

- Chapter 2 presents the literature review of available thermal energy storage technologies, along with the estimations of heating and cooling needs for various buildings throughout Europe. In order to enhance the comprehensiveness of the document, some useful data though not on the primary focus of the analysis are presented in the Annex.
- Chapter 3 regards the potential renewable energy input to MiniStor system. It is divided into two parts: i) the identification of methods to integrate MiniStor with RES systems and ii) the overview of RES utilisation in several European countries.
- Chapter 4 focuses on the restrictions imposed by the use of ammonia by MiniStor and their impacts on the system installation.

- Chapter 5 concerns the system operation and comprises two sections: i) the definition of the system operation modes, ii) the overview of the corresponding operating conditions along with the main specifications of the basic system components
- Finally, chapter 6 includes the thermal load calculations for the Santiago de Compostela demo site.

As already discussed, D2.4 receives useful input from Deliverables 2.1, 2.2 and 2.3, all of them compiled in the framework of WP2. Additional input is provided by tasks of WPs 3, 4 and 6. In addition to its function as a "user manual", D2.4 will also provide feedback to WP3, WP5, WP6 and WP7. Figure 1 presents the connections of the document five parts with the other activities of the project.

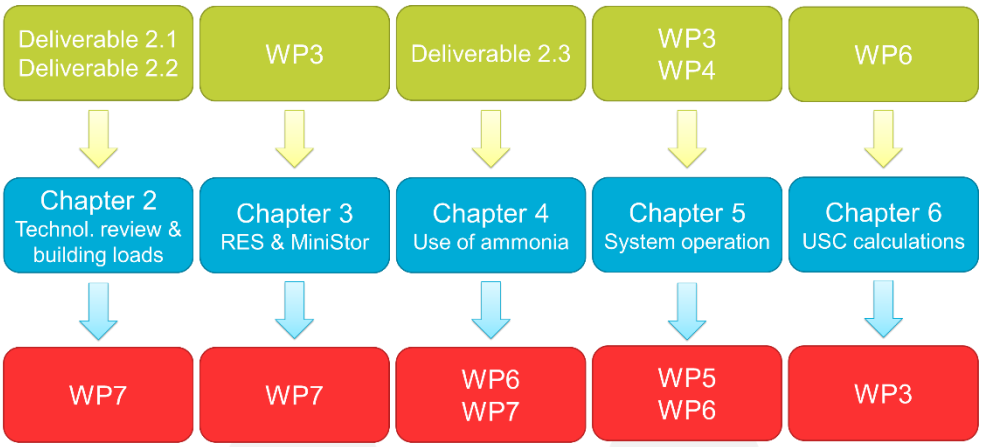

Figure 1: Deliverable structure and connections

2 Context description, Stakeholder and User Characterisation

2.1 Review of energy storage technologies

Thermal energy storage (TES) systems have an increasingly important role in the current and future energy systems. The storage of thermal energy allows for increasing the levels of integration of renewable energy sources (RES) on the energy system as it addresses the mismatch between the energy production from the variable RES and demand. In addition, the use of TES may also lead to improved performance of conventional systems. Furthermore, it offers demand-side management services through shifting the electricity demand for heating applications and leading to the use of off-peak electricity, thus resulting in significant reduction in the energy bills of households and flexibility services to the energy system (Renaldi, 2018). Ultimately, effective energy storage in the building sector may lead to increased levels of energy security and reliability of the energy systems as well as to a reduction in the greenhouse gases emissions (Dincer & Rosen, 2010).

Thermal energy storage systems are classified in three main categories based on the mechanism involved in the storage process:

- Sensible heat storage, where the energy is stored in a solid or liquid medium resulting in an increase of its temperature
- Latent heat storage, where energy is stored in a medium mainly in the form of latent energy required during the phase change of that medium (from solid to liquid or liquid to gas). Heat is also stored in the form of sensible heat prior and after the change of phase, however sensible storage is only a small fraction of the overall storage capacity. For this reason, the mediums used in this process are also referred to as Phase Change Materials (PCMs). Latent heat storage systems comprise inorganic or organic PCMs.
- Thermochemical heat storage, where the energy is stored through reversible endothermic chemical reactions or sorption.

The main types of thermal energy storage systems are presented in Table 1 below:

Table 1: Classification of thermal Energy Storage Systems (Sarbu & Sebarchievici, 2018)

Thermal Energy Storage systems					
Sensible Heat Storage		**Latent Heat Storage**		**Thermochemical Storage**	
Solid	Liquid	Inorganic	Organic	Reaction	Sorption
- Clay - Concrete - Bricks - Soil/Earth - Rock	- Water - Water/glycol	- Water - Ice - Salt hydrates	- Paraffins - Sugar Alcohols	- Hydration - Carbonation	- Ammoniates - Hydrates - Metal hydrides

The various systems are at different stage of development and technology readiness to enter the market. The level of maturity for some common thermal and electricity storage technologies is presented in Figure 2 below.

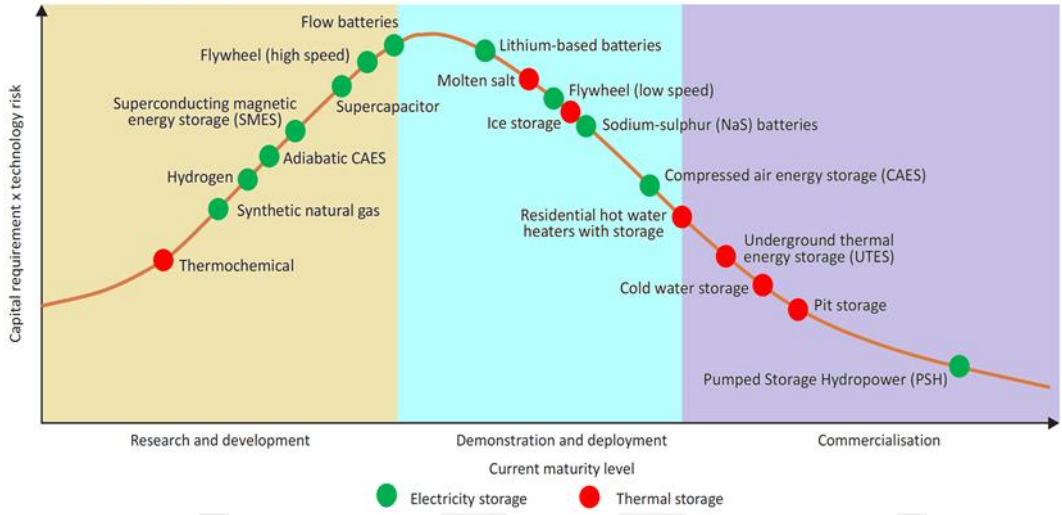

Figure 2: Maturity level of various thermal and electricity storage technologies (adapted from (IEA, 2014))

Storage systems may be defined by one or more of the following attributes (IEA-ETSAP & IRENA, 2013):

- Capacity, defines the amount of energy stored. Storage capacity relies on many factors such as the storage procedure, the storage medium and the size of the system
- Power, defines the rate at which the stored energy can be charged and discharged from the storage system.
- Efficiency, the ratio of the energy delivered to the user divided by the energy required to charge the storage system
- Storage period, the period for which the energy is stored in the system and ranges from several hours up to months
- Charge/discharge time, the time required for a fully charge or discharge of the storage system.
- Cost per unit of storage, either cost per unit of energy or per unit of power, including both the capital and the operational costs.

2.1.1 Sensible Heat Storage Systems

Sensible Heat Storage (SHS) is the simplest form of energy storage where heat is stored in a medium in the form of temperature rise of the material. The most commonly SHS material is water as it is cheap, abundant and has a high heat capacity; other materials include rocks, molten salts, soil etc. SHS is the cheapest method of heat storage whilst it is also the safest as the materials involved are non-toxic. However, this

type of storage has the lowest energy density requiring large storage volumes which makes it difficult to use in applications with limited space availability. Efficiency of SHS systems varies between 50-90% (Ould Amrouche et al., 2016).

The most commonly used sensible TES systems for the domestic sector that are also applicable for single family residential buildings, are the following:

- Water storage tanks. The use of hot water tanks is the most widely used technology for thermal energy storage. TES Tanks are commonly used as buffer tanks in space heating applications as well as daily energy storage in hot water applications and are usually combined with solar thermal systems. Currently, TES Tanks are being used in combination with heat pumps (air-to-water, water-to-water and brine-to-water) and low-temperature emitters in new and retrofitted buildings. This enhances the usable temperature differences in the water tank and increases their efficiency. In district heating systems, large scale water tanks may also be used for seasonal storage. Working temperatures are between 80-90 °C in the charging phase. Water storage tanks are very cost-effective. The technology is mature and its efficiency can be improved by using stratification elements, and installing increased levels of thermal insulation. In addition, water has a high specific heat capacity and is a safe and chemically stable material to use. The main drawbacks are the lower energy density compared to PCMs and TCM technologies and its variable discharging temperature (IEA-ETSAP & IRENA, 2013).
- Underground thermal energy storage. With regard to single family residential buildings borehole storage is an applicable solution of underground energy storage; boreholes are usually vertical ground heat exchangers that store heat in the thermal mass of underground soil (clay, rock, etc.). The system charging/discharging rate is defined and restricted by the area and the thermal conductivity of the pipe arrays and the heat transfer properties (thermal conductivity, heat capacity) of the surrounding soil. Insulation may be used at the ground surface (Sarbu & Sebarchievici, 2018). Ground heat exchangers may be used in combination with heat pumps for covering the space heating requirements and domestic hot water needs (IEA-ETSAP & IRENA, 2013). Borehole storage combined with solar thermal systems may also be used for seasonal thermal storage through a suitable arrangement of a number of pipes, although this is mostly applicable to large community scale installations.
- Packed-bed storage. A packed-bed or pebble-bed is a storage unit filled with solid material (rocks, pebbles, ceramic) with a stream of heat-transfer fluid (HtF – usually air) circulating in order to store or remove heat from the storage medium. Air flow takes place in one direction for heat addition and the opposite for removal; therefore, charging and discharging of the storage unit cannot take place simultaneously. They are cheap and can be used in a wide temperature range from low-temperature applications such as solar air heaters to high temperature ones (solar thermal power plants) (Gautam & Saini, 2020). In domestic applications they are usually combined with solar air heaters and have the advantage of being highly stratified; the temperature of the storage medium at the inlet of the hot air stream is higher than the temperature at the outlet. Effectiveness of the system may be increased with the control of the flow of the HtF. In (Nemś et al., 2017), efficiency of a ceramic brick packed-bed unit in a single family home in the range of 72-96% for variable air flow rates was demonstrated. The storage unit was incorporated into the existing heating system of the building and would be eventually connected to a concentrated solar thermal system.

2.1.2 Latent Heat Storage

Latent Heat Storage offers specific advantages compared to the sensible storage systems. Phase Change Material systems have higher energy density than sensible storage systems, thereby requiring less volume for the same storage capacity. Furthermore, PCMs are characterised by stable temperatures during the heat discharge process. These attributes offer significant benefits in solar thermal and waste heat utilization applications (Zalba et al., 2003). They also render latent heat storage systems favourable in terms of building integration and facilitate the efficient operation of integrated systems. Nevertheless, PCM systems are more expensive than sensible storage systems whilst certain types might be corrosive or toxic which make their containment in tanks and use on building applications challenging.

Phase change in latent heat storage systems takes place in various material forms: solid-liquid, liquid-gas and solid-solid. In domestic applications solid-liquid systems are used; liquid-gas systems have very high enthalpy, however they are difficult to control due to the high volume increase occurring as a result of the transition from liquid to the gas state. On the contrary, solid-liquid systems experience low levels of volume variations and have a considerably high enthalpy; typical storage density of a PCM material is in the order of 100 kWh/m^3, four times higher than the energy density of 25 kWh/m^3 for typical SHS systems (IEA-ETSAP & IRENA, 2013). PCMs can be used for both short and long-term storage with an efficiency of 75-90% (Ould Amrouche et al., 2016).

PCMs are classified as organic or inorganic materials. Organic materials are either paraffin waxes or non-paraffin materials (fatty acid, esters, alcohols, glycols and eutectics) while inorganic PCMs comprise salt hydrates, nitrate salts, carbonate salts, chlorine salts, sulphate salts, fluorine salts, hydroxides, metal, alloys and salt eutectics (Kampouris et al., 2020; Sarbu & Sebarchievici, 2018). The most commonly used organic PCMs are paraffins and fatty acids whilst salt hydrates and salts are the most commonly used inorganic materials (Cabeza, 2019). For space heating and domestic hot water applications the former three are most commonly used as they have most suitable melting points for these applications (da Cunha & Eames, 2018). The main characteristics of these materials are presented below (Cabeza, 2019; Sarbu & Sebarchievici, 2018):

- Paraffins are alkanes with variable melting points, ranging from 0 to 120 °C, depending on the length of the alkane chain; both the melting point and the latent heat increase with the length of the chain. Paraffins are generally characterised of high energy density and they do not present significant sub-cooling. They have low thermal conductivity but this can be improved by means of thin encapsulation or graphite-matrix (de Gracia & Cabeza, 2015). However, they are flammable and they are usually not compatible with plastic containments; only with metal ones.
- Fatty acids have similar melting points to paraffins and they do not present sub-cooling either. However, they are characterised by low conductivity whilst they can also be corrosive to metal containers.
- Inorganic salt hydrates on the other hand have a higher latent heat density than paraffins and fatty acids and a higher thermal conductivity compared to the organic PCMs. The main disadvantages are that they are corrosive and they show sub-cooling as well as phase segregation. The melting point salt hydrates is between 5 and 130 °C.

The table below presents the main advantages and disadvantages of the organic and inorganic latent heat storage materials as well as recommended methods for improving their performance. It is also interesting to note that as defined in D4.2 “PCM storage material characterization and optimal implementation in PCM storage vessels”, the selected for use in MiniStor hot PCMs are inorganic materials (based on Sodium Acetate Trihydrate), whereas the cold PCMs are organic ones (the preferred material is based on dimethyl adipate and an alternative is based on methyl laurate).

Table 2: Main characteristics of organic and inorganic materials (adapted from (Cabeza et al., 2011))

	Organic	Inorganic
Advantages	- Non corrosives - Low or none sub-cooling - Chemical and thermal stability	- Greater phase change enthalpy - Non-flammable - Inexpensive - Higher thermal conductivity
Disadvantages	- Lower phase change enthalpy - Low thermal conductivity - Flammability	- Sub-cooling - Corrosion - Phase separation - Phase segregation, lack of thermal stability
Methods for improvement	- Use of high thermal conductivity additives - Use of fire-retardant additives	- Mixing with nucleating and thickening agents - Thin layer arranged horizontally - Mechanical stir

2.1.3 Thermochemical Storage

Thermochemical storage takes place under reversible endothermic reactions or sorption processes following the general representation below:

$$AB + Q \leftrightarrow A + B$$

Where, AB is a compound of parts A and B. When heat, Q, is supplied to the system (endothermic reaction) the products A and B are separated. This is the charging stage of the thermochemical TES. Energy is released (discharging) in the reverse exothermic reaction when parts A and B are combined in suitable conditions of pressure and temperature to form AB.

Thermochemical storage has a higher energy density than latent heat storage technologies and higher efficiency ranging from 75 to 100% (Ould Amrouche et al., 2016). Since the losses are due to the sensible losses occurring at the storage units of the separated components; these are usually significantly lower to the overall heat released during the reaction process (Renaldi, 2018). These high levels of storage capacity in combination with reduced losses make thermochemical storage suitable for the transportation of thermal energy (IEA, 2014) as well as for long-term storage of heat.

Selection of the most appropriate thermochemical TES process relies on the following characteristics (Milone, Kato, & Mastronardo, 2019):

- Increased amount of heat required for the reaction;
- Favourable reversibility of the process;
- Fast rate of charging/discharging;
- High levels of products stability;
- Reaction products can be easily stored, i.e. reactants should not be toxic, corrosive, flammable or explosive;
- Low-cost and availability of the compound.

The term *sorption* collectively describes the mechanisms of absorption and adsorption of a gas in a liquid or solid material. In absorption, the gas molecules enter the liquid or solid material and change its composition whilst adsorption refers to the mechanism where the gas molecules are bound in the surface of a solid or porous material (Krese et al., 2018). In the sorption process, the gas is called *sorbate* and the solid or liquid that is adsorbing or absorbing the gas is called *sorbent* (Frazzica et al., 2019). Thermochemical storage systems are classified as open and closed based on the type of storage of the reactant gas. In closed systems there is no mass exchange with the environment. The charging process involves the input of heat to the reactor and the sorbate vapour desorbed from the sorbent, thereby regenerating it. The sorbate vapour is then condensed and stored in the condenser. The discharging process involves the evaporation of the condensed sorbate which is then fed to the sorbent material resulting in the heat release due to the exothermic reaction. In open systems there is mass exchange with the environment; for this reason, open systems operate only with water vapour. Regeneration of the sorbent (desorption of the sorbent vapour, i.e. water) takes place with the flow of heated and dried external air through the reactor that contains the sorbent material. The discharging process occurs when cooled and humid stream of external air passes through the reactor that contains the dry sorbent thereby enabling the sorption of the water vapour and releasing heat through the exothermic process that is driven to cover the heat load (Frazzica et al., 2019). The table below presents the main advantages and disadvantages of the open and closed systems.

Table 3: Main advantages and disadvantages of the open and closed reactor TCM systems (Scapino et al., 2017)

	Disadvantages	Advantages
Open	- Requirement for fan operation to drive the moist flow through the reactor - Humidifier may also be required so that the sorbent stream can reach the desired vapour pressure - Temperature over the reactor subject to the flow mass	- Simple system with fewer component requirements compared to the closed systems - Adequate heat transfer rate may be achieved - Forced ventilation may increase heat transfer - No hazardous materials involved

	- Requirement for heat recovery unit to obtain space heating and DHW temperatures - Increased flow rates lead to pressure drops	
Closed	- Requirement for additional storage vessel, evaporator and condenser - System complexity with additional components required compared to open systems - Requirement for periodic system evacuation and maintenance to address the issue of non-condensable gases - Energy requirements for the evaporation of the sorbate	- No requirement for fan operation to drive the sorbent - Higher temperatures at the system discharge may be achieved - Isolated from the environment with no mass exchange involved - May act as adsorption heat pump

Thermochemical storage is currently not commercially available for building applications with most systems demonstrated being currently at the pilot and lab-demonstration stage. In order to develop market ready systems there are several issues that need to be addressed, mainly related to the high costs, corrosion, environmental impact of materials and inadequate levels of heat and mass transfer achieved (de Gracia & Cabeza, 2015; Krese et al., 2018). The challenge is to deliver low-cost sorbent materials with adequate energy density and stability at the required temperature range for building applications (Scapino et al., 2017). Furthermore, material degradation and chemical instability during the charging/discharging processes is another issue for TCM storage systems. In (Sögütoglu et al., 2018), the authors investigated the energy density, power output and chemical stability of three thermochemical materials (K2CO3, MgCl2 and Na2S) used as sorbents in open and closed systems. It was found that K2CO3 presented the most favourable performance with a power output of 283 - 675 kW/m^3 (energy density of 1.28GJ/m^3 and 0.95GJ/m^3 for the closed and open system respectively) and high thermal stability. MgCl2 and Na2S were not chemically stable as they showed significant degradation in multiple charging/discharging cycles; MgCl2 is expected to become inactive after 30 cycles and Na2S is air sensitive resulting in a reduction in the energy density. Therefore, they were not found to be preferable despite the fact that both materials had higher energy density measured in the first cycle compared to K2CO3.

Several prototype systems have been developed for space heating and domestic hot water applications. An overview of current and previous prototype systems developed for building related applications is provided by (Krese et al., 2018) and (Scapino et al., 2017). It was found that in most cases the energy density expected was not met mainly due to inadequate levels of heat and mass transfer achieved in practice. In that respect open systems performed better as they are simpler and HtF is in direct contact to the sorbent material. Furthermore, open systems have a lower cost than closed ones as they are simpler and involve less components.

Table 4: Summary of prototype open and closed TCM systems developed

	System	Sorbent material	T_{des}	T_{sorp}
HYDES ("High energy density sorption heat storage for solar space heating," 1998)	Closed	Silica-gel	82	-
MODESTORE ("Modular high energy density sorption heat storage," 2008)	Closed	Silica-gel	88	-
Schreiber et al. (Schreiber et al., 2015)	Closed	Zeolite 13X	200	120
Lass-Seyoum et al. (Lass-Seyoum et al., 2012; Lass-Seyoum et al., 2016)	Closed	Unspecified	100-120	65-70
Lu et al. (Lu et al., 2003)	Closed	Zeolite 13X	-	125

TNO (Cuypers et al., 2012; Finck et al., 2013)	Closed	Zeolite 5A	-	-
MONOSORP (H. Kerskes, Heidemann, & Müller-Steinhagen, 2004)	Open	Zeolite 4A	180	20
SolSpaces (Weber et al., 2016)	Open	Zeolite 13X	-	-
CWS (Henner Kerskes et al., 2012)	Open	Zeolite and salt composite	180	35
ZAE Bayern (Hauer, 2007)	Open	Zeolite 13X	130 (heating) 50 (cooling)	25-30
Zettl et al (Zettl, Englmair, & Steinmaurer, 2014)	Open	Zeolite 4A/Zeolite 13X	-	-
Johannes et al (Johannes et al., 2015)	Open	Zeolite 13X	-	-
Flow TCS (van Helden et al., 2016)	Open	Zeolite and salt impregnated zeolite	-	-

2.1.4 Strengths and Weaknesses for each competing technology

MiniStor combines two different storage technologies, i.e. thermochemical and latent heat storage, offering significant energy storage density, increased flexibility and better control of the induced heat flows. Contrary to the previously mentioned thermochemical storage systems, it capitalizes on a commercially available technology utilised in sectors of the cold supply chain and especially in the transportation of food and pharmaceutical products. In these applications, usually characterised by low power (on the order of several hundred watts), $MnCl2(NH3)6/2$ salts are used for the provision of cooling at temperature levels of -20/-10 °C. In MiniStor system the implementation of different ammoniated salts is proposed ($CaCl2(NH3)8/4$ and $CaCl2(NH3)4/2$) for the provision of both heating and cooling, while utilising RES as heat input. The chemical properties and reacting stability of the selected salts have been analysed in the literature (N'Tsoukpoe et al., 2015) and they have been experimentally tested in sorption refrigeration and solar cooling applications. Thus, the TCM unit of MiniStor can justifiably be considered to be of higher technological maturity compared to those of other thermochemical storage systems. Because of the use of ammonia, the thermochemical storage system of MiniStor is a closed one, i.e. all the reactants and products of the reactions are in a sealed reactor and no mass exchange with the environment occurs. Table 5 summarizes the main strengths and weaknesses identified for each of the above-mentioned competitive storage technologies. The relevant characteristics of the MiniStor system are also presented.

Table 5: Summary of prototype open and closed TCM systems developed

Technology	Main strengths	Main weaknesses
Electrical storage heaters	- Low cost - Mature technology - Possibility to use PV technology as an energy source (seasonal)	- Low system efficiency - Low energy storage capacity - Application only for Domestic Hot Water systems
Sensible Heat Storage based systems	- Low-cost TES material - Mature technology - Large availability - No toxic TES material - Chemical stability - Easy integration to existing systems with water-based emitters units - Market ready - Increased stratification for packed-bed storage	- Large temperature variation during the discharge process - Low energy density - High volume required - Lower storage efficiencies than competing technologies

	- Efficiency increase with the use of stratification elements and insulation levels - Suitable for short and long term storage - Integration with geothermal and solar thermal applications	
PCM TES based systems	- Higher energy density - Compact system - Stable temperature during the discharging process - Low toxicity - Easy integration to existing systems with water-based emitters units - Low levels of volume variation (solid-liquid systems) - Relatively high enthalpy - Suitable melting points for domestic application - High energy efficiency	- Low maturity (mainly at the development stage and demonstration projects) - High cost. The total cost should include the material, the container, and the overhead cost. - Low thermal conductivity of PCMs (can be improved with additives) - Inorganic PCMs are normally corrosive to metal containers - Organic PCMs are flammable (use of fire-retardants recommended)
TCM TES systems	- Higher energy density than both Sensible and Latent Heat Storage systems - High levels of energy efficiency - Suitable for short and long-term storage - Suitable for heat transport - Open systems do not have hazardous materials - Closed systems are isolated from the environment (no mass exchange)	- Low maturity (lab-based or pilot systems) - Higher cost than SHS - Poor heat and mass transfer performance - Subject to degradation and chemical instability - Corrosive and hazardous materials (closed systems) - Complex systems with high number of peripheral components (closed) - Requirement for fan operation and humidifier in open systems reduces efficiency - Risk of material chemical degradation
MiniStor system	- Very high energy density - Low mass and volume of storage materials. - High exergetic efficiency - High operating temperature - Relatively easy integration to existing heating and cooling systems with water-based emitters units. - Combination of different storage technologies with internal heat pump. - Can provide heating and cooling.	- Low maturity compared to Sensible and Latent Heat Storage systems - Much more complex and expensive than the TES-based tanks - Risk of degradation of the TCM material properties during charging and discharging processes. - Regulation limitation in the use of ammonia in refrigeration systems for residential sector. - Low technical knowledge by the installer companies.

2.2 Estimations of peak heating & cooling loads for various residential buildings throughout Europe

In order to investigate the market potential and the applicability of the Ministor system, in this section the heating and cooling loads of residential buildings in several key-countries identified as most suitable for its use are presented. Based on the market analysis presented in "D2.1 - Definition of stakeholder requirements, market demands and application challenges" and taking into account factors such as

geographical region, market size and solar availability the following countries were considered in this investigation:

- Greece
- Hungary
- Germany
- France
- Italy
- Spain

Due to the various climatic conditions found throughout Europe, building characteristics differ considerably from one country/city to another. For reasons of consistency, the various building typologies of each country were grouped in three main types of dwellings that are common in all countries:

- Detached houses, that are stand-alone dwellings not attached to any other building
- Semi-detached houses, that are dwellings attached to a neighbouring building, side by side (or back to back) without any dwellings above or below
- Flats, that are residential units of apartment buildings with three or more dwellings

This classification is also in accordance with the findings of "D2.2 – Definition of system context and limits of use". As described in Deliverable D2.1, the Ministor system can be used in any of these types of dwellings in a different manner. Therefore, the heating and cooling loads for these three main building types were determined with the use of the methodology described in the following paragraphs. In addition, as the system may also be used for providing domestic hot water, the DHW requirements in each country were also calculated.

2.2.1 Methodology for determining the heating and cooling loads

Determining the load for space heating and cooling requires to calculate first the heating and cooling requirements. Defining the heating requirements of dwellings in the EU has been the subject of various studies and projects that provide such information to various degrees of detail at the building stock level. However, this is not the case for the cooling demand of dwellings where available information is limited (Jakubcionis & Carlsson, 2017). As the study was conducted for the various countries and the different building types presented, there was a need to derive a concise methodology along with the use of homogenized data in order to determine the space heating requirements of the buildings in a manner that is consistent for all countries examined. Furthermore, there was a need for the methodology to be able to overcome the barrier of limited data and deliver a consistent estimation of the space cooling demands for all building types.

The first step of the methodology considered the definition of the space heating demand of the buildings. The Tabula Webtool[1] that has been developed within the framework of the European projects Tabula and Episcope[2] was used. During these projects the typical building typologies of 15 European countries were developed considering different time periods and (in some cases) different regions within each country. Furthermore, the specific space heating demand (kWh/m^2) and the typical area (m^2) for each building of the respective time period and region were determined. This information was used to establish the heating demand Q_{ht} for each type of building.

The heating load for each building was then determined considering the Heating Degree Hours and the annual heating requirements calculated through the Tabula Webtool. Using the following formula, the total building Heat Loss Coefficient was determined:

$$Q_{ht} = HLC \cdot (T_b - T_{ext})^+ \cdot H_r = HLC \cdot HDH \qquad \text{Equation 1}$$

Where,

HLC: is the overall Heat Loss Coefficient of the building. This is a collective term that includes both the transmission and ventilation losses from a building and is expressed in W/K

[1] https://webtool.building-typology.eu/#bm

[2] https://episcope.eu/welcome/

HDH: is the number of Heating Degree Hours during a year. A *HDH* is the product of the temperature difference between the external temperature, T_{ext}, and a base temperature, T_b for that hour times that hour (H_r). The base temperature is a predefined temperature when no heating is required. HDHs are defined only in the case when the external temperature is lower than the base temperature (denoted by the symbol "+" in Equation 1), otherwise they are considered zero (i.e. there is no heating demand for that hour). The total number of Heating Degree Hours throughout the year is the summation of the individual HDHs and is a measure of both the magnitude and the distribution of the heating demand and is expressed in K·h (Kelvin-hours).

The overall Heat Loss Coefficient is determined from Equation 1 through the ratio of the annual heating demand and the annual heating degree hours. After determining its value, the maximum heating load for each building was calculated by multiplying the HLC with the maximum value of HDH observed, i.e. the hour with the maximum value of heating demand of the year. Finally, the maximum cooling load of the buildings was calculated by multiplying the overall HLC with the maximum Cooling Degree Hour (CDH) observed in the year. Similar to the concept of the Heating Degree Hour, a Cooling Degree Hour is the temperature difference between the external temperature and a predefined base temperature (when no cooling is required). CDHs are defined only when the external temperature is higher than the base temperature for cooling. The total number of Cooling Degree Hours throughout the year is the summation of the individual CDHs and is a measure of both the magnitude and the distribution of the cooling demand (Figure 3). However, it should be noted that the resulting cooling loads are approximations mainly suitable for qualitative analysis, as in reality heat gains from human activities, household devices and solar irradiance (through building transparent elements) also contribute to the build-up of each building cooling needs.

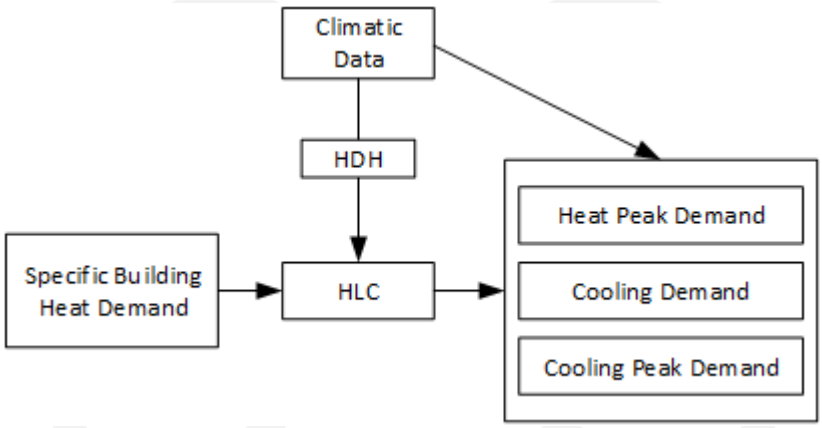

Figure 3: Simplified diagram of the estimation procedure.

Of particular importance for the calculation of HDHs and CHDs is the selection of suitable base temperatures. The latter should take into consideration local weather conditions as well as specific building characteristics (Kadioğlu, Şen, & Gültekin, 2001) and may be different for each country as there are no universally accepted values. In the current analysis, the choice of base temperatures for heating and cooling and for each country was based on literature. Their values are presented in Table 6 below. Finally, the ambient temperature values used in HDHs and CHDs computations, were derived from Typical Meteorological Years (TMY). TMY files are sets of meteorological data with hourly values for a typical year for a specific location (Team E3P - DG JRC). In this analysis, TMY files for representative cities of each region and country were used ("Climate.OneBuilding,").

Table 6: Base temperature selection for each country

Country	Base temperature for HDH	Base Temperature for CDH
Greece (Papakostas, Mavromatis, & Kyriakis, 2010)	15°C	24°C
Hungary (Skarbit et al., 2017)	15°C	18.3°C
Germany (Heitkoetter et al., 2020; Olonscheck, Holsten, & Kropp, 2011)	15°C	22°C

France (J. Spinoni, Vogt, & Barbosa, 2015)	15.5°C	22°C
Italy (Petralli, Massetti, & Orlandini, 2011)	17°C	22°C
Spain (Petri & Caldeira, 2015)	17°C	22°C

2.2.2 Heating and Cooling Demand calculation

Following the methodology described above, the heating and cooling load was determined for each building type in the countries examined. Furthermore, the analysis considered also the climatic zones where the buildings may be situated as well as the time period of construction as shown in Table 7, as these parameters have a significant effect on the building loads. Table 8 gives the representative cities and used TMY files for each region and country considered in this analysis. Results are presented in the following paragraphs.

Table 7: Analysis index

Country	Number of Climatic Zones	Time classes / periods	House Types	Comments
Greece	4	4	2	Each zone presents different building characteristics
France	3	7	3	All zones present the same building characteristics per type
Italy	1	6	3	-
Hungary	1	5	2	-
Germany	15	7	3	All zones present the same building characteristics per type
Spain	1	5	3	-

Table 8: Representative cities and corresponding TMY files for each region and country considered

Country	Climatic Zone	City	TMY file
Greece	A	Herakleion	GRC_CR_Heraklion-Kazantzakis.AP.167540_TMYx.2004-2018
Greece	B	Athens	GRC_AT_Athinai-Hellinikon.AFB.167160_TMYx.2004-2018
Greece	C	Thessaloniki	GRC_MH_Thessaloniki-Makedonia.AP.166220_TMYx.2004-2018
Greece	D	Kozani	GRC_EM_Kozani-Filippos.AP.166320_TMYx.2004-2018
France	H1	Paris	FRA_IF_Paris.MontSouris.071560_TMYx.2004-2018
France	H2	Toulouse	FRA_LP_Toulouse-Blagnac.AP.076300_TMYx.2004-2018
France	H3	Marseille	FRA_PR_Marseille.Provence.AP.076500_TMYx.2004-2018
Italy	-	Rome	ITA_LZ_Rome-Fiumicino-da.Vinci.AP.162420_TMYx.2004-2018
Hungary	-	Budapest	HUN_CEN_Budapest.Ferenc.Liszt.Intl.AP.128390_TMYx.2004-2018
Germany	CR1	Bremerhaven	DEU_HB_Bremerhaven.101290_TMYx
Germany	CR2	Rostock-Laage	DEU_MV_Rostock-Laage.AP.101720_TMYx.2004-2018
Germany	CR3	Hamburg-Schmidt	DEU_HH_Hamburg-Schmidt.AP.101470_TMYx.2004-2018
Germany	CR4	Potsadam	DEU_BB_Potsdam.103790_TMYx
Germany	CR5	Essen	DEU_NW_Essen.DWD.104100_TMYx

Germany	CR6	Bad Marienberg	DEU_RP_Bad.Marienberg.105260_TMYx
Germany	CR7	Kassel	DEU_HE_Kassel.Calden.AP.104360_TMYx.2004-2018
Germany	CR8	Braunlage	DEU_NI_Braunlage.104520_TMYx
Germany	CR9	Chemnitz-Stelzendorf	DEU_SN_Chemnitz-Stelzendorf.105770_TMYx
Germany	CR10	HoF	DEU_BY_Hof.106850_TMYx.2004-2018
Germany	CR11	Fichtelberg	DEU_SN_Fichtelberg.105780_TMYx
Germany	CR12	Mannheim	DEU_BW_Mannheim.107290_TMYx.2004-2018
Germany	CR13	Passau	DEU_BY_Passau.108930_TMYx
Germany	CR14	Stuttgard	DEU_BW_Stuttgart.AP.107380_TMYx.2004-2018
Germany	CR15	Garmisch	DEU_BY_Garmisch-Partenkirchen.109630_TMYx
Spain	Continental	Madrid	ESP_MD_Madrid-Barajas-Suarez.AP.082210_TMYx.2004-2018

2.2.2.1 Greece

Greece is divided in four climatic zones, Zones A-D, whilst the building stock has been grouped in two building types (detached dwellings and flats) and four time periods: prior to 1980, 1981 – 2000, 2001 – 2010 and 2011 – 2020.
The total HLC for each building type in each zone and time period is presented in Table 9 and Table 10 below along with the estimated heating and cooling load.

Table 9: Area, Heat Loss Coefficient, Peak Heating and Peak Cooling load of the typical detached dwellings in the four climatic zones in Greece

	Zone A		Zone B		Zone C		Zone D	
Year	Area (m^2)	HLC (W/K)	Area (m^2)	HLC (W/K)	Area (m^2)	HLC (W/K)	Area (m^2)	HLC (W/K)
Pre - 1980	111	1053.23	162	1137.20	187	865.87	156	646.27
1981 - 2000	86	1051.56	293	1305.53	149	721.01	180	523.46
2001 - 2010	217	895.72	115	491.18	179	450.16	111	307.51
2011 - 2020	128	387.12	255	517.68	153	259.27	111	205.96
Peak Heating Load (kW)								
Year	Zone A		Zone B		Zone C		Zone D	
Pre - 1980	12.64		17.29		16.45		14.28	
1981 - 2000	12.62		19.84		13.70		11.57	
2001 - 2010	10.75		7.47		8.55		6.80	
2011 - 2020	4.65		7.87		4.93		4.55	
Peak Cooling Load (kW)								
Year	Zone A		Zone B		Zone C		Zone D	
Pre - 1980	12.64		18.65		12.12		7.76	
1981 - 2000	12.62		21.41		10.09		6.28	
2001 - 2010	10.75		8.06		6.30		3.69	
2011 - 2020	4.65		8.49		3.63		2.47	

Table 10: Area, Heat Loss Coefficient, Peak Heating and Peak Cooling load of the typical flats in the four climatic zones in Greece

	Zone A		Zone B		Zone C		Zone D	
Year	Area (m^2)	HLC (W/K)	Area (m^2)	HLC (W/K)	Area (m^2)	HLC (W/K)	Area (m^2)	HLC (W/K)
Pre - 1980	63	328.1	53	225.5	39	183.5	72	219.1

1981 - 2000	69	491.3	96	568.7	59	283.8	117	339.2
2001 - 2010	60	178.4	50	166.2	98	247.1	60	117.7
2011 - 2020	80	174.9	81	108.1	85	134.9	73	94.9

Peak Heating (kW)				
Year	Zone A[3]	Zone B	Zone C	Zone D
Pre - 1980	3.94	3.43	3.49	4.84
1981 - 2000	5.90	8.64	5.39	7.50
2001 - 2010	2.14	2.53	4.69	2.60
2011 - 2020	2.10	1.64	2.56	2.10

Peak Cooling (kW)				
Year	Zone A	Zone B	Zone C	Zone D
Pre - 1980	3.94	3.70	2.57	2.63
1981 - 2000	5.90	9.33	3.97	4.07
2001 - 2010	2.14	2.73	3.46	1.41
2011 - 2020	2.10	1.77	1.89	1.14

2.2.2.2 Hungary

The residential buildings in Hungary were grouped in five different time periods (pre-WWII, 1945 – 1979, 1980 – 1989, 1990 – 2005, 2006 – 2020) and two different typologies (detached dwellings and flats), whilst there are no defined climatic zones.

The areas and the total HLC as well as the estimated heating and the cooling load for each building type and time period are presented in Table 11 below.

Table 11: Area, Heat Loss Coefficient, Peak Heating and Peak Cooling load of the typical detached houses and flats in Hungary

Detached dwellings				
Year	Area (m^2)	HLC (W/K)	Peak Heating (kW)	Peak Cooling (kW)
Prior WWII	102	278.89	7.53	4.66
1945 – 1979	116	325.66	8.79	5.44
1980 – 1989	103	245.29	6.62	4.10
1990 – 2005	110	182.69	4.93	3.05
2006 – 2020	132	164.48	4.44	2.75
Flats				
Year	Area (m^2)	HLC (W/K)	Peak Heating (kW)	Peak Cooling (kW)
Prior WWII	58	139.7	3.77	2.33
1945 – 1979	52	98.5	2.66	1.65
1980 – 1989	57	123.4	3.33	2.06
1990 – 2005	57	82.0	2.21	1.37
2006 – 2020	75	74.8	2.02	1.25

2.2.2.3 Germany

Germany is divided in fifteen climatic zones, CR1 to CR15, whilst the building stock has been grouped in three building types (detached, semi-detached and flats) and seven time periods: pre-WWII, 1945 – 1970, 1971 –1980, 1981 – 1990, 1991 – 2000, 2001 - 2010 and 2011 – 2020.

[3] The temperature difference between the minimum external temperature and the base temperature for heating (15°C) as well as the maximum external temperature and the base temperature for cooling (24°) were the same in Zone A resulting in identical heating and cooling loads

The total area and HLC for each building type in each zone and time period along with the estimated heating and cooling load are presented in Table 12 to Table 15 below.

Table 12: Heat Loss Coefficient for the detached, semi-detached and multifamily dwellings in Germany

	Detached		Semi Detached		Flats	
Year	Area (m^2)	HLC (W/K)	Area (m^2)	HLC (W/K)	Area (m^2)	HLC (W/K)
Pre – WWII	194	457.79	120	233.20	93	192.70
1945 – 1970	121	289.07	117	161.00	88	148.50
1971 –1980	173	351.43	106	174.25	68	110.50
1981 – 1990	216	344.74	108	177.54	23	35.10
1991 – 2000	150	262.80	128	161.79	78	122.50
2001 - 2010	135	185.58	151	163.63	98	106.30
2011 – 2020	187	234.47	196	210.99	129	143.60

Table 13: Peak Heating and Peak Cooling Load of the detached dwellings in Germany

Detached								
Peak Heating (kW)								
Year	CR1	CR2	CR3	CR4	CR5	CR6	CR7	CR8
Pre – WWII	11.44	11.44	13.28	14.74	12.45	11.12	15.34	11.95
1945 – 1970	7.23	7.23	8.38	9.31	7.86	7.02	9.68	7.54
1971 –1980	8.79	8.79	10.19	11.32	9.56	8.54	11.77	9.17
1981 – 1990	8.62	8.62	10.00	11.10	9.38	8.38	11.55	9.00
1991 – 2000	6.57	6.57	7.62	8.46	7.15	6.39	8.80	6.86
2001 - 2010	4.64	4.64	5.38	5.98	5.05	4.51	6.22	4.84
2011 - 2020	5.86	5.86	6.80	7.55	6.38	5.70	7.85	6.12
Peak Heating (kW)								
Year	CR9	CR10	CR11	CR12	CR13	CR14	CR15	
Pre – WWII	15.02	15.56	14.74	10.53	13.73	12.82	15.52	
1945 – 1970	9.48	9.83	9.31	6.65	8.67	8.09	9.80	
1971 –1980	11.53	11.95	11.32	8.08	10.54	9.84	11.91	
1981 – 1990	11.31	11.72	11.10	7.93	10.34	9.65	11.69	
1991 – 2000	8.62	8.94	8.46	6.04	7.88	7.36	8.91	
2001 - 2010	6.09	6.31	5.98	4.27	5.57	5.20	6.29	
2011 - 2020	7.69	7.97	7.55	5.39	7.03	6.57	7.95	
Peak Cooling (kW)								
Year	CR1	CR2	CR3	CR4	CR5	CR6	CR7	CR8
Pre – WWII	3.16	4.03	4.12	4.17	3.16	2.75	4.58	2.79
1945 – 1970	1.99	2.54	2.6	2.63	1.99	1.73	2.89	1.76
1971 –1980	2.42	3.09	3.16	3.2	2.42	2.11	3.51	2.14
1981 – 1990	2.38	3.03	3.1	3.14	2.38	2.07	3.45	2.1
1991 – 2000	1.81	2.31	2.37	2.39	1.81	1.58	2.63	1.6
2001 - 2010	1.28	1.63	1.67	1.69	1.28	1.11	1.86	1.13
2011 - 2020	1.62	2.06	2.11	2.13	1.62	1.41	2.34	1.43
Peak Cooling (kW)								
Year	CR9	CR10	CR11	CR12	CR13	CR14	CR15	
Pre – WWII	3.71	4.58	1.37	6.41	4.49	5.49	4.12	
1945 – 1970	2.34	2.89	0.87	4.05	2.83	3.47	2.60	
1971 –1980	2.85	3.51	1.05	4.92	3.44	4.22	3.16	
1981 – 1990	2.79	3.45	1.03	4.83	3.38	4.14	3.10	
1991 – 2000	2.13	2.63	0.79	3.68	2.58	3.15	2.37	
2001 - 2010	1.5	1.86	0.56	2.6	1.82	2.23	1.67	
2011 - 2020	1.9	2.34	5.89	0.74	0.30	0.60	0.18	

Table 14: Peak Heating and Peak Cooling Load of the semi-detached dwellings in Germany

Semi-detached								
Peak Heating (kW)								
Year	CR1	CR2	CR3	CR4	CR5	CR6	CR7	CR8
Pre – WWII	5.83	5.83	6.76	7.51	6.34	5.67	7.81	6.09
1945 – 1970	4.03	4.03	4.67	5.18	4.38	3.91	5.39	4.20
1971 –1980	4.36	4.36	5.05	5.61	4.74	4.23	5.84	4.55
1981 – 1990	4.44	4.44	5.15	5.72	4.83	4.31	5.95	4.63
1991 – 2000	4.04	4.04	4.69	5.21	4.40	3.93	5.42	4.22
2001 - 2010	4.09	4.09	4.75	5.27	4.45	3.98	5.48	4.27
2011 - 2020	5.27	5.27	6.12	6.79	5.74	5.13	7.07	5.51
Peak Heating (kW)								
Year	CR9	CR10	CR11	CR12	CR13	CR14	CR15	
Pre – WWII	7.65	7.93	7.51	5.36	7.00	6.53	7.91	
1945 – 1970	5.28	5.47	5.18	3.70	4.83	4.51	5.46	
1971 –1980	5.72	5.92	5.61	4.01	5.23	4.88	5.91	
1981 – 1990	5.82	6.04	5.72	4.08	5.33	4.97	6.02	
1991 – 2000	5.31	5.50	5.21	3.72	4.85	4.53	5.48	
2001 - 2010	5.37	5.56	5.27	3.76	4.91	4.58	5.55	
2011 - 2020	6.92	7.17	6.79	4.85	6.33	5.91	7.15	
Peak Cooling (kW)								
Year	CR1	CR2	CR3	CR4	CR5	CR6	CR7	CR8
Pre – WWII	1.61	2.05	2.10	2.12	1.61	1.40	2.33	1.42
1945 – 1970	1.11	1.42	1.45	1.47	1.11	0.97	1.61	0.98
1971 –1980	1.20	1.53	1.57	1.59	1.20	1.05	1.74	1.06
1981 – 1990	1.23	1.56	1.60	1.62	1.23	1.07	1.78	1.08
1991 – 2000	1.12	1.42	1.46	1.47	1.12	0.97	1.62	0.99
2001 - 2010	1.13	1.44	1.47	1.49	1.13	0.98	1.64	1.00
2011 - 2020	1.46	1.86	1.90	1.92	1.46	1.27	2.11	1.29
Peak Cooling (kW)								
Year	CR9	CR10	CR11	CR12	CR13	CR14	CR15	
Pre – WWII	1.89	2.33	0.70	3.26	2.29	2.80	2.10	
1945 – 1970	1.30	1.61	0.48	2.25	1.58	1.93	1.45	
1971 –1980	1.41	1.74	0.52	2.44	1.71	2.09	1.57	
1981 – 1990	1.44	1.78	0.53	2.49	1.74	2.13	1.60	
1991 – 2000	1.31	1.62	0.49	2.27	1.59	1.94	1.46	
2001 - 2010	1.33	1.64	0.49	2.29	1.60	1.96	1.47	
2011 - 2020	1.71	2.11	0.63	2.95	2.07	2.53	1.90	

Table 15: Peak Heating and Peak Cooling Load of the typical flats in Germany

Germany Flats								
Peak Heating (kW)								
Year	CR1	CR2	CR3	CR4	CR5	CR6	CR7	CR8
Pre – WWII	4.82	4.82	5.59	6.21	5.24	4.68	6.46	5.03
1945 – 1970	3.71	3.71	4.31	4.78	4.04	3.61	4.98	3.88
1971 –1980	2.76	2.76	3.20	3.56	3.01	2.69	3.70	2.88
1981 – 1990	0.88	0.88	1.02	1.13	0.96	0.85	1.18	0.92
1991 – 2000	3.06	3.06	3.55	3.95	3.33	2.98	4.11	3.20
2001 - 2010	2.66	2.66	3.08	3.42	2.89	2.58	3.56	2.77
2011 - 2020	3.59	3.59	4.16	4.62	3.90	3.49	4.81	3.75

Peak Heating (kW)								
Year	CR9	CR10	CR11	CR12	CR13	CR14	CR15	
Pre – WWII	6.32	6.55	6.21	4.43	5.78	5.40	6.53	
1945 – 1970	4.87	5.05	4.78	3.42	4.46	4.16	5.04	
1971 –1980	3.62	3.76	3.56	2.54	3.32	3.09	3.75	
1981 – 1990	1.15	1.19	1.13	0.81	1.05	0.98	1.19	
1991 – 2000	4.02	4.17	3.95	2.82	3.68	3.43	4.15	
2001 - 2010	3.49	3.61	3.42	2.44	3.19	2.98	3.60	
2011 - 2020	4.71	4.88	4.62	3.30	4.31	4.02	4.87	
Peak Cooling (kW)								
Year	CR1	CR2	CR3	CR4	CR5	CR6	CR7	CR8
Pre – WWII	1.33	1.70	1.73	1.75	1.33	1.16	1.93	1.18
1945 – 1970	1.03	1.31	1.34	1.35	1.03	0.89	1.49	0.91
1971 –1980	0.76	0.97	0.99	1.01	0.76	0.66	1.11	0.67
1981 – 1990	0.24	0.31	0.32	0.32	0.24	0.21	0.35	0.21
1991 – 2000	0.85	1.08	1.10	1.12	0.85	0.74	1.23	0.75
2001 - 2010	0.73	0.94	0.96	0.97	0.73	0.64	1.06	0.65
2011 - 2020	0.99	1.26	1.29	1.31	0.99	0.86	1.44	0.88
Peak Cooling (kW)								
Year	CR9	CR10	CR11	CR12	CR13	CR14	CR15	
Pre – WWII	1.56	1.93	0.58	2.70	1.89	2.31	1.73	
1945 – 1970	1.20	1.49	0.45	2.08	1.46	1.78	1.34	
1971 –1980	0.90	1.11	0.33	1.55	1.08	1.33	0.99	
1981 – 1990	0.28	0.35	0.11	0.49	0.34	0.42	0.32	
1991 – 2000	0.99	1.23	0.37	1.72	1.20	1.47	1.10	
2001 - 2010	0.86	1.06	0.32	1.49	1.04	1.28	0.96	
2011 - 2020	1.16	1.44	0.43	2.01	1.41	1.72	1.29	

2.2.2.4 France

France is divided in three climatic zones, H1, H2 and H3, whilst the building stock has been grouped in three building types (detached dwellings, semi-detached dwellings and flats) and seven time periods: pre-WWII, 1945 – 1969, 1970 –1979, 1980 – 1989, 1990 – 1999, 2000 - 2009 and 2010 – 2020.

The total HLC for each building type in each zone and time period along with the estimated heating and cooling load are presented in Table 16 to Table 19 below.

Table 16: Area and Heat Loss Coefficient of the typical detached dwellings, semi-detached dwellings and flats in France

	Detached		Semi Detached		Flats	
Year	Area (m^2)	HLC (W/K)	Area (m^2)	HLC (W/K)	Area (m^2)	HLC (W/K)
Pre – WWII	87	444.88	120	422.15	55	194.20
1945 – 1969	79	378.33	87	372.51	68	224.70
1970 –1979	94	471.77	116	426.66	85	250.60
1980 – 1989	137	327.37	86	251.17	74	180.60
1990 – 1999	107	247.99	171	196.02	72	112.10
2000 - 2009	122	230.78	69	113.47	73	90.30
2010 – 2020	103	149.14	93	119.71	72	48.90

Table 17: Peak Heating and Peak Cooling Load of the typical detached dwellings in France

Detached	
Peak Heating (kW)	

Year	H1	H2	H3
Pre – WWII	8.72	9.16	8.63
1945 – 1969	7.42	7.79	7.34
1970 –1979	9.25	9.72	9.15
1980 – 1989	6.42	6.74	6.35
1990 – 1999	4.86	5.11	4.81
2000 - 2009	4.52	4.75	4.48
2010 – 2020	2.92	3.07	2.89
Peak Cooling (kW)			
Year	H1	H2	H3
Pre – WWII	5.87	7.74	5.56
1945 – 1969	4.99	6.58	4.73
1970 –1979	6.23	8.21	5.9
1980 – 1989	4.32	5.7	4.09
1990 – 1999	3.27	4.32	3.1
2000 - 2009	3.05	4.02	2.88
2010 – 2020	1.97	2.6	1.86

Table 18: Peak Heating and Peak Cooling Load of the typical semi-detached dwellings in France

Semi-Detached			
Peak Heating (kW)			
Year	H1	H2	H3
Pre – WWII	8.27	8.7	8.19
1945 – 1969	7.3	7.67	7.23
1970 –1979	8.36	8.79	8.28
1980 – 1989	4.92	5.17	4.87
1990 – 1999	3.84	4.04	3.8
2000 - 2009	2.22	2.34	2.2
2010 – 2020	2.35	2.47	2.32
Peak Cooling (kW)			
Year	H1	H2	H3
Pre – WWII	5.57	7.35	5.28
1945 – 1969	4.92	6.48	4.66
1970 –1979	5.63	7.42	5.33
1980 – 1989	3.32	4.37	3.14
1990 – 1999	2.59	3.41	2.45
2000 - 2009	1.5	1.97	1.42
2010 – 2020	1.58	2.08	1.5

Table 19: Peak Heating and Peak Cooling Load of the typical flats in France

Flats			
Peak Heating (kW)			
Year	H1	H2	H3
Pre – WWII	3.81	4.00	3.77
1945 – 1969	4.40	4.63	4.36
1970 –1979	4.91	5.16	4.86
1980 – 1989	3.54	3.72	3.50
1990 – 1999	2.20	2.31	2.18
2000 - 2009	1.77	1.86	1.75
2010 – 2020	0.96	1.01	0.95
Peak Cooling (kW)			

Year	H1	H2	H3
Pre – WWII	2.56	3.38	2.43
1945 – 1969	2.97	3.91	2.81
1970 –1979	3.31	4.36	3.13
1980 – 1989	2.38	3.14	2.26
1990 – 1999	1.48	1.95	1.40
2000 - 2009	1.19	1.57	1.13
2010 – 2020	0.65	0.85	0.61

2.2.2.5 Italy

The residential buildings in Italy were grouped in six different time periods (pre-WWII, 1945 – 1960, 1961 – 1975, 1976 – 1990, 1991 – 2005 and 2006-2020) and three different typologies (detached dwellings, semi-detached dwellings and flats), whilst there are no defined climatic zones. Results are presented in Table 20 below.

Table 20: Heat Loss Coefficient, Peak Heating and Peak Cooling load for the typical detached dwellings, semi-detached dwellings and flats in Italy

Detached				
Year	Area (m2)	HLC (W/K)	Peak Heating (kW)	Peak Cooling (kW)
Pre-WWII	123	623.67	12.47	7.48
1945 – 1960	162	780.21	15.6	9.36
1961 – 1975	156	784.05	15.68	9.41
1976 – 1990	199	687.31	13.75	8.25
1991 – 2005	172	498.61	9.97	5.98
2006 - 2020	174	410.96	8.22	4.93
Semi-Detached				
Year	Area (m2)	HLC (W/K)	Peak Heating (kW)	Peak Cooling (kW)
Pre-WWII	116	482.75	9.66	5.79
1945 – 1960	111	433.12	8.66	5.20
1961 – 1975	89	377.35	7.55	4.53
1976 – 1990	125	399.71	7.99	4.80
1991 – 2005	111	319.41	6.39	3.83
2006 - 2020	127	300.85	6.02	3.61
Flats				
Year	Area (m2)	HLC (W/K)	Peak Heating (kW)	Peak Cooling (kW)
Pre-WWII	60	225.7	4.51	2.71
1945 – 1960	76	283.0	5.66	3.40
1961 – 1975	46	170.5	3.41	2.05
1976 – 1990	58	192.4	3.85	2.31
1991 – 2005	87	224.2	4.48	2.69
2006 - 2020	82	187.5	3.75	2.25

2.2.2.6 Spain

The residential buildings in Spain were grouped in five different time periods (pre-1936, 1937 – 1959, 1960 – 1979, 1980 – 2006 and 2007 – 2020) and three different typologies (detached, semi-detached and flats). According to Tabula, three climatic zones are defined in Spain, namely Mediterranean, Continental and Atlantic. However, the database is still incomplete for this country and therefore only one zone (continental) for which reasonable data were derived, is considered in the current analysis. Results are presented in Table 21 below.

Table 21: Heat Loss Coefficient, Peak Heating and Peak Cooling load for the typical detached dwellings, semi-

detached dwellings and flats in Spain

Detached				
Year	Area (m2)	HLC (W/K)	Peak Heating (kW)	Peak Cooling (kW)
Pre – 1936	129	302.17	6.77	5.23
1937 – 1959	780	1103.48	24.72	19.09
1960 – 1979	171	385.03	8.62	6.66
1980 – 2006	163	174.02	3.9	3.01
2007 – 2020	119	123.65	2.77	2.14
Semi-Detached				
Year	Area (m2)	HLC (W/K)	Peak Heating (kW)	Peak Cooling (kW)
Pre – 1936	224	536.59	12.02	9.28
1937 – 1959	59	251.25	5.63	4.35
1960 – 1979	251	349.72	7.83	6.05
1980 – 2006	162	166.01	3.72	2.87
2007 – 2020	143	76.84	1.72	1.33
Flats				
Year	Area (m2)	HLC (W/K)	Peak Heating (kW)	Peak Cooling (kW)
Pre – 1936	108	181.0	4.05	3.13
1937 – 1959	89	156.6	3.51	2.71
1960 – 1979	107	140.4	3.14	2.43
1980 – 2006	134	78.3	1.75	1.35
2007 – 2020	96	56.0	1.26	0.97

2.2.3 Methodology for determining the domestic hot water requirements

The energy demand for hot water Q_{dhw} has been estimated by the calorimetry equation:

$$Q_{dhw} = \rho \cdot V \cdot c_p \cdot N_{d,m} \cdot (T_{dhw} - T_{ws}) \quad \text{Equation 2}$$

Where T_{ws} is the water supply temperature to the building, which for this case has been assumed equal to the average monthly ground temperature at 0.5m and has been acquired from the TMY files repository ("Climate.OneBuilding,") for a representative metering station of each country and zone (where this is possible). All the considered in these calculations water supply temperature values are summarized in the Annex. Finally, $N_{d,m}$ is the number of days for the *m* month. The other parameters are:

- Volume of hot water per day per person: V=60L
- Hot water temperature: T_{dhw}=60°C
- Water special thermal capacity Cp=4.18 kJ/(kg ·K)
- Water density ρ=1kg/L

The application of the above mentioned equation for the countries of Greece, France, Italy, Hungary, Germany and Spain and their Climatic zones are presented in the following tables (Table 22 to Table 27, respectively).

Table 22: Monthly Energy Demand for DWH for Greece

Monthly Energy Demand (kWh/person)				
Month	Zone A	Zone B	Zone C	Zone D
January	100.90	115.78	113.97	106.88
February	92.27	101.77	109.51	102.82
March	99.93	106.58	123.23	115.71
April	93.34	97.58	117.60	110.39
May	87.34	89.93	111.70	104.70
June	77.73	81.49	97.44	91.17
July	75.59	82.61	90.34	84.33

August	74.14	85.52	82.84	77.16
September	74.13	89.26	78.06	72.67
October	82.05	100.62	84.18	78.44
November	86.46	105.36	89.66	83.75
December	96.11	114.31	103.34	96.75

Table 23: Monthly Energy Demand for DWH for Hungary

Monthly Energy Demand (kWh/person)	
January	126.28
February	115.89
March	124.70
April	115.22
May	104.31
June	89.91
July	85.24
August	82.91
September	84.08
October	95.72
November	104.06
December	118.50

Table 24: Monthly Energy Demand for DWH for Germany

Monthly Energy Demand (kWh/person)								
Month	CR1	CR2	CR3	CR4	CR5	CR6	CR7	CR8
January	118.98	118.89	110.12	120.10	117.55	124.27	125.20	112.26
February	112.32	112.63	107.15	113.86	110.88	117.27	114.48	108.81
March	125.82	126.28	123.86	127.68	124.18	131.35	123.99	126.86
April	120.53	120.89	121.39	122.20	118.98	125.84	115.77	125.90
May	117.29	117.08	122.30	118.24	115.91	122.52	108.26	131.07
June	105.65	104.79	111.52	105.71	104.56	110.44	96.29	122.91
July	101.53	100.04	106.47	100.75	100.62	106.19	93.58	120.14
August	95.98	94.05	97.88	94.61	95.26	100.45	91.79	111.94
September	91.33	89.33	89.14	89.83	90.66	95.60	91.79	101.49
October	96.97	95.11	90.75	95.72	96.21	101.46	101.66	100.96
November	99.90	98.59	91.06	99.34	98.98	104.48	107.18	97.79
December	111.14	110.42	101.05	111.42	109.95	116.15	119.19	105.11
Monthly Energy Demand (kWh/person)								
Month	CR9	CR10	CR11	CR12	CR13	CR14	CR15	
January	127.74	131.46	131.85	121.89	122.50	124.29	131.59	
February	116.77	115.54	124.12	111.62	116.40	113.78	120.34	
March	126.56	121.03	138.93	120.60	130.62	122.97	130.34	
April	118.34	110.81	133.17	112.19	124.94	114.47	121.74	
May	111.14	102.17	130.10	103.69	120.51	106.02	113.99	
June	99.21	92.59	117.73	91.21	107.28	93.42	101.47	
July	96.71	93.88	113.71	87.88	101.81	90.17	98.70	
August	94.94	97.16	107.96	85.95	95.24	88.22	96.82	
September	94.8	101.41	102.87	86.38	90.31	88.57	96.79	
October	104.64	114.27	109.00	96.58	96.41	98.87	107.10	
November	109.91	119.63	111.77	102.93	100.49	105.19	112.82	
December	121.87	129.77	123.68	115.46	113.19	117.83	125.37	

Table 25: Monthly Energy Demand for DWH for France

Monthly Energy Demand (kWh/person)			
Month	Zone H1	Zone H2	Zone H3
January	104.51	115.78	105.43
February	100.81	101.77	100.60
March	115.97	106.58	112.99
April	113.51	97.58	107.99
May	114.68	89.93	103.56
June	105.25	81.49	91.52
July	101.44	82.61	86.13
August	94.25	85.52	80.02
September	86.55	89.26	75.70
October	88.31	100.62	81.10
November	88.16	105.36	85.19
December	96.90	114.31	96.75

Table 26: Monthly Energy Demand for DWH for Italy

Monthly Energy Demand (kWh/person)	
January	110.21
February	96.85
March	101.46
April	92.88
May	85.63
June	77.58
July	78.66
August	81.42
September	84.98
October	95.78
November	100.28
December	108.80

Table 27: Monthly Energy Demand for DWH for Spain

Monthly Energy Demand (kWh/person)	
January	117.77
February	102.78
March	106.06
April	95.53
May	84.85
June	75.05
July	75.55
August	79.24
September	84.96
October	98.46
November	105.44
December	115.89

2.2.4 Relevance to the energy needs of MiniStor project demo sites

The previously presented information regarding the peak heating and cooling loads of representative dwellings in several EU countries, are summarized in Figure 4 and Figure 5 respectively. In order to enhance

the figures comprehensiveness, average values of detached, semi-detached houses and flats energy needs are provided for the various climatic zones in the cases of Greece, France and Germany. As it can be observed, the general pattern concerns a decrease of thermal loads in buildings of newer construction. In addition, the detached dwellings in all examined countries tend to present increased energy needs compared to the semi-detached ones, whereas the flats seem to be the less energy intensive dwellings. For buildings built after 1980 (all MiniStor demo sites were constructed after that year as explained below), the peak heating needs are in the range of 2.8 – 14.4 kW for detached dwellings, 1.8 – 8 kW for semi-detached ones and 1 – 6.9 kW for flats. The corresponding peak cooling demands are in the range of 1.6 – 12.6 kW, 1.3 – 4.8 kW and 0.3 – 5.8 kW respectively.

Figure 4: Peak heating loads in all examined building types and countries

Figure 5: Peak cooling loads in all examined building types and countries

Regarding the buildings where MiniStor system will be demonstrated, Cork demo site involves a semi-detached two-storey dwelling constructed in 1980. Its peak heating load as estimated in the framework of D3.1 is around 3.8 kW. In Kimmeria, MiniStor will supply heat and cold to five rooms of a student residences

building constructed in 1997. Their cumulative peak heating and cooling needs were approximated to be in the range of 6.6 kW and 5.8 kW respectively. In the case of Sopron, a newly (2019) built and highly insulated single-family house (including two floors and a cellar) will be used for demonstration activities, with estimated heating and cooling needs equal to 4 kW and 8.1 kW accordingly. In Thessaloniki pre-pilot, MiniStor will feed a large room of a demonstration platform shaped like real house and constructed in 2017. Its heating and cooling needs were approximated in D3.1 to 3.6 kW and 8.1 kW respectively. However, it should be underlined that cooling demand in the cases of Sopron and Thessaloniki was considerably shaped by devices and solar irradiance heat gains. Finally, in the case of Santiago de Compostela an apartment located in a student residence building of the city university will be used for MiniStor demonstration. Its maximum heating needs are estimated in Chapter **Error! Reference source not found.** to around 5.2 kW.

It is evident that the estimated peak heating loads of the project demo sites are well within the defined load ranges of the corresponding dwelling types for buildings constructed after 1980. The demo sites' cooling needs approximations exceed the statistically defined values, but this is mainly owed to the limitations of the method used for the latter process and load calculations. Consequently, the MiniStor performance assessment in terms of heating and cooling needs coverage to be conducted in the framework of the project activities along with any corresponding findings, can fairly be considered valid for the majority of recently constructed dwellings in the examined countries.

3 Methods to integrate MiniStor with RES systems

3.1 Identification of RES suitable for integration with MiniStor system

One of the main advantages of MiniStor energy storage system is its ability to utilize renewable energy as energy source. In this way, it can provide sustainable heating, cooling and electricity to residential buildings, decrease their consumption through the advanced energy management system it incorporates along with its high COP, generate energy cost savings and reduce the corresponding GHG emissions. Therefore, it can contribute to the increase of energy efficiency in the residential sector and the achievement of the EU Energy Policy targets.

Another important characteristic of MiniStor is the compactness of the used storage materials (< 0.72 m^3 as defined by KPI_1 in Deliverable 6.1 "Design of the monitoring system and KPI definition"). This is achieved by the increased energy storage density of the system (182 kWh/m^2 as defined by KPI_7), which is mainly determined by the density of the utilized thermochemical material. The latter is in turn defined by the activation and the degree of advancement of the involved chemical reactions. Thus, there is a requirement for delivering heat to the TCM reactor at a quite high temperature and more specifically above 55 °C. For this reason, the heat supply to the reactor is activated when a heat-source outlet temperature of 60 °C is achieved.

Apart from the above described temperature requirement, the energy source of MiniStor should also be suitable for installation in residential buildings, considering the space limitations, safety requirements and microclimatic conditions that characterize urban environments. Taking also this information into account, the RES technologies identified as most suitable for integration with MiniStor system are the following:

- Hybrid photovoltaic thermal panels (PVTs), possibly combined with solar thermal collectors
- Photovoltaic panels (PVs) in combination with heat pumps (HPs).
- Biomass boilers.

In the next paragraphs, the combination of each technology with MiniStor is discussed, while at the end of paragraph 3.1 the pros and cons of each option are summarized.

3.1.1 Integration of hybrid photovoltaic thermal panels and solar thermal collectors

Photovoltaic thermal systems are hybrid modules comprising of "regular" photovoltaic panels integrated into solar thermal collectors and thus simultaneously producing electricity and heat (Hasan & Sumathy, 2010). This is achieved by recovering part of the waste heat produced by PVs and utilising it for covering various thermal needs. Additionally, the cooling of the PV module has positive effects on its electrical

efficiency, as the latter decreases when the PV cell temperature increases (Tyagi, Kaushik, & Tyagi, 2012). The main PVTs advantages are:

- The same system is able to produce both heat and electricity, resulting in a cost-effective utilization of solar energy (Hasan & Sumathy, 2010).
- Generation of higher amounts of thermal and electrical energy compared to a combination of conventional PVs and non-hybrid solar thermal collectors of equal sizes and matching combined area (Zondag et al., 2002). Reported overall efficiency is in the range of 60% - 80% (Bergene & Løvvik, 1995; Chow, 2003; Robles-Ocampo et al., 2007)
- It presents flexibility and wide application potential, especially in residential building sector (Hasan & Sumathy, 2010)

There are several PVT designs utilising different heat-removal fluids and / or materials for the construction of the PV modules. In general, the currently available PVTs can be classified in the following categories (Hasan & Sumathy, 2010):

- Liquid PVT collectors
- Air PVT collectors
- Ventilated PVs with heat recovery
- PVT concentrator

Liquid PVT collectors are similar to conventional solar thermal flat-plate collectors, utilising a liquid substance (usually water or a mixture of it) for removing heat from the PV module. They are grouped into four main categories (Zondag et al., 2002): sheet-and-tube collectors, channel collectors, free-flow collectors, and two-absorber collectors. Air PVT collectors utilise air for heat removal and their function presents many similarities with conventional solar air heaters. An advantage of this type compared to the previous one is the avoidance of fluid boiling or freezing during severe weather conditions, along with a diminished danger for damages in case of a leakage. On the other hand, due to the properties of air they present low heat transfer rates, require higher volume flow rates of fluid, whereas heat losses can be significant in the case of air leakage. Both liquid and air PVT collectors are characterised as glazed or unglazed, depending on the existence or absence of an absorber-covering glass respectively. In general, glazed panels have lower thermal losses than the unglazed ones, at the expense of lower electricity output (Hasan & Sumathy, 2010).

Ventilated PVs with heat recovery, are practically PV facades or rooftop PVs with an air gap at the rear for cooling purposes that utilise the heat of this air stream for covering thermal needs of the building. Finally, PVT concentrators utilize reflectors to concentrate solar radiation in a limited area, where its transformation into useful heat and electricity takes place. In general, this type can yield hot water of higher temperature compared to the flat-plate design (Tyagi et al., 2012), achieving higher efficiencies, but it has increased cooling requirements of PV material (Hasan & Sumathy, 2010). To conclude, PVTs seem ideal for residential building applications, where space for panel (PV, conventional solar thermal or PVT) installation is limited, as they can efficiently cover both electrical and heating needs in a sustainable way. Figure 6 summarizes the main categories of solar energy converting collectors.

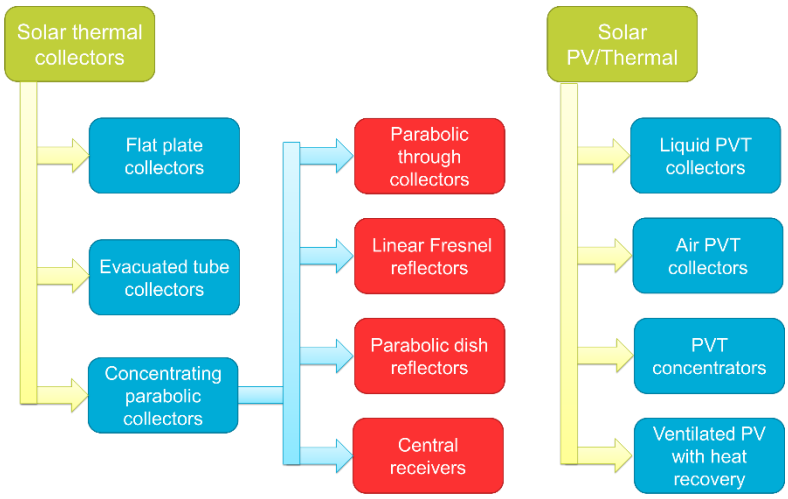

Figure 6: Main types of solar thermal collectors and PVTs (adapted from (Tyagi et al., 2012))

Although the PVTs are able to supply sufficient heat for regular residential applications (i.e. DHW production) all year round, they might not be capable of providing the needed amount of energy and at the high temperatures required by the TCM reactor during winter. In that case, the PVTs can be combined with conventional solar thermal collectors, as the latter present high thermal efficiency utilising both beam and diffusive solar radiation, without the need of solar tracking (Duffie & Beckman, 2013). Their most common type is the flat plate collector (FPC). They are usually used in low or medium temperature applications (< 100 ^{o}C) and mainly consist of a solar energy absorbing plate and attached structures (tubes, passages, channels etc.) in which the HtF flows. Insulation layers along with transparent covers of the absorber are used in order to reduce the convective and radiative heat losses (Tyagi et al., 2012).

Other types of solar thermal collectors are the evacuated tube collectors (ETC) and the concentrating ones. The first design achieves higher efficiencies than FPCs at temperatures higher than 80 ^{o}C, by combining vacuum insulation with selective surface coating materials of the absorber (Tyagi et al., 2012). The latter consists of several long and narrow segments that are place along with the attached tubes within evacuated glass envelopes. The low-pressure conditions inside the envelopes lead to significantly decreased heat losses (Duffie & Beckman, 2013). Another characteristic of the ETC type is that the heat-transfer fluid evaporates during the absorption of solar energy and condenses when this energy is rejected, thus experiencing a constant evaporating-condensing cycle. In applications involving very high temperatures, concentrating collectors are used. These are categorized into parabolic through collectors (PTCs), linear Fresnel reflectors (LFRs), central receivers and parabolic dish reflectors (PDRs). Their general operating principle involves the concentration of solar radiation, through reflection of refraction, into an area quite limited compared to the aperture one. This is achieved by using lens or mirroring surfaces and leads to reduced losses, higher HtF induced temperatures and lower per absorber unit area cost compared to FPCs or ETCs. On the other hand, they usually require solar tracking mechanisms as they mainly utilise only the beam solar radiation (Tyagi et al., 2012).

The initial plan for MiniStor demonstration activities involved the utilization of liquid-based PVT panels for providing the necessary energy to the TCM reactor. Thus, in the framework of Task 3.3 and as described in the corresponding deliverable “D3.4 Design and integration of improved PVT electrical generation system”, EndeF modified the designs of two liquid-based PVT models currently produced by the company (one glazed and one unglazed), implementing several improvements in various layers of the collector (i.e. absorber design, its integration with PV laminates, the characteristics of the latter etc.). The improved prototypes, along with those of a completely new design (transparent PV laminate glazed and unglazed) were tested and glazed prototypes proved to be more suitable for integration with MiniStor due to their higher thermal output. However, the PVTs electricity yield should not be very low as there are specific voltage thresholds imposed by the inverters available in the market. Therefore, a glazed prototype based on the commercial model Ecomesh is selected due to its balanced thermal and electrical outputs, with obtained overall efficiency up to 80%.

Because of the space limitations in the demo sites, the PVTs have to be combined with solar thermal collectors in order to meet the temperature requirements of the TCM unit in winter. Commercial off-the-shelf FPC and ETC models were considered and their output was numerically investigated in the context of Task 3.1, resulting in small differences in terms of thermal output between the two types. Finally, the FPC design was chosen as this it presents simpler construction, robustness, lower maintenance requirements and cost than ETCs. Therefore, a combination of PVTs and FPCs will be installed in the Thessaloniki pre-pilot, as well as the Sopron and Cork demo sites as described in D3.8 “Design of the electrical storage system”, with the collectors’ area in each case being displayed in Table 28. The solar field is accompanied by several auxiliary components usually used in solar applications such as:

- Water tank, which will act as a buffer between the reactor and the collectors’ outlet, mitigating the oscillations of fluid temperature at the latter point. Its temperature will be utilised for the control of the circulating pumps’ operation (both of the solar field pump and the pump circulating HtF to the TCM unit), whereas a back-up heater (i.e. in the form of electrical resistance) can be installed inside it.
- Pump, for circulating the HtF between the collectors and the tank
- Air dissipator that will protect the collectors from increased temperature and over-pressure by rejecting excess heat to the ambient.

- Differential control of the solar circuit along with the necessary sensors and actuators.
- Hybrid inverter, responsible for managing the electrical energy flows between the PVTs, the battery and MiniStor system as well as for DC-AC power conversion.
- Electrical battery, enabling the storage of produced electricity by the PVTs.
- Electrical panel and wiring, housing all the necessary protections of the electrical circuit and connecting its main elements.

Table 28: Total area of PVTs and FPCs foreseen to be installed in MiniStor demo sites

Demo site	Total absorber area of PVTs (m^2)	Total absorber area of FPCs (m^2)	Configuration
Thessaloniki pre-pilot	15.50	11.55	Group 1: PVTs in parallel Group 2: FPCs in parallel Group 1 & Group 2 in series
Sopron	13.95	13.86	Group 1: PVTs in parallel Group 2: FPCs in parallel Group 1 & Group 2 in series
Cork	9.30	7.20	Group 1: PVTs in parallel Group 2: FPCs in parallel Group 1 & Group 2 in series

3.1.2 Integration of photovoltaic panels combined with heat pump

The basic idea of this configuration is similar to the previous one, i.e. the utilization of solar radiation for feeding the MiniStor system. Its major difference is the conversion of solar energy solely into electricity instead of a combination of thermal and electrical energy. This can be achieved by utilising conventional PVs, comprising of cells that generate DC current by exploiting the energy of photons through the photovoltaic effect (Shubbak, 2019). The main technologies of PV cells, depicted also in Table 29, are commonly classified as following:

- First generation cells, mainly referring to various crystalline silicon wafer-based cells (monocrystalline, polycrystalline, heterojunction with intrinsic thin layer (HIT), and microcrystalline)
- Second generation cells that include thin-film cells utilizing PV materials such as cadmium telluride (CdTe), cadmium sulphide (CdS), copper indium gallium di-selenide (CIGS) and amorphous silicon (a-Si). Single-junction gallium arsenide (GaAs) cells are also a variation of thin-film cells, but are usually considered a distinct category due to their different electronic behaviour.
- Third generation cells. This category concerns multi-junction cells, used almost exclusively in space applications, as well as technologies still in research stage such as organic polymer-based cells, Perovskites, and dye-sensitized solar cells (DSSC).

Nowadays, first generation cells, namely multi-crystalline and poly-crystalline silicon-based ones, dominate civil applications with a market share of around 93% (Freitas Gomes, Perez, & Suomalainen, 2020). They also present higher efficiencies than thin-film cells, up to 22.3% for polycrystalline and 27.6% for monocrystalline cells, but on the other hand involve high economic and environmental cost.

Table 29: Main technologies of solar PV cells (adapted from (Shubbak, 2019))

Cell technology	Max. Efficiency (%)	Market share (%)	Application
1st generation			
Monocrystalline silicon	26.1 – 27.6	24	Civil
Polycrystalline silicon	22.3	69	Civil
HIT	26.6	< 1	Civil
Microcrystalline silicon	21.2		Civil
2nd generation (thin-film)			
CIGS	22.9 – 23.3	< 2	Civil
CdTe	22.1	3	Civil

Amorphous silicon	14	3	Civil
GaAs	29.5 – 30.1		Space
3rd generation			
Multi-junction	46		Space
Organic	15.6		Research
DSSC	11.9		Research
Perovskite	24.2 – 28		Research

The electrical energy produced by the PVs is fed to an air-to-water heat pump. This is a combination currently being on the focus of scientific research, especially regarding its potential application in residential buildings. Several numerical (Beck et al., 2017; Bellos et al., 2016) and experimental (Aguilar, Aledo, & Quiles, 2016; Franco & Fantozzi, 2016; Litjens, Worrell, & van Sark, 2018) studies have been conducted, assessing its ability (in some cases combined with electrical storage) to provide self-sufficiency in terms of electricity, space heating and / or DHW generation, to promote the concept of Nearly Zero Energy Buildings (NEZBs) and to reduce the corresponding GHG emissions of residential sector. The concept of PVs – HP integration is also investigated in the framework of European Research projects such as SunHorizon[4].

The utilised in the current application HP should be able to operate efficiently at relatively low ambient temperatures so as to be able to charge uneventfully the TCM reactor under such weather conditions. In addition, its condensing conditions should comply with the reactor temperature charging requirements, i.e. the water discharge should be as high as 60 °C. The first precondition is more easily met by two- or generally multi-stage heat pumps, as this type mitigates the disadvantages of single-stage ones at low ambient temperatures (namely insufficient heat output, compressor overheating, decrease of COP, need for cycling at high temperatures if the design point is close to low ambient temperature values (Bertsch & Groll, 2008)). Multi-stage HPs can be of compound design, i.e. having the compression stages connected in series, or of cascade one which involves two separate refrigeration cycles exchanging heat via an intermediate heat exchange (Chua, Chou, & Yang, 2010). The latter concept enables the utilisation of different refrigerants in each cycle, offering high flexibility. Regarding the temperature heat sink requirement imposed by the TCM, there are several commercial HP models able to supply heat sink temperatures from 90 °C up to 165 °C and characterized as high or very-high temperature heat pumps (HT / VHT-HPs). However, they are mainly oriented to industrial applications, whereas their minimum capacity in the range of 20 kW (Arpagaus et al., 2018) makes them unsuitable for integration with Ministor. On the other hand, the majority of residential heat pumps can supply hot water in the range of 40 – 60 °C (Zhang et al., 2016). This means that MiniStor requirements are at the upper limit of the aforementioned temperature interval, which may imply a non-efficient heat supply or even a limited ability of operation. Nevertheless, during the recent years several air-to-water HP models have been introduced, capable of supplying efficiently the required heat sink temperature and oriented for domestic use.

Alternatively, to the utilisation of conventional PVs, unglazed PVTs can be used. As discussed in the previous paragraph, this type of PVTs presents lower thermal efficiency and higher electrical one. Nevertheless, it maintains the advantage of dual generation capability, which can be very useful for covering low-temperature thermal needs of buildings. Therefore, a configuration of unglazed PVTs with a heat-pump will be installed in Santiago de Compostela demo site. The exact number of collectors along with the specifications of the HP and all the other auxiliary components are to be defined within the framework of Task 3.4. Preliminary estimations regard a number of 20 PVTs, as adequate for providing the necessary electricity to the heat pump. Their total absorber area will be equal to 33m^2 and they will be arranged in two groups to be connected in series (10 PVTs per group connected in parallel).

A further future development of this concept would be the adoption of the solar-assisted heat pump (SAHP) scheme. In a wider definition, as SAHPs can be characterised all the techniques aiming to use solar energy for reducing the HP primary energy consumption (Buker & Riffat, 2016). In the current case, more suitable seems the concept which involves the utilisation of solar radiation as the evaporating heat source. Several relevant studies have been published recently exploring numerically (Chow et al., 2010; Safijahanshahi & Salmanzadeh, 2019), experimentally (Ji et al., 2008; Kuang & Wang, 2006) or with both methods (Hawlader,

[4] https://www.sunhorizon-project.eu/

Rahman, & Jahangeer, 2008; Ji et al., 2009) the performance of such SAHPs schemes in water heating applications. These schemes concerned either direct expansion configurations where refrigerant circulates directly through the solar collectors or indirect expansion in which an intermediate heat exchanger is used to transfer heat form the solar circuit HtF to the HP refrigerant. Ambient heat can also be used as an additional heat source for evaporation (connected in parallel or in series with the solar source), increasing the configuration flexibility. The results of the aforementioned studies showed an increase of HP efficiency compared to conventional systems due to the increase of evaporating temperature (Chua et al., 2010), whereas the SAHP as a combined unit performed more efficiently than separate HP and solar systems (Chow et al., 2010; Ji et al., 2008). Therefore, this concept is worthy of consideration as a potential energy supply system for MiniStor.

3.1.3 Integration of biomass boilers

Biomass is regarded as a carbon-neutral energy source, because of the zero-net balance of CO_2 absorption and release into the atmosphere throughout the plants' growth and combustion cycle (Perea-Moreno, Manzano-Agugliaro, & Perea-Moreno, 2018). This fact combined with its worldwide availability, renders biomass as a key type of renewable energy for achieving the UN Sustainable Development Goals, defined in the context of 2030 Agenda (IEA Bioenergy, IRENA, & FAO, 2017). Within EU member states bioenergy is the main source of renewable energy, accounting for 59% of all renewables and 10% of the gross final energy consumption (Scarlat et al., 2019). The major share (75%) of bioenergy is directed to the heating and cooling sector, with biomass boilers being one of the main devices used for this energy conversion.

Commercially available small scale biomass boilers present efficiencies in the range of 73-89% based on the fuel gross calorific value (Hebenstreit et al., 2011). Despite of their lower efficiency compared to gas or oil-fired boilers, they present lower SOx and NOx emissions (Perea-Moreno et al., 2018). They are capable of delivering hot water suitable for both low and high temperature heating systems, i.e. up to 90 ^{o}C (Sarbu & Sebarchievici, 2017), well above the MiniStor temperature requirements. Thus, the integration of biomass boilers with MiniStor would be an attractive option especially in the case of large buildings, due to the high thermal inertia and the specific operating schedules of the corresponding heating systems. However, their operation is related to significant particle emissions (Gröhn et al., 2009). In condensing boilers, i.e. boilers that are equipped with a flue-gas condensing heat exchanger, the efficiency can be increased by 10-15%, based on the fuel low calorific value, depending on the fuel moisture, the air to fuel ratio and the heat sink temperature (Cornette et al., 2021; Hebenstreit et al., 2011). In addition, this type of boilers is characterised by lower emissions of particles and other harmful substances, such as sulphuric acid and chlorides, compared to the standard biomass boiler design (Chen et al., 2012). On the other hand, condensing boilers require low return water temperatures (in the range of 25-35 ^{o}C, (Chen et al., 2012; Hebenstreit et al., 2011)), which may hinder their integration with MiniStor.

A possible way to mitigate the disadvantages of biomass boilers is their combination with PVTs or solar thermal collectors. In this configuration the working medium to heat the TCM unit can be heated only by the solar systems in case of high solar radiation or preheated up to a certain point if the weather conditions are cloudy. In the latter case, the biomass boiler could supplement the solar system by providing the necessary temperature rise to meet the MiniStor requirements, resulting in limited GHG and particle emissions. Another advantage of this combination is that it renders the MiniStor charging process independent of the solar energy intermittent nature. On the other hand, the capital cost of the equipment used for providing energy input is increased. Thus, this concept could be very attractive in cases of dwellings already using biomass boilers in their heating system. In Kimmeria demo site, a system of similar operating principle is used for proving space heating and DHW to the student residencies buildings. It consists of a solar thermal park with area of 1889 m^2 and a 1.15 MW_{th} biomass boiler, while 4 hot water storage tanks of 10m^3 capacity each are used for thermal energy storage. In the framework of MiniStor demonstration activities, this system will supply heat to the TCM unit and it can be considered that the heat provision at the specified temperature level will be realised regardless of solar energy availability.

3.1.4 Strengths and weaknesses for each RES technologies

Except from the above-mentioned cases, MiniStor can be integrated with other RES technologies too. For instance, possible energy inputs could originate from: i) small wind turbines in combination with heat pump

or ii) from geothermal heat pumps either standalone or in combination with PVTs. However, the application of these technologies is case specific, as wind turbines can be potentially installed only in rural dwellings, whereas the implementation of geothermal heat pumps requires easy access to subsoil and presence of a low enthalpy geothermal resource. Information about the availability of geothermal resources throughout Europe is presented in paragraph 3.2.4, giving a sufficient picture of the potential use of this energy source. Finally, Table 30 summarises the main advantages and disadvantages of the previously described RES configurations and identified as suitable for integration with MiniStor.

Table 30: Main strengths and weaknesses of the RES systems suitable for integration with MiniStor

RES system	Main strengths	Main weaknesses
PVTs and solar thermal collectors	- Renewable energy source, covering both thermal and electric energy needs of MiniStor - No emissions of any nature (GHG, particle, NOx, SOx etc.) - No fuel supply is required - It can be combined with batteries for electricity storage, enabling DR schemes	- Operation of intermittent nature - Significant open space requirements for installation - MiniStor temperature requirements may be met with difficulty in days with limited solar radiation
PVs and heat pump	- No emissions of any nature (GHG, particle, NOx, SOx etc.) - No fuel supply is required - It can be combined with batteries for electricity storage, enabling DR schemes - HP could have dual operation, covering MiniStor heating needs and also being coupled with the building heating and / or cooling system - High flexibility as HP can utilise energy from the grid if necessary	- Operation of intermittent nature - Significant open space requirements for installation - In days with limited solar radiation, PVs may not be able to cover all electricity needs of the system - Higher cost compared to the utilization of only PVTs and solar thermal collectors
Biomass boiler	- Mature technology - Operation independent of weather conditions - MiniStor temperature requirements can be easily met - Limited space requirements - Easy integration and lower CAPEX if a biomass boiler already exists	- Significant particle emissions - Emissions of NOx and SOx (relevant to the fuel composition) - Requires constant fuel supply - It cannot offer electricity storage - Increased equipment cost if a biomass boiler is not already available - Regular boiler maintenance is necessary

3.2 Exploration of compatible with MiniStor RES utilisation throughout Europe

Renewable energy sources are playing a very important role in European Union policies for reducing negative impact on environment and reaching a net-zero CO2 emission economy. During last two decades share of renewables in energy production increases constantly, and now it is on the path to reach the target

of 32% of energy generation in 2030, according to European Commission plan set in 2018 ("Energy: new target of 32% from renewables by 2030 agreed by MEPs and ministers," 2018). Currently, in the entire European Union, share of RES in energy generation is approximately 34% in gross electricity production and 20.5% for heating and cooling purposes.

Within this framework, the analysis of suitable for integration with MiniStor system renewable energy systems would be very useful to start with indicating the share of RES in the energy production structure of each European country. A dedicated tool called SHARES (Eurostat, 2019) and provided by Eurostat gives a complete overview of the use of renewable energy in all EU member states, while harmonized methods are used for the corresponding statistical calculations. The RES shares in the energy production structures in 2019 for all 28 EU countries are presented in Figure 7 below and indicate quite large differences among them.

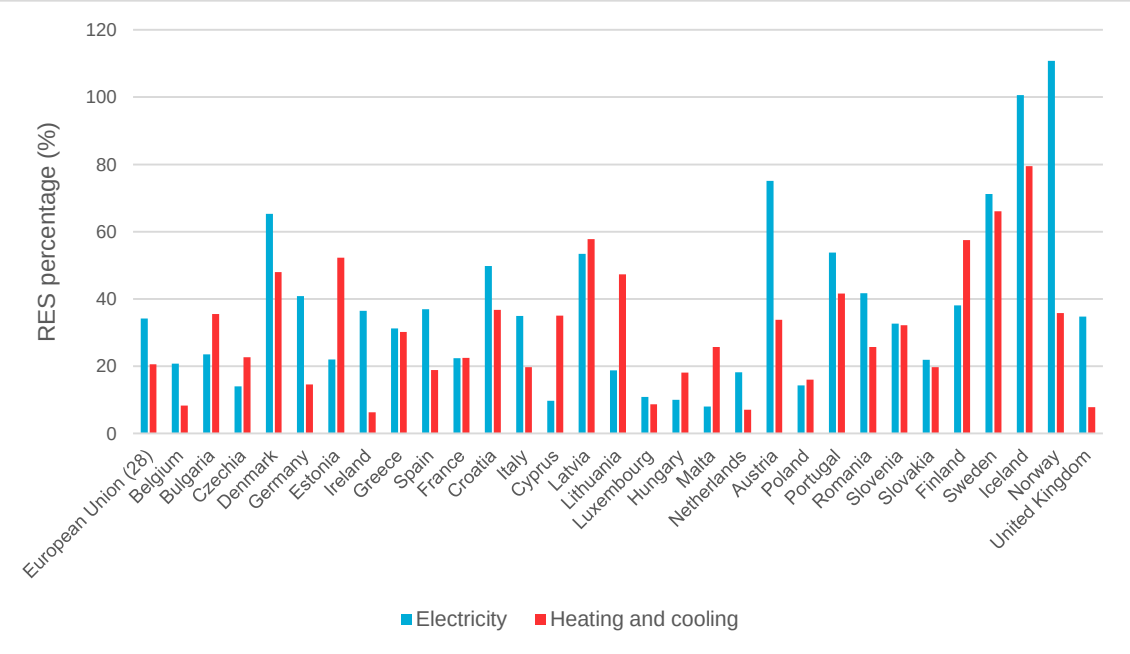

Figure 7: Share of energy from renewable sources in EU + UK for electricity and heating and cooling purposes (2019). Source: (Eurostat, 2019)

The above figure clearly shows that in terms of the share of renewable energy sources in the structure of energy production, both in the form of electricity and thermal energy, the Scandinavian countries - Iceland, Norway, Sweden and Denmark - present the highest values. In the case of thermal energy, the Baltic countries (Estonia, Latvia and Lithuania) also have high RES shares in the structure of its production (over 50%). On the other hand, Hungary, Poland, Luxemburg and Netherlands present the lowest RES penetration.

However, it should also be noted that the countries with significant RES share mentioned above present a relatively low absolute level of energy consumption, which results directly from their size and population. Therefore, particular attention should be paid to countries with high electricity and thermal energy consumption, such as Germany, France, Italy and the United Kingdom. In their case, the share of RES in the structure of electricity production ranges from 20% (France) to 40% (Germany), whereas regarding thermal energy, this share ranges from 8% (UK) to 22% (France).

From the point of view of integrating the MiniStor system with the existing RES installations throughout Europe, the investigation of RES structure per individual energy source is particularly important. As mentioned in previous subchapter, MiniStor is most suitable for use with PVT panels or solar collectors, photovoltaic installations and biomass boilers. The design of the system and its orientation towards covering the needs of residential buildings makes it more difficult to integrate with systems based on hydro or wind energy. The structure of the use of individual RES in the production of electricity and thermal energy in individual countries is presented below.

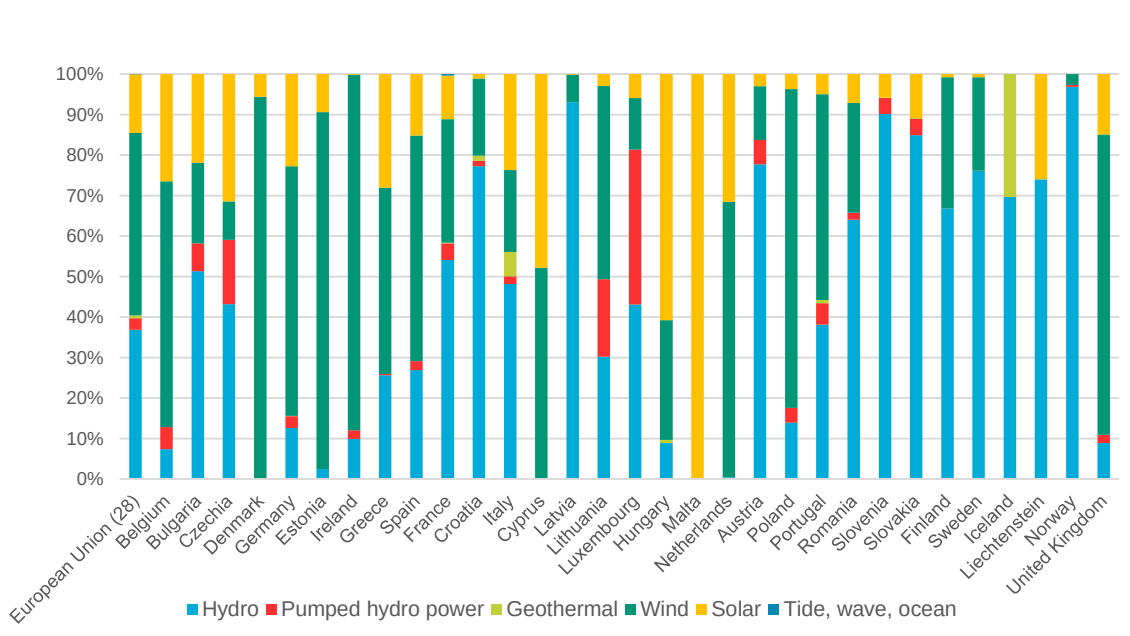

Figure 8: Structure of RES used in gross electricity production in EU countries in 2019 (excluding biofuels). Source: (Eurostat, 2019)

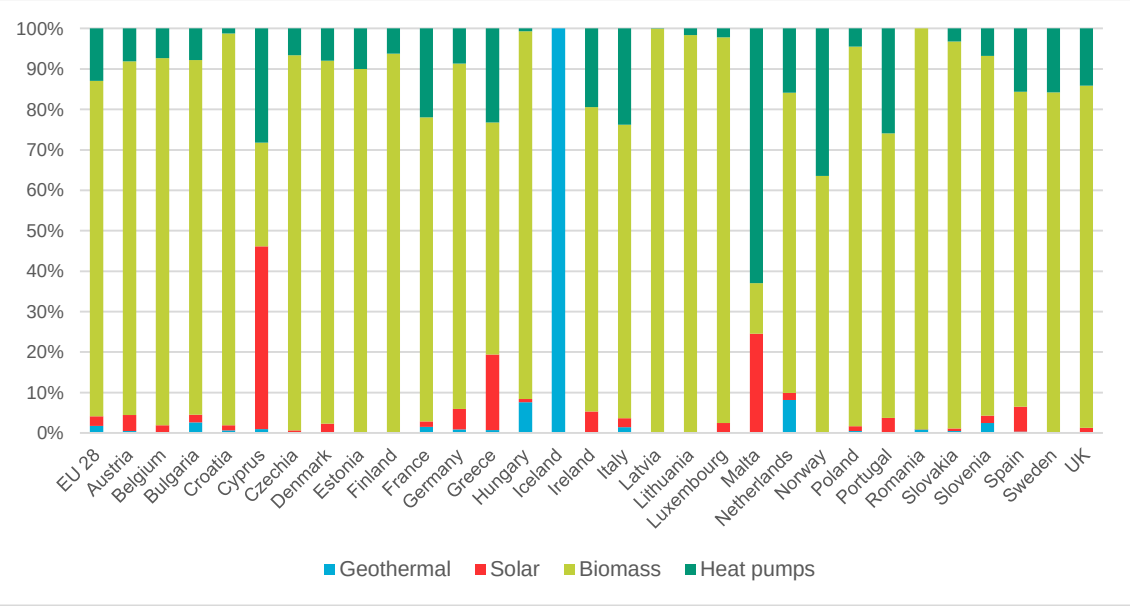

Figure 9: Structure of RES used in heat and cool production in EU countries in 2019. Source: (Eurostat, 2019)

The above diagrams show that in the case of electricity generation, the two dominant renewable energy sources in Europe are hydropower and wind energy. However, the share of solar energy is also significant and at EU-28 level it accounts for around 12.5% of the gross electricity produced from RES. In the case of renewable thermal energy, biomass combustion is by far the most common form of energy source, being total of over 80% of its production.

3.2.1 Solar Energy

3.2.1.1 Solar Thermal

Solar collectors and concentrating technologies account for only 2.4% of renewable thermal energy in the EU. They are mainly used for the production of domestic hot water. As shown in Figure 9, solar thermal

technology has a significant (higher than 20%) share in the structure of RES-based thermal energy production only in relatively small countries with very high solar radiation levels - Cyprus (47%), Malta (24%) and Greece (20%). A significant advantage of solar thermal technology in the context of integration with the MiniStor system is the fact that most installations of this type in Europe are residential ones. Therefore, there is wide experience in its use and combination with thermal energy storage devices in dwellings.

3.2.1.2 Photovoltaics

Photovoltaics is a much more common renewable energy technology that harvests solar irradiance. It is responsible for around 12.5% of all electricity produced in the EU from renewable energy sources. It is the dominant source of renewable electricity in Malta (97%, after considering the contribution of biofuels to RES-based electricity), whereas it presents significant shares in Cyprus (43%), Hungary (32%), Greece (26%), Netherlands (24%), Czech Republic and Belgium (in both cases around 22.5%).

Moreover, this field currently experiences a rapid growth, occurring since 2018. Thus, last two years there can be observed an increase in installed PV capacity by approximately 10% from year to year. This increase is due to a significant improvement in the lifetime of photovoltaic modules and a decrease in their prices. Currently, there is a 117 GW capacity of PV installations in the EU, and as much as 15.1 GW was installed only in 2019. The forecasts prepared by the IEA indicate that in 2024 the installed capacity of PVs in EU member states will exceed 200 GW (IEA, 2020). There are three main types of installations of photovoltaics: large-scale (utility) systems, commercial systems and residential systems. The current structure of the installed capacity in each type of this technology is presented in Figure 10.

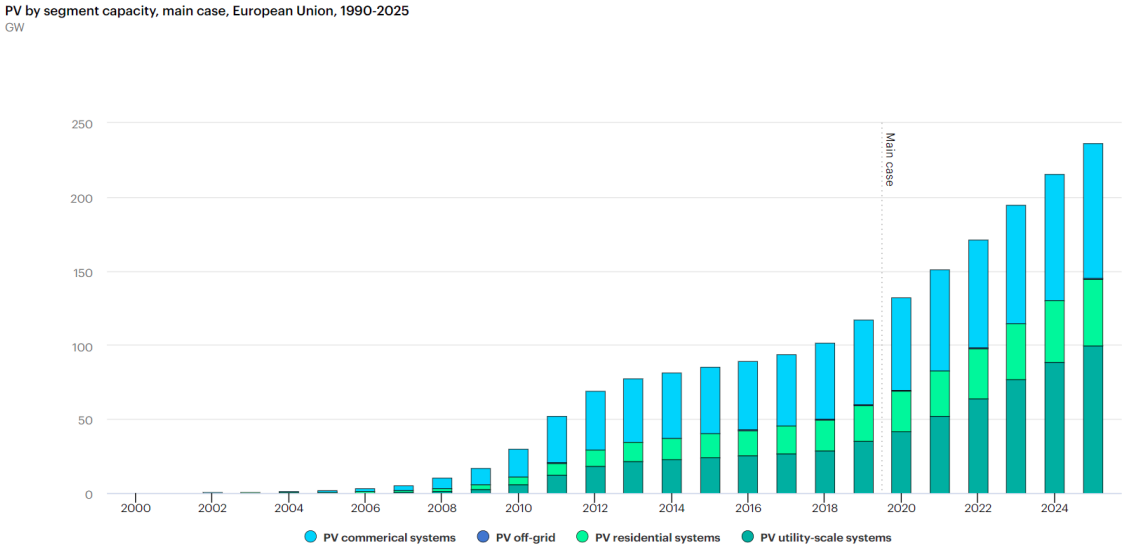

Figure 10: PV capacity installed in European Union (adapted from (IEA, 2020))

From the MiniStor point of view, residential systems are the most interesting group of installations. This is because when combined with heat pump of suitable heat sink, they can successfully provide MiniStor with the necessary energy input, as indicated in previous subchapter. The largest markets for residential PVs in Europe are Germany, Italy, the Netherlands and Belgium, as these countries present the highest installed capacities of this PV type. Currently, the total installed capacity of residential PVs is around 25 GW. Assuming an average installation size of about 6 kW, the total number of installations of this type can be over 40,000,000, revealing the widespread application of this technology.

In the case of the largest countries, it is also worth looking at the IEA's forecasts predicting increase in photovoltaic capacity in the coming years. Figure 11 - Figure 14 show the forecasted power annual increase in the next 5 years in Germany, Italy, France and United Kingdom respectively and for each group of PVs. The presented forecasts clearly show that residential PV technology will continue to be an attractive option for consumers and consequently there will be additional installations in homes in the coming years.

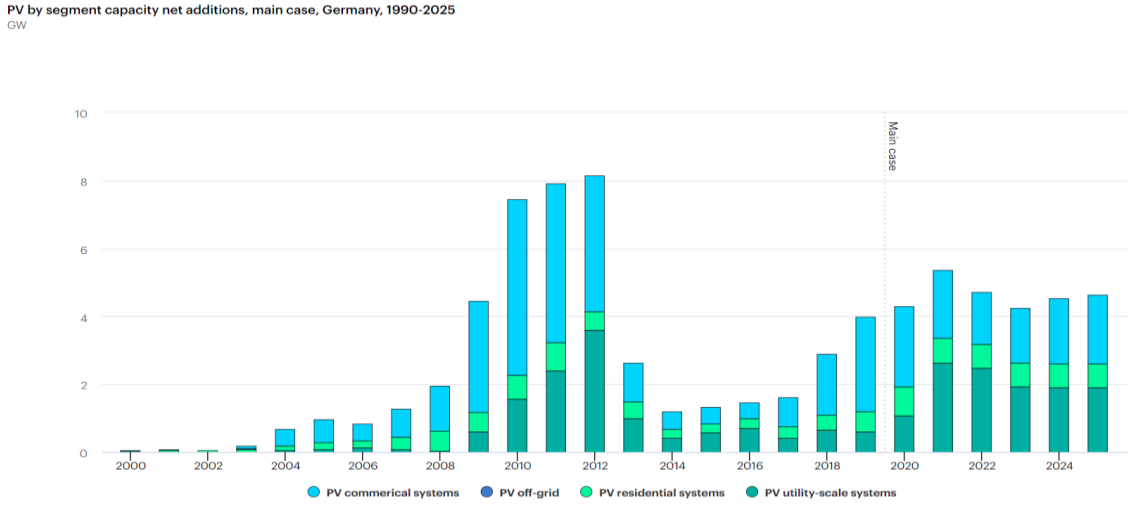

Figure 11: Historical and forecasted PV capacity net add-ons in Germany (adapted from (IEA, 2020))

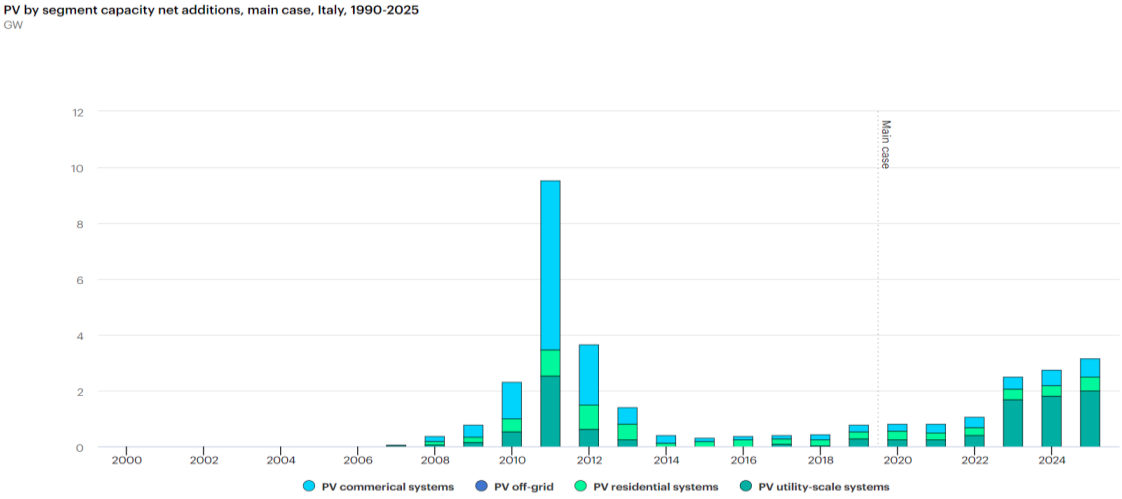

Figure 12: Historical and forecasted PV capacity net add-ons in Italy (adapted from (IEA, 2020))

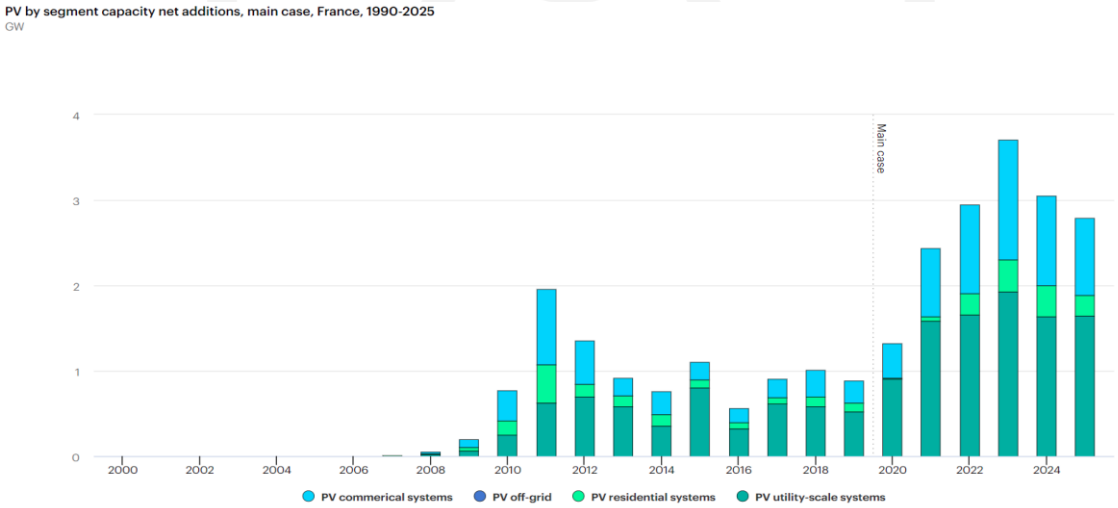

Figure 13: Historical and forecasted PV capacity net add-ons in France (adapted from (IEA, 2020))

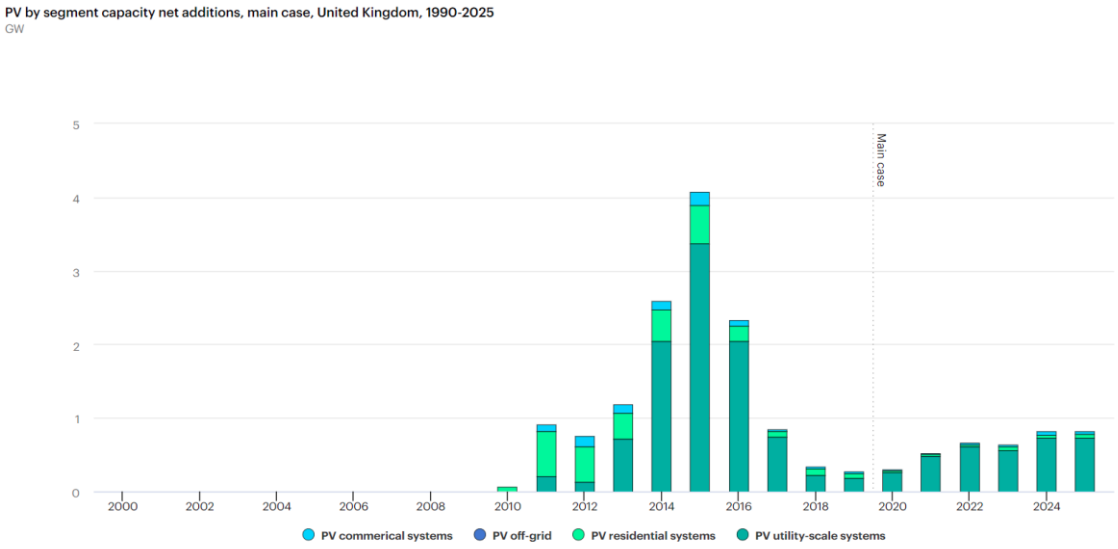

Figure 14: Historical and forecasted PV capacity net add-ons in United Kingdom (adapted from (IEA, 2020))

3.2.2 Heat Pumps

Photovoltaic systems, although they primarily provide electricity, can also be indirectly used for heating purposes. The most effective way to produce heat from photovoltaic modules is to use the produced electricity to feed heat pumps. The combination of these components is considered as one of the potential ways to supply the MiniStor system with RES driven heat. The presented in Figure 9 data on the share of individual RES in the structure of renewable thermal energy production also depict the contribution of RES driven heat pumps. In this case, the largest share of this source is observed in Malta, Cyprus and Norway. There is also a clear pattern indicating a relatively high share of heat pumps in the renewable thermal energy structure in all southern countries (Italy, Greece, Spain, Portugal, etc.). It results mainly from the use of heat pump-based systems in air-conditioning systems in these countries. Below is a summary of the number of heat pumps installed in individual EU countries. It is obvious that aerothermal HPs are quite more common than ground source ones, due to the increased installation costs of the latter. Notable exceptions to this pattern are Greece, Austria and Lithuania.

Table 31: Total number of heat pumps in operation in 2019 in European Union (EurObserv'ER, 2020)

Country	Aerothermal HP	Ground source HP	Total HP
Italy	19,600,000	14,100	19614100
France	6,994,156	161,250	7155406
Spain	4,157,961	10,793	4168754
Sweden	1,349,857	551,776	1901633
Portugal	1,610,677	909	1611586
Germany	762,336	392,784	1155120
Finland	836,620	127,964	964584
Netherlands	660,806	71,065	731871
Denmark	380,995	68,997	449992
Malta	425,237	0	425237
Belgium	321,593	15,804	337397
United Kingdom	201,946	36,877	238823
Austria	126,246	109,695	235941
Bulgaria	215,971	4,272	220243
Estonia	161,747	17,625	179372

Czechia	150,440	26,316	176756
Poland	112,950	60,196	173146
Slovakia	94,586	3,964	98550
Slovenia	34,300	10,648	44948
Ireland	36,436	4,722	41158
Hungary	12,800	2,745	15545
Lithuania	4,145	3,311	7456
Greece	1,403	3,700	5103
Luxembourg	1,834	831	2665

*Data from Italy, France, Spain and Portugal cannot be directly compared with other countries, as it includes HP that primary function is cooling.

3.2.3 Biomass

Another type of renewable energy source is biomass, widely used in the production of heat. As stated previously, this source of energy is responsible for over 80% of renewable heat in EU. A very important feature in this case, is that many installations are wood-fired residential-scale systems, i.e. suitable for integration with MiniStor. Figure 15 presents the share of energy generated by residential installations in the total thermal energy produced from biomass.

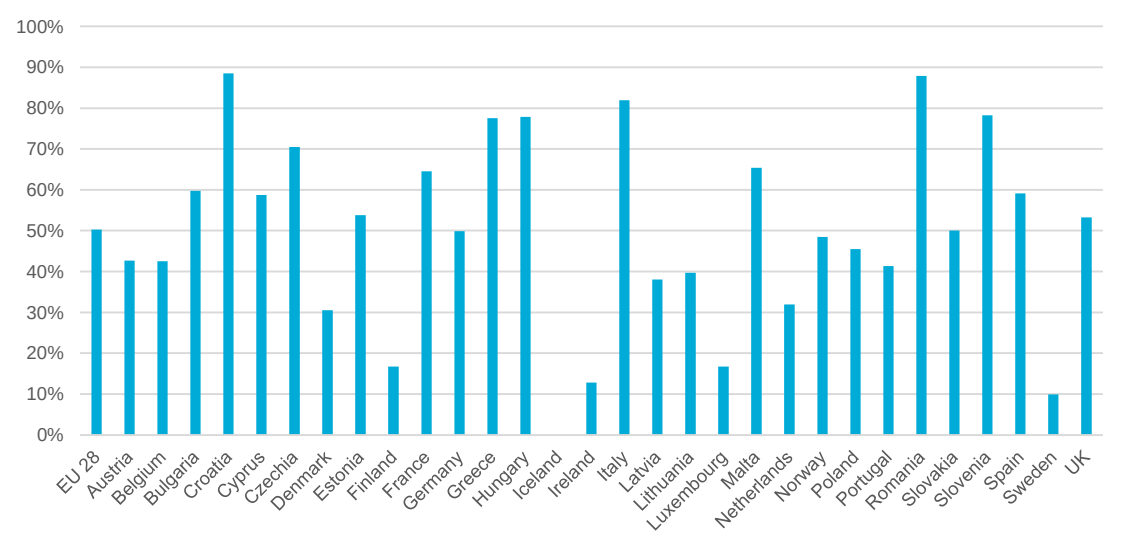

Figure 15: Share of energy generated in residential biomass installations in total amount of biomass heat generation in each country. Source: (Eurostat, 2019)

The share of residential installations in the EU as a whole is around 50%, which renders the integration of the MiniStor system with these biomass boilers as a very promising combination and can significantly increase the market penetration of this solution. On the other hand, striking is the limited use of residential scale systems in Sweden and Finland, i.e. two countries presenting an overwhelmingly biomass-based renewable thermal energy generation.

3.2.4 Geothermal potential

Finally, another promising renewable energy source is geothermal energy. However, its use is determined to a great extent by the occurrence of natural resources in the area of interest that would allow the exploitation of this type of energy. The graphic below shows the geothermal potential in Europe.

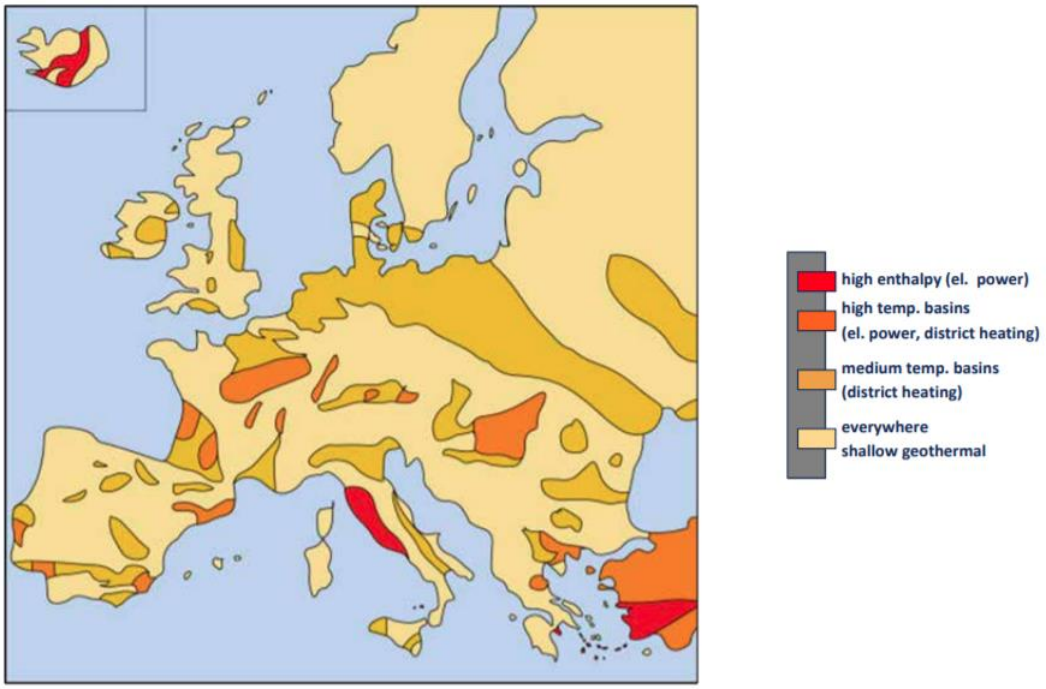

Figure 16: Geothermal resources in Europe (adapted from (Große et al., 2017))

As showed in the Figure 16 above, in some parts of Europe the geothermal potential is significant. Examples of such regions are mainly Iceland and central Italy, where high enthalpy basins are located. The connection of the use of this form of energy with the availability of natural resources is clearly visible when analyzing the electricity and heat production from geothermal sources in EU countries presented in Figure 17.

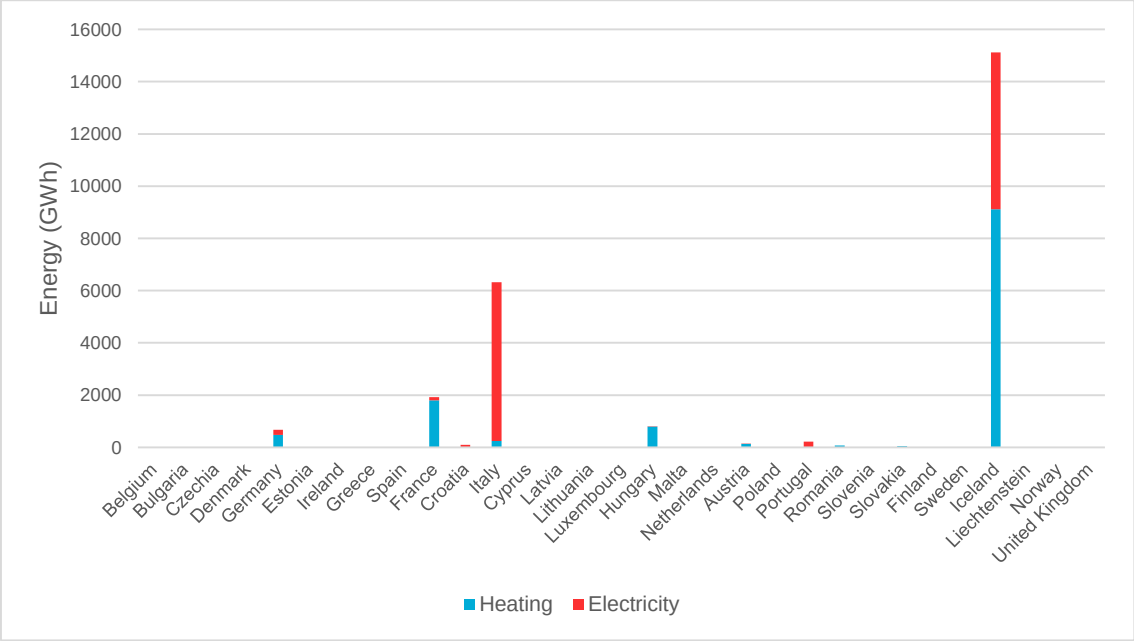

Figure 17: Energy (electricity and heat) generation from geothermal resources throughout Europe. Source: (Eurostat, 2019).

From the above figure it is evident that the aforementioned two countries, namely Iceland and Italy, which have the best geothermal conditions present also the highest energy generation in absolute values. However, this is translated differently in terms of geothermal energy share in the total RES contribution, as in Iceland this involves almost 100% of renewable thermal energy and 30% of renewable electricity, whereas in Italy only 5% of RES-based electricity is produced by geothermal sources, with the share in

renewable thermal energy generation being negligible. In addition, and as indicated by Figure 16, favorable geothermal conditions, in the form of high temperature basins, also exist in the area of Hungary and in Northern France, which is also reflected in energy generation. However, extensive medium temperature basins suitable for generating heat are located in several regions, especially in Germany, Poland, Denmark and Netherlands. This implies that geothermal resources perhaps can be considered as underexploited in Europe.

To conclude, geothermal sources in Europe, despite the lack of great potential, are being used in some countries for energy generation purposes. Therefore, it is worth considering the definition of guidelines for the combination of MiniStor system with this renewable energy source, especially if the system is to be introduced in the market of such countries.

4 Assessment of application barriers on MiniStor installation

In this chapter, the applicability of Ministor system in the various building typologies examined at the previous sections will be assessed. Due to the use of ammonia by the system, there are specific restrictions in place regarding the permitted mass of ammonia to be used by the system and the requirements for the system location. These restrictions are based on the European Standard 378 ("European Standard EN 378-1:2016 - Refrigerating systems and heat pumps - Safety and environmental requirements," 2016) covering safety and environmental requirements for refrigerating systems and heat pumps and are discussed extensively in Deliverable D2.3 - “Analysis of relevant legislation and standards for system application”. Briefly, based on the EN 378 Standard the systems that use ammonia as refrigerant are subject to charge limitations due to the refrigerant toxicity and flammability properties. Ammonia belongs to class B regarding its toxicity and to class 2L regarding its flammability. The corresponding values of maximum permissible charge (one base on toxicity and another based on flammability) are determined taking into account i) the access category of the conditioned space and ii) the location classification of the refrigerating equipment and the maximum charge is the lowest one from these two values.

As the system is proposed to be used in residential buildings, the Access Category “A” of Standard EN 378 is considered, i.e. there is general access to the conditioned building. This implies that ammonia usage as refrigerant can be regarded safe only if a Location Class III (Machinery room or open-air) is realized, i.e. all parts of the system that contain ammonia will be located either in a machinery room or open-air. In addition, the proposed setup of Ministor (Figure 18) is classified as a double indirect system, i.e. the heat-transfer fluid (primary circuit) is in direct contact with ammonia containing parts, but the heat is directed to the conditioned space with a secondary indirect circuit that exchanges heat with the primary one. In general, double indirect systems are considered to be placed in Location Class III.

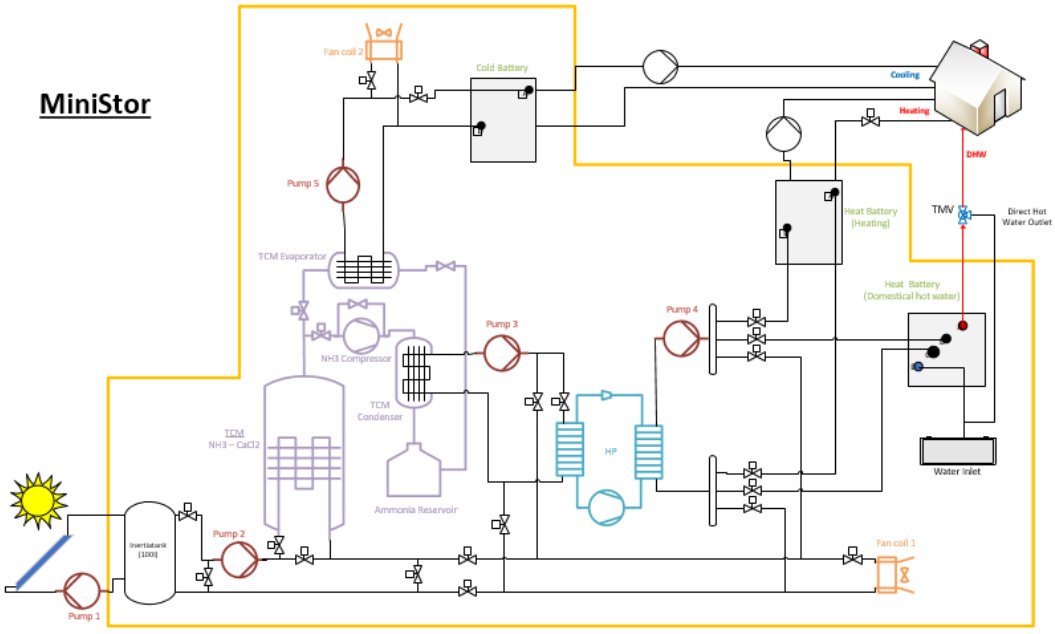

Figure 18: Overall configuration of the MiniStor system components

Part 3 of the European Standard EN 378 sets the specific requirements for the installation of the refrigerating equipment in the open-air and the machinery rooms. With regard to the former, it is required that provisions are taken so that the refrigerant is not allowed to flow into any ventilation opening, door or similar opening in case of leak, whilst if the equipment is located outside and sheltered, then natural or forced ventilation should be provided. If, despite the outdoor installation, a release of refrigerant can stagnate, then the provisions regarding the detection of gas and mechanical ventilation for the machinery rooms apply in this case as well.

With regard to the installation of the refrigeration equipment in machinery rooms, there are several requirements that need to be met. Within the context of residential buildings, the main requirements are:

- Access should be provided only to instructed personnel.
- No airflow from the machinery room to the rest of the building should take place and any potential escaping gas should be vented outside.
- Exterior openings from the machinery room should be at least 2m away from openings of the building (windows, vents etc.).
- In case there are combustion systems, boilers and air compressors then provisions should be taken so that the air to these systems is ducted from the outside.
- Doors should be tight fitting, self-closing and should provide at least 1-hour fire resistance.
- Open flames should be avoided unless for necessary maintenance activities.
- The storage of other substances should be avoided.
- A remote emergency switch should be provided outside of the closed space.
- Normal and emergency lighting should be available.
- Dimensions of the machinery room should be adequate to allow the installation and maintenance of the equipment.
- Any ducts that pass through building elements should be sealed and the seal should provide the same fire resistance as the element.
- Emergency exit leading to the outside or to an emergency exit passageway should be included.
- Service ducts should be sealed and adequately vented to avoid the build-up of ammonia in case of leakage.
- Mechanical ventilation for normal operation and emergencies should be included.
- Additional equipment specific to systems containing ammonia include drainage to collect any liquid ammonia that may leak, equipment for emergency washing and exhaust gas ventilation. Furthermore, specific requirements for fire sprinkler systems are in place.
- Specific alarm systems and gas detectors.

It is apparent that meeting the requirements for the installation of the refrigeration equipment of Ministor system in an existing machinery room of a building is a challenging task. Furthermore, in case of a retrofit it might not be possible to identify a suitable space for meeting the requirements on the size and the location of the openings. In addition, meeting these requirements might lead to a significant cost. Therefore, in such cases it seems more feasible to install the equipment outside. The latter can either be placed under an open shelter providing basic protection from weather conditions or can be located inside a closed box (e.g. a container) that will operate as a regular machinery room supplementary to the existing one. The first option involves lower cost, but the second one guaranties higher levels of safety, as the equipment will be inside a space with restricted access and equipped with all the necessary safety instrumentation (i.e. for ventilation, drainage, firing control, ammonia scrubbing etc.). Because of these advantages, the usage of a closed box is preferred for the MiniStor installation and operation in the demo sites during the current project activities. However, it should be underlined that accordingly hydraulic and electrical connections of this closed space with the building's water and electricity networks are necessary to be realised in order to ensure the smooth operation of the safety equipment (sensors, fans, firing suppression system etc.).

From all the above, it can be deduced that the system appears to be more suitable for installation in a detached or semi-detached dwelling where the refrigeration equipment can be more easily installed outside. Requirements set by EN 378 – Part 3 should be met at all times. Installing the refrigeration

equipment in individual flats is more difficult due to the limited amount of open space. In this case, installing larger systems corresponding to whole or a significant part of a multifamily building is more feasible, but remains challenging given the size of units required. A possible location for the system is the roof of the building (in case of buildings with flat accessible roofs), provided all requirements for safety and static control are met. However, there are space limitations on the roof too, especially considering that this is the most probable location for the RES systems that supply energy to MiniStor (i.e. PVT panels) as well. The overall weight of the system may be an additional limiting factor that must be taken into account.

5 MiniStor specifications and operation modes

5.1 Definition of the conceptual operation modes of MiniStor system

This section includes a summary of main operational modes of the MiniStor system, yet only referred to the thermal devices. For all main modes, a basic description of the involved steps is included first, and a more detailed description of the subsequent processes is presented afterwards.

5.1.1 Introduction to operation modes definition

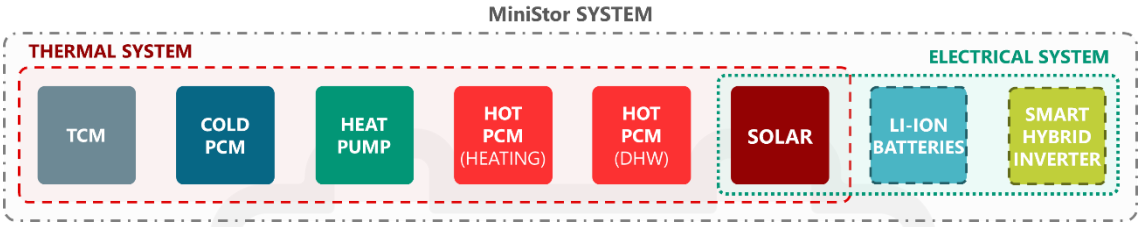

Figure 19: Main subsystems within the MiniStor system

From an operational perspective, the MiniStor system is constituted by eight sub-systems, both thermal and electrical: TCM (which includes also the ammonia cycle), heat pump, hot PCM for heating, hot PCM for DHW, cold PCM, solar, smart hybrid inverter and Li-Ion batteries. These subsystems are interconnected to provide a dynamic operation of the system as a whole, and in turn, from a functional point of view within the MiniStor system, can be divided into three main types:

Table 32: MiniStor subsystems by functional typology

Sub-system	Thermal	Electrical
Production	Solar (FPC + PVT)	
Storage	TCM (Ammonia cycle) Hot PCM (heating) Hot PCM (DHW) Cold PCM	Li-Ion batteries
Transformer	Heat Pump	Smart hybrid inverter

Despite both thermal and electrical systems operate in an integrated manner (i.e., interact with each other depending on the given conditions), both systems have independent control systems. Thus, the interaction of both electrical and thermal systems is inherent to the nature of the solar subsystem: the solar modules produce both electricity and heat. While the electricity is managed in the smart hybrid inverter, which decides if electrical energy needs to be stored in the li-ion batteries or can be consumed, either in the building or in the MiniStor system[5], the heat is sent to the thermal circuit (where PCM storage, the TCM and the heat pump are included), where electricity is required for the operation of the different devices. Nevertheless, from a control perspective, both thermal and electrical systems can operate properly in an isolated manner: the electrical system does not require any operational or control inputs from the thermal system because the main control is done by the smart hybrid inverter, and the thermal system does require

[5] Additionally, electricity produced in the solar field might be sent into the grid, but only in cases where this is allowed by technical conditions and applicable regulation.

electricity, but, from an operational perspective, the source of that electricity is not relevant. This separation allows for a more robust configuration of the system, as well as for a simpler definition of the operation modes.

The operation of the MiniStor electricity system was previously presented in D3.8, where a detailed description of all possible scenarios according to technical and regulation restrictions was included. Consequently, only thermal operation modes will be included in detail in this document. In any case, a basic description of the operation modes for the MiniStor electricity system is included next. The system, mainly constituted by a hybrid inverter, PVT modules, electrical batteries, the main grid and the electrical load, can operate according to nine different operation modes, depending on the energy flows between these elements;

- Mode 1: the system shows a *production excess* (a positive difference between PVT electrical production and the load to be covered). Solar energy production is used to charge batteries. Load is covered from grid. In addition, batteries are also charged from grid.
- Mode 2: the system shows a *production deficit* (a negative difference between PVT electrical production and the load to be covered). Solar energy production is used to charge batteries. Load is covered from grid. In addition, batteries are also charged from grid. The difference between this mode and Mode 1 is that the energy coming from grid will be higher due to the production deficit in Mode 2, in comparison with the production excess in Mode 1. Consequently, both modes are equivalent from an operational perspective, but from a control approach need to be differentiated.
- Mode 3: Load is covered from solar energy production and both production excess and energy storage in batteries are sold to the grid.
- Mode 4: Production deficit is bought from grid. Batteries are not used.
- Mode 5: Production excess is used to charge batteries. Energy is not bought nor sold to grid.
- Mode 6: Production deficit is covered by batteries. Besides, energy from batteries is sold to grid.
- Mode 7: Solar energy production is used to charge batteries, while load is covered by grid
- Mode 8: Production deficit is covered by batteries. Energy is not bought nor sold to grid.
- Mode 9: Load is covered directly from production. Production excess cannot be used and it is dumped.

For illustrative purposes, the electrical energy flow for Mode 2 is represented in Figure 20 as an example. The rest of diagrams representing the different modes are included in the Annex A4 of D3.8.

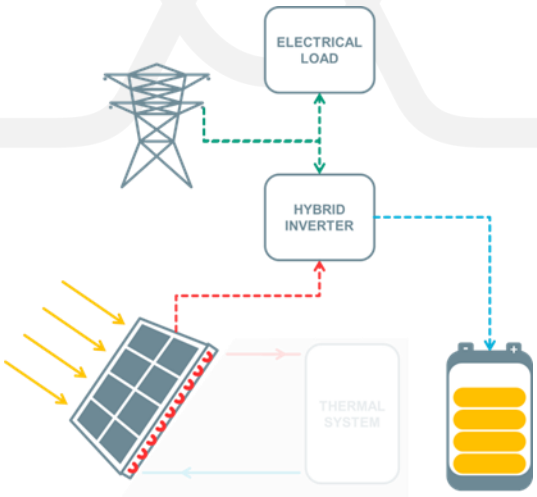

Figure 20: Electrical energy flow representation for the Operation mode 2.

5.1.2 Main thermal operation modes

Main sub-systems of the MiniStor thermal system as well as their main possible thermal interactions are displayed in Figure 21, although these interactions do not occur at the same time. Associated electrical consumptions, and additional auxiliary devices for all the sub-systems to interact with each other (e.g.

pumps, valves, fan coils), are not included in this simplified representation. This diagram will be used as a basis to describe the basic concepts of main operation modes in subsequent sections.

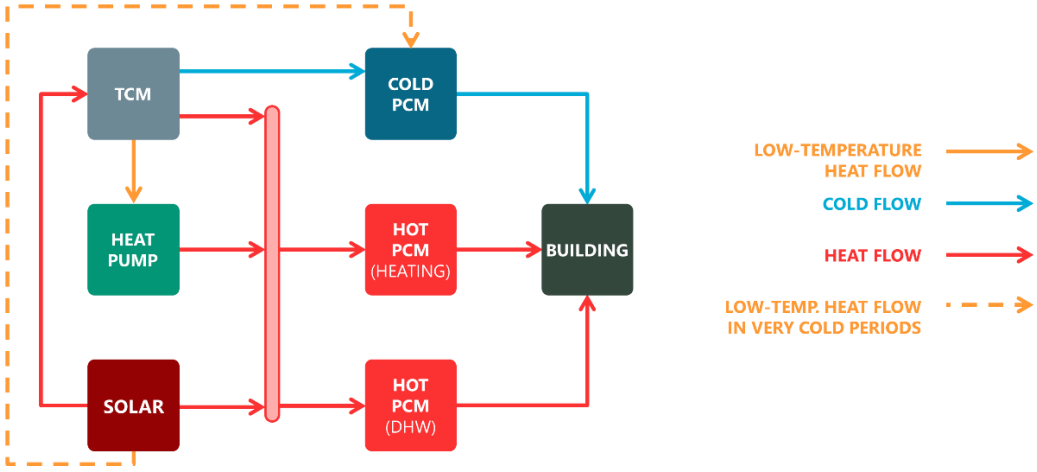

Figure 21: Basic diagram of the MiniStor thermal system, including main interactions among main sub-systems

Figure 22 represents the layout of the MiniStor thermal system, and contains the main components from a functional perspective, both within the boundaries of each subsystem, and in between the sub-systems, to connect them. This diagram will be set as a basis to show a detailed representation of the main operation modes. This includes the position of valves and active thermal flows, displaying their direction and temperature in a qualitative way, following the colour code displayed in the previous figure.

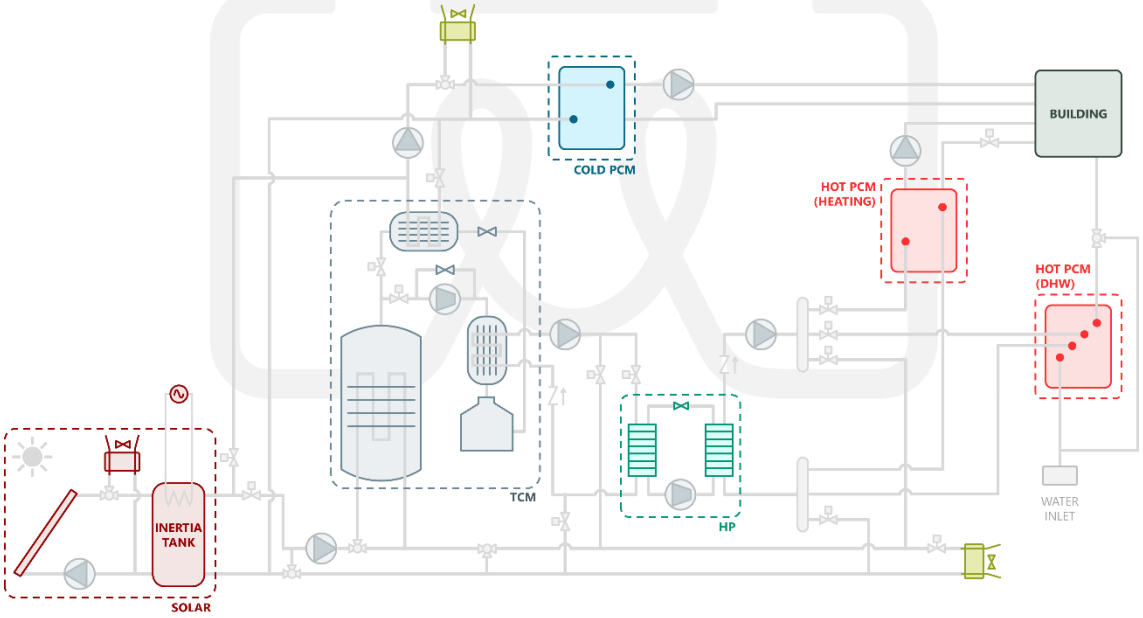

Figure 22: Detailed layout of the MiniStor thermal system

Despite the system complexity, all operation modes of the MiniStor thermal system can be divided into four main groups, which are summarized in Figure 23. As it can be seen, within the operation mode “TCM discharge”, there are three different variations depending on the season and the ambient conditions, but all of them share the same concept as a basis (see next sections).

Apart from these four main modes, a large number of combinations of these operation modes or sub-modes can occur, yet all of them could be simplified into one or more than these main modes. For instance, within the TCM discharge mode, thermal demand could be either only cold and DHW (while heating is not needed), heating and DHW demand but not cold, or any of these types of demands separately (i.e. DHW, cold or heating), and a different set of PCM units would receive energy accordingly. Nevertheless, all these

combinations have been considered sub-modes of the TCM discharge mode for simplicity reasons. Additionally, some variants representing specific operational conditions may also happen (e.g. heat rejection using a fan coil because the PCM units are fully charged, heat rejection for safety reasons). All these operation modes that are subject to technical and control restrictions. They will be explained in more detail in D5.1 "Initial design of the Energy Management System".

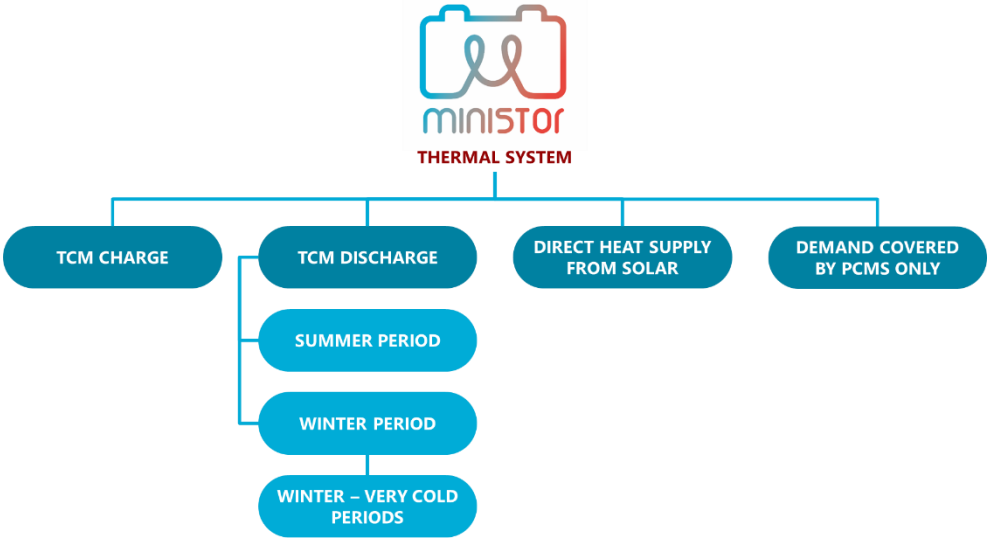

Figure 23: Main operation modes of the MiniStor thermal system

Next, the main operation modes are described for the MiniStor thermal system. As previously stated, for each mode a basic explanation is included first as a preliminary and conceptual approach, followed by a more detailed description of the different processes occurring in every case.

It is important to note that next descriptions aim at providing a conceptual perspective of the main operation modes, and need to be considered for illustrative purposes only. Thus, represented operation modes are generic, and include a combination of different operation sub-modes that might not happen at the same time. Consequently, non-feasible scenarios are represented in some cases in terms of thermal demand, for instance, a simultaneous supply of cold and heat to the building (see "TCM discharge" or "Demand covered by PCM units only" modes), which will not occur in a real environment. Additionally, the diagrams do not reflect the sequential progress of the different steps, but a static picture of the main steps taking place at the same time.

5.1.3 Operation mode: TCM charge

5.1.3.1 Basic description

In this operation mode, the solar resource is used to provide the required heat to charge the TCM, and, as a result of this process, additional heat is provided to the hot PCM units, which can be used in the building. Cold production does not occur in this mode.

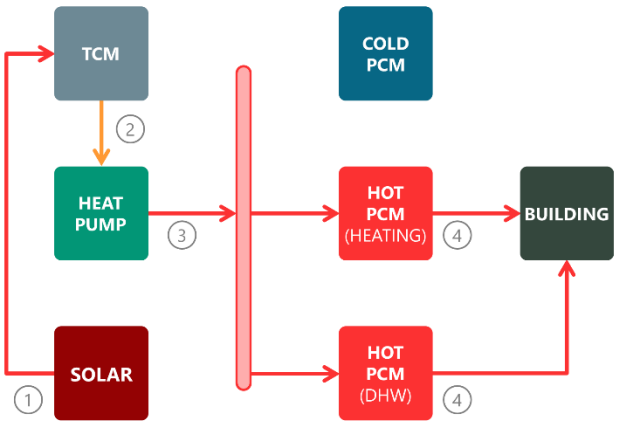

Figure 24: Operation mode "TCM charge". Basic diagram

Main steps:

1. The heat produced in the solar field is firstly used to perform the charging process of the TCM system.
2. As a result, a low-temperature heat flow is produced and sent into the heat pump.
3. In the heat pump, the temperature is increased and the resulting heat is introduced into the hot PCM units.
4. Finally, the heat is released from the PCM units and sent to the building whenever it is necessary.

5.1.3.2 Detailed description

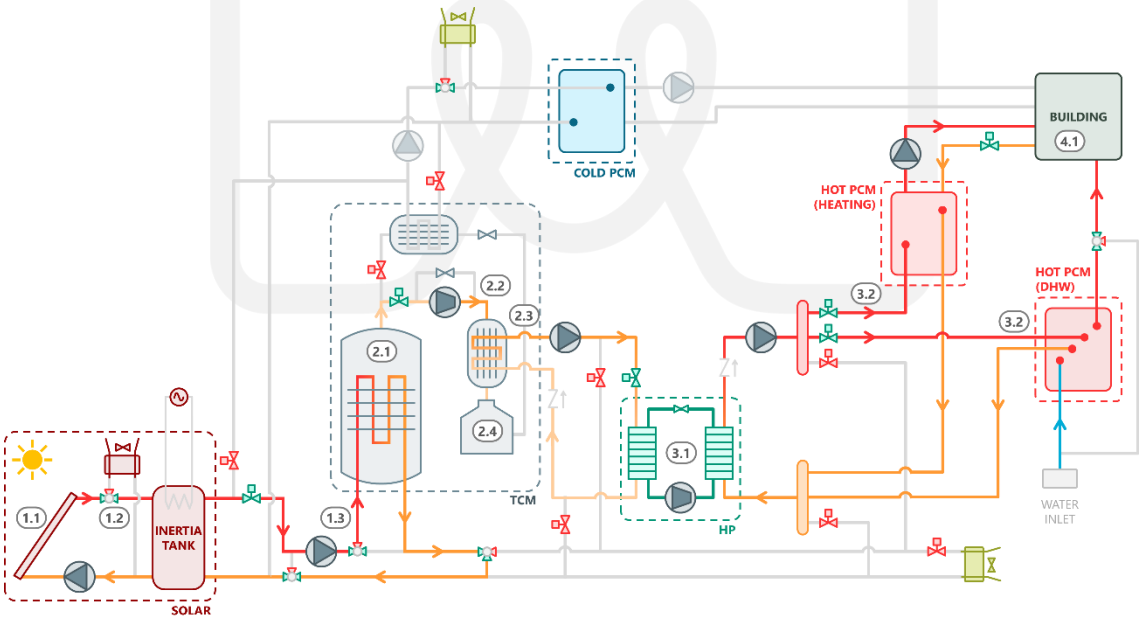

Figure 25: Operation mode "TCM charge". Detailed diagram

Detailed steps:

1.1 First, during periods of sufficient solar insolation, the temperature of the HtF flowing through the solar field is increased.

1.2 The heat from the solar modules flows into the inertia tank, where it is stored until a specific temperature threshold is reached.

1.3 Once this minimum temperature is reached, the heat from the solar system is supplied to the TCM during the charging process, by means of a hydraulic circuit that passes through the reactor and exchanges heat with it.
2.1 The heat in the reactor is used for the decomposition reaction, which results in the gaseous ammonia exiting the reactor.
2.2 The ammonia is driven through a compressor, which also causes an increase in its temperature.
2.3 In the TCM condenser, this heat from the ammonia is transferred to a different flow that is connected to the evaporator of the heat pump.
2.4 After this heat exchange, liquid ammonia is stored in a reservoir.
3.1 The heat recovered from the ammonia flow, is connected to the evaporator of the heat pump, which increases its temperature and releases it to a hydraulic line connected to the heat pump condenser.
3.2 From the heat pump condenser, the heat is sent into the hot PCM units, where it is transferred and stored in the PCM material.
4.1 The heat that is stored in the hot PCM units is transferred to the heating and DHW circuits in the building to cover the thermal requirements.

5.1.4 Operation mode: TCM discharge

5.1.4.1 Basic description

For this operation mode, the precondition is the TCM being fully charged. During this process, the TCM process is reverted, hence the ammonia is re-introduced into the reactor. As a consequence of this process, both cold and heat are produced, which can be stored into the PCM units, and subsequently used in the building.

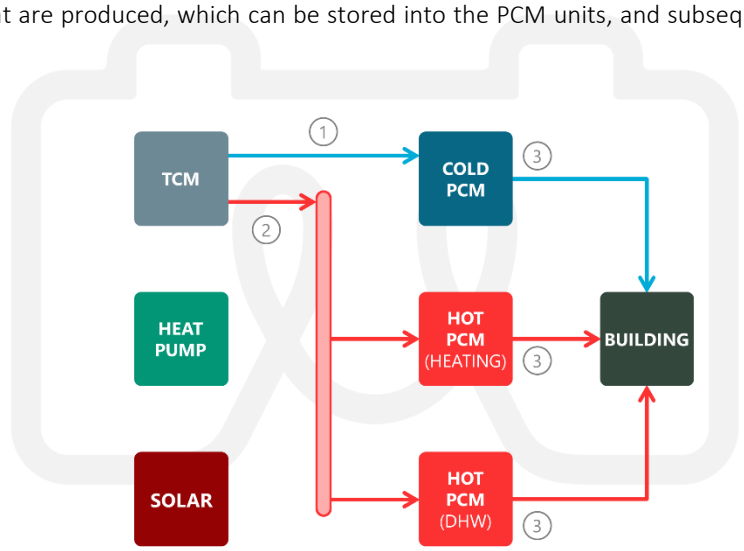

Figure 26: Operation mode “TCM discharge”. Basic diagram

Main steps:

1. During the first stage of the discharging cycle of the TCM, cold is produced in the TCM evaporator, which is sent into the cold PCM unit during summer period or very cold periods in winter, or rejected to the ambient through a fain coil during mild periods in winter.
2. As a second stage, the exothermal reaction in the TCM reactor produces heat, which can be introduced into the hot PCM units in winter, or rejected into the ambient using a fan coil in summer (not explicitly represented in previous basic diagram).
3. Both cold and heat are released from the PCM units when necessary (cold in summer, only), and are used in the building to cover the corresponding demand.

5.1.4.2 Detailed description

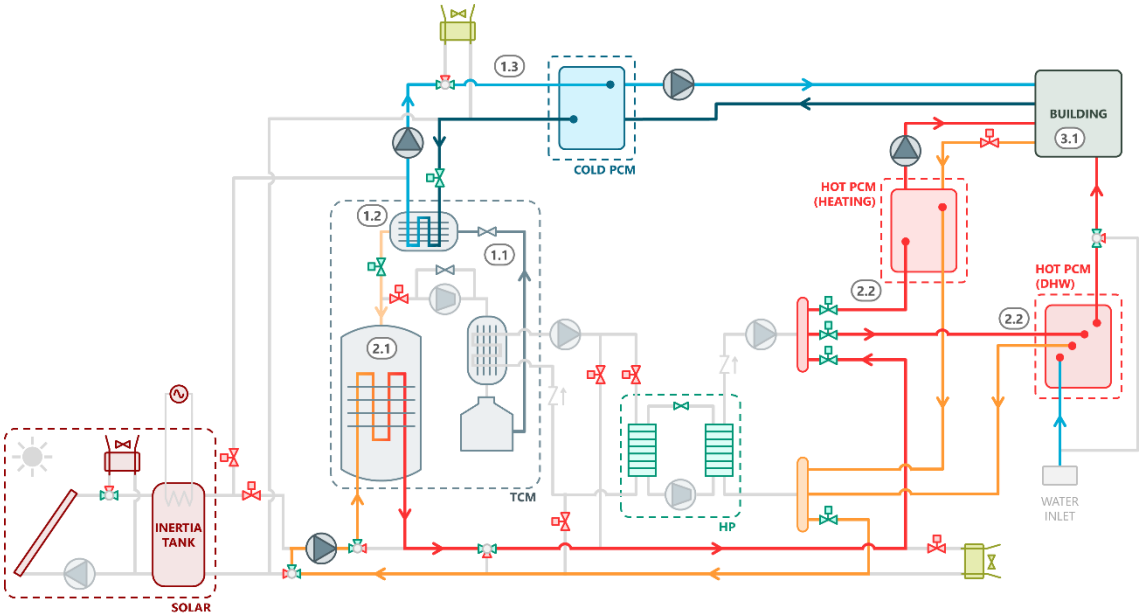

Figure 27: Operation mode "TCM discharge". Detailed diagram

Detailed steps:

1.1 Once the TCM charging cycle is complete (i.e. the decomposition reaction is finished), the ammonia can exit the reservoir, and subsequently its temperature decreases as a result of the expansion process.

1.2 In the evaporator, the cold from the ammonia is exchanged with the hydraulic circuit that drives it to the cold PCM or to a fan coil, and then the ammonia enters the reactor.

1.3 The flow leaving the evaporator goes into the cold PCM unit during summer or very cold winter periods, where cold is stored. In other winter periods, i.e. when external ambient temperature is not very low, the flow from the TCM evaporator passes through the outdoor fan coil, and cold is rejected into the ambient.

2.1 In the TCM reactor, the ammonia interacts with the salts of calcium chloride, which results in an exothermal reaction.

2.2 The heat produced during the reaction, is transferred to a passing flow, which sends this heat into the hot PCMs during winter, where it is stored. In summer, released heat from the TCM reactor is rejected into the ambient.

3.1 As a last step, cold and heat from the PCM batteries is sent into the building to cover the thermal demand of the demo sites, i.e. cooling, heating and DHW. Nevertheless, it is to be noted that the exact scenario included in Figure 27 does not reflect any realistic situation; cold and heating demand are not expected to occur during the same discharging cycle, but only heating and DHW demands, cold and DHW demands, or any of the demands separately.

5.1.4.3 TCM discharge during very cold periods

Unlike for most of the year (i.e. summer and mild winter periods), for which no additional steps are required and only small variations differ depending on the given conditions, during very cold periods, an additional step is required prior to the previously described process (step 0). This step allows to ensure the required temperatures and pressures to operate the reactor. Apart from this previous procedure, the rest of the steps are the same as those explained in previous section.

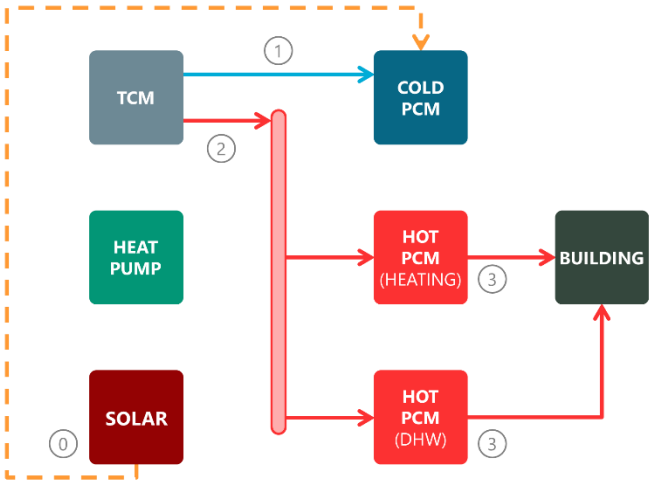

Figure 28: Operation mode "TCM discharge - Very cold periods". Basic diagram

Additional step:

0. In very cold periods, low-temperature heat from the solar sub-system will be sent into the cold PCM to keep a minimum temperature inside the unit.

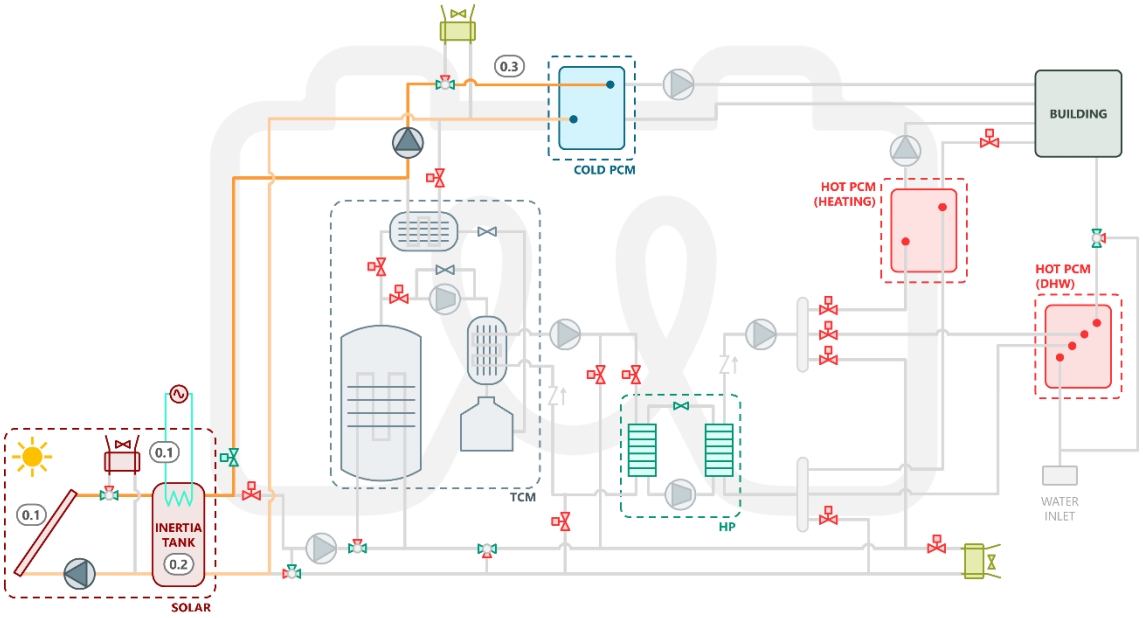

Figure 29: First phase of the operation mode "TCM discharge - Very cold periods". Detailed diagram

Main processes within the preliminary step:

0.1 During moments for which solar radiation is low, heat gained by the solar modules will be limited, but may still contribute to increasing the temperature of the HtF flowing through the solar circuit. Alternatively, in cases for which solar radiation is too low to reach a minimum temperature, an electrical resistance may be used as a backup heater for a limited amount of time.

0.2 Heat from the solar field or from the electrical heater will increase the overall temperature of the HtF stored inside the inertia tank.

0.3 A hydraulic circuit connected to the cold PCM unit will send heat into it, so that a minimum temperature is always kept, hence the pressure at the TCM evaporator can be increased during the discharging process, and the required temperature in the TCM reactor remains within appropriate limits for charging the hot PCMs.

5.1.5 Operation mode: Direct supply from solar

5.1.5.1 Basic description

This operation mode mainly consists in the direct use of energy from the solar sub-systems for the charging process of hot PCMs. Given the temperature requirements in the PCM units and the limited solar resource during winter periods, this operation mode will occur, except for extraordinary situations, during the summer period. Consequently, heat will be mainly used in the hot PCM for DHW, and will be unlikely to be used in the hot PCM for heating.

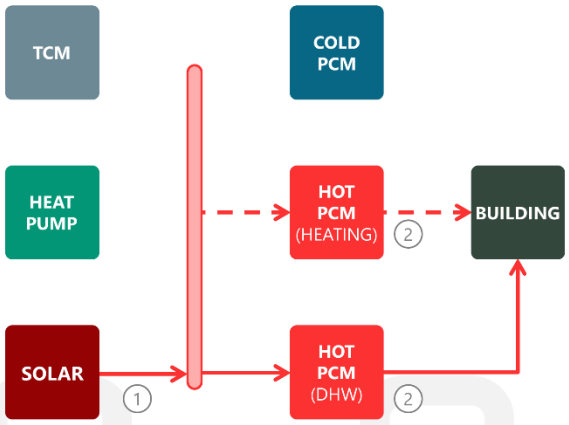

Figure 30: Operation mode “Direct supply from solar”. Basic diagram

Main steps:

1. In cases where the TCM subsystem is fully charged and there is enough solar energy available at the required temperature, heat from the solar field can be sent into the hot PCMs[6].
2. Heat stored in the hot PCM units is then sent into the building when required, to cover the thermal needs.

[6] The red-dotted arrows symbolizing the heat flowing into and out of the hot PCM for heating represents the improbability of this scenario to happen, since the heating PCM will be only used in winter, and, during this period, solar energy is not likely to be enough for this operation mode.

5.1.5.2 Detailed description

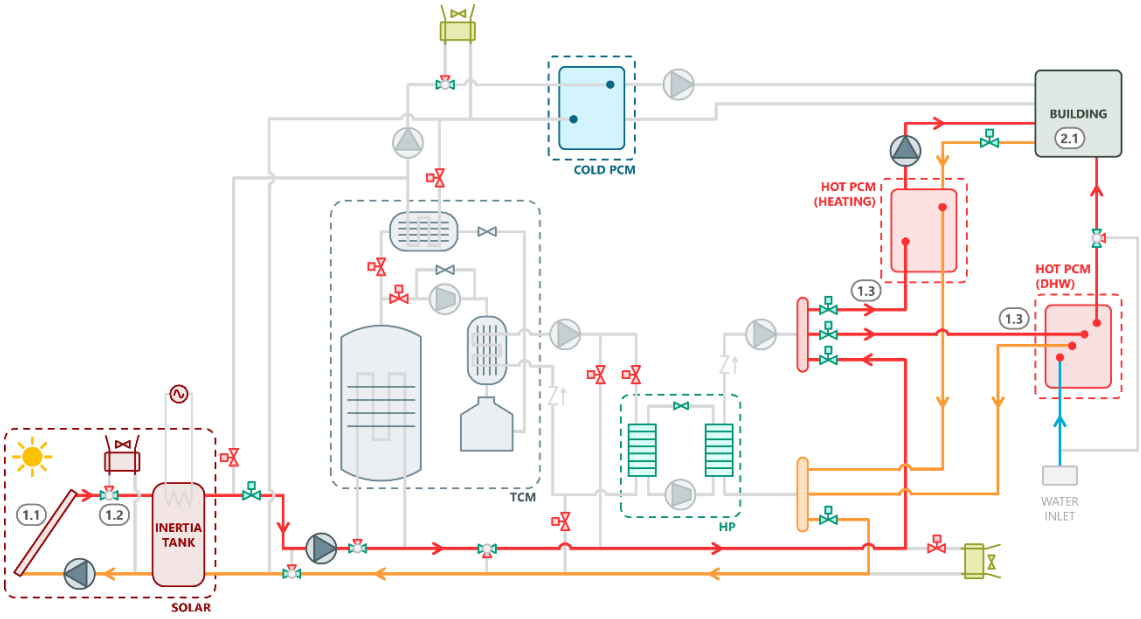

Figure 31: Operation mode “Direct supply from solar”. Detailed diagram

Detailed steps:

1.1 Following the same procedure as that corresponding to the operation mode “TCM charge”, the temperature of the HtF flowing through the solar field is firstly increased, during periods of sufficient solar insolation.
1.2 Next, the heat from the solar modules flows into the inertia tank, where it is stored until a specific temperature threshold is reached.
1.3 The heat from the inertia tank is driven into the hot PCM units (one or both) where it is stored.
2.1 Heat from the PCM batteries is sent into the building to cover the heat demand of the demo sites, i.e. DHW and heating demand.

5.1.6 Operation mode: Demand covered by PCM units only

5.1.6.1 Basic description

In cases when both solar and TCM sub-systems are not available, PCM thermal storage units can be used to cover the demand of the building, using the energy that previously has been introduced into them.

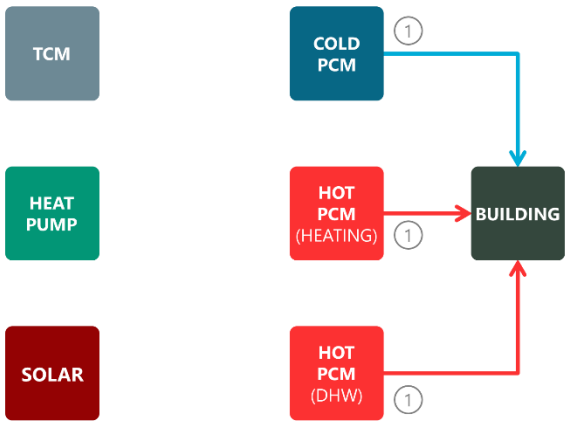

Figure 32: Operation mode “Demand covered by PCM units only”. Basic diagram

Main step:

1. Heat and cold stored in the PCM units can be sent into the building to cover the thermal needs. The rest of sub-systems do not participate in this operation mode.

5.1.6.2 Detailed description

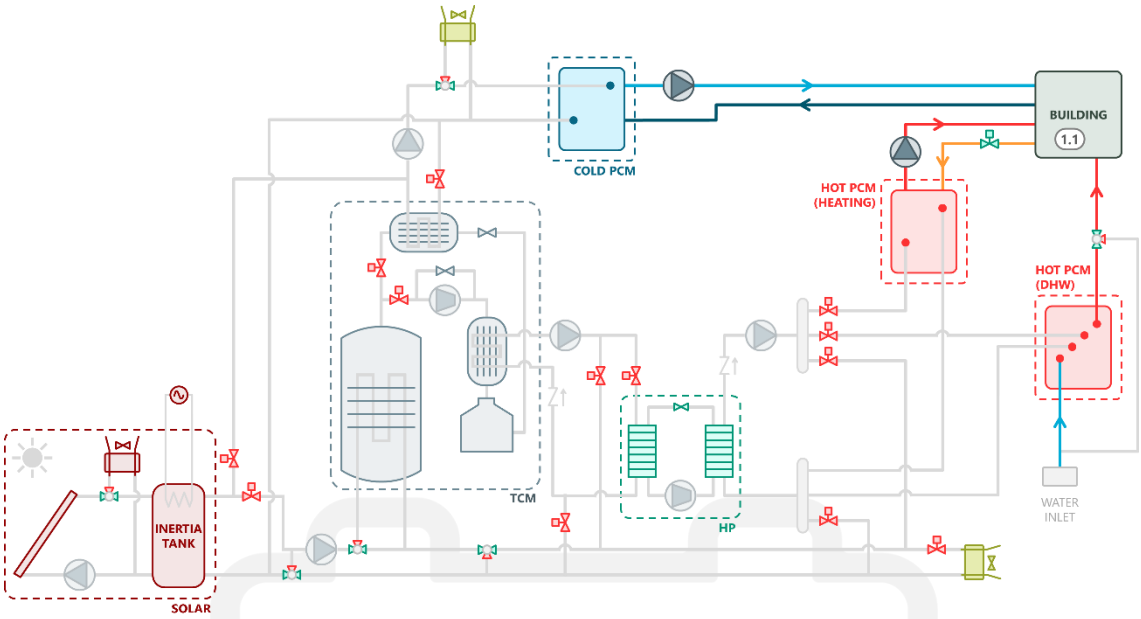

Figure 33: Operation mode “Demand covered by PCM units only”. Detailed diagram

Main process:

1.1 The PCM units constitute thermal storage devices which can be used to cover the demand in the buildings. In cases where the energy in the solar subsystem is not available, and the TCM is not fully charged or is preferred not to start the discharging process, the PCM units can release the stored heat and cold by exchanging the energy available to the thermal-consumption circuit of the building.

5.2 Overview of system operating conditions and system main specifications

5.2.1 Factors shaping the system operating conditions

MiniStor is characterised by rather stable operating conditions at each operation mode, which however vary between summer and winter periods. This is attributed to the fact that these conditions are imposed on the one hand by the specifications of the storage subsystems and on the other hand by the ambient conditions, as there is a frequent heat exchange between the system and the environment. Table 33 summarizes the characteristics temperatures of the incorporated storage subsystems.

Table 33: Characteristic temperatures of the storage subsystems

Storage Subsystem	Characteristic Temperature	Description
TCM	60 °C	Necessary inlet temperature of HtF in order to achieve the targeted energy storage density of 200 kWh/m^3 (mentioned in D4.1 “Reactive salt optimal implementation in thermochemical reactor and vessel design”)

Hot PCM (heating & DHW)	58 °C	Phase change temperature of the preferred PCM (identified in D4.2). Alternatively a different PCM with a lower melting point (48 °C) can be used
Cold PCM	11 °C	Melting temperature of the preferred PCM (identified in D4.2). Alternatively a different PCM with a lower melting point (5.5 °C) can be used

The phase change temperatures of PCMs impose preconditions to the inlet temperature of HtF. Thus in order to charge, i.e. melt, the hot PMC an inlet temperature of 63 °C is required, whereas for charging, i.e. solidifying, the cold PCM the corresponding maximum value is about 8 °C. Table 34 depicts the main interactions between the various subsystems and the ambient. As it can be easily seen, these heat exchanges regard only the TCM storage subsystem, however they are not limited to only one of its components but involve several of them. In general, a system unhindered operation for ambient conditions of 35 °C in summer and -10 °C in winter is desired.

Table 34: Main interactions between MiniStor subsystems and the environment

MiniStor subsystem	Subsystem component	Usual period of interaction
TCM	TCM reactor	Summer
TCM	TCM condenser	Summer
TCM	TCM evaporator	Winter

5.2.2 Operating conditions in the defined main operating modes

5.2.2.1 Operating conditions in TCM charge mode

During TCM charge mode in winter the system operating conditions are determined by the TCM and PCM characteristic temperatures. First of all, the heat supply to the TCM should be in the range of 60 °C, if an energy storage density of 200 kWh/m^3 is to be achieved. This in turn means that the reactor equilibrium temperature and pressure are approximately 55 °C and 2 bar respectively (Figure 34). On the other hand, the hot PCMs phase change temperature of 58 °C means that the heat sink of the HP, acting as the "energy transformer" between TCM and hot PCMs subsystems, should be approximately 63 °C. The intermediate ammonia condensation conditions (28 °C, approx. 11 bar), are defined by two factors: i) the characteristics of commercially available ammonia compressors, namely their compression ratio which is usually not higher than 6 and thus for a suction pressure of 2 bar determine a maximum condensation pressure of 12 bar, and ii) the characteristics of available heat pumps, since machines being able to provide the required from the PCMs heat sink conditions require heat source temperatures in the range of 20-30 °C. For achieving high HP COP values, very low condensation temperatures should be avoided.

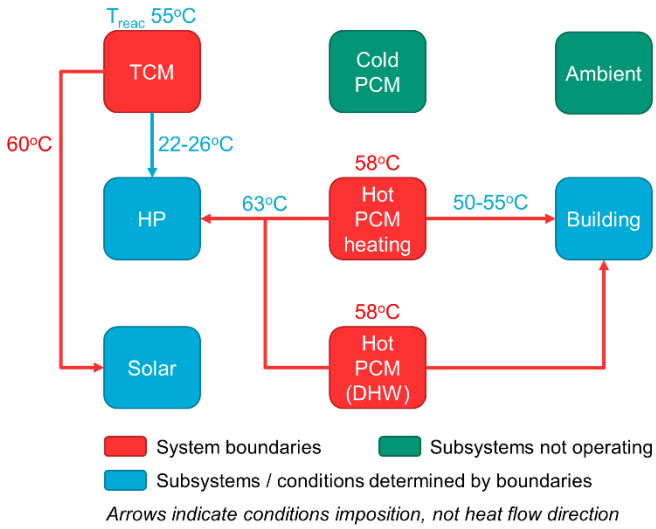

Figure 34: Boundaries of operating temperatures in winter TCM charge mode

In TCM charge mode in summer, the characteristic hot PCMs temperature does not impose any restrictions on the system operating conditions, as these vessels are foreseen to be charged under the direct supply from solar operation mode. This also means that the operation of the HP for heat upgrade is not necessary. Nevertheless, restrictions are imposed by the outdoor conditions and more particularly by the need to reject the TCM condensation heat to the ambient (Figure 35). Considering an ambient temperature of 35 °C, the ammonia condensation should be realized under a temperature of around 40 °C and a corresponding pressure of 16 bar. Thus, the equilibrium conditions inside the reactor should be at least 3 bar and 63-64 °C, which in turn require a solar heat input to approximately 68 °C. Since in summer the solar radiation presents its higher annual values, a prerequisite of a 70 °C heat supply to the TCM is reasonable which would further reduce the compression ratio and the ammonia compressor electrical consumption. Cold and DHW PCMs, if charged, may discharge covering the corresponding energy needs of the building.

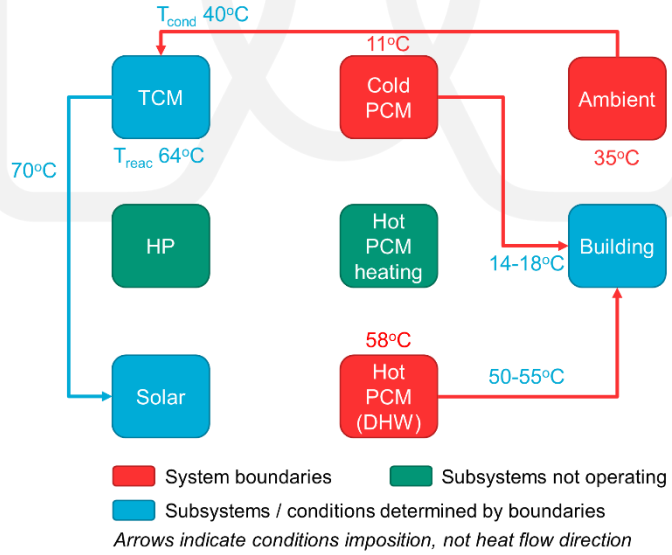

Figure 35: Boundaries of operating temperatures in summer TCM charge mode

5.2.2.2 Operating conditions in TCM discharge mode

In winter TCM discharge mode, the TCM should generate heat at a temperature appropriate for realising the hot PCMs charging. Thus, the phase change temperature of the latter is the one boundary of the system operating conditions, translated into a minimum equilibrium temperature inside the reactor of 63-65 °C (Figure 36). The corresponding pressure is approximately 4.5-5 bar, while the evaporation pressure should

be a bit higher than this value in order to enable a gaseous ammonia flow towards the reactor. However, the evaporation pressure is also linked with the TCM evaporator – environment interaction, as the latter is the heat source of the ammonia evaporation process. For an evaporation pressure of 4.5 bar the corresponding temperature is about 2 °C, resulting in a minimum ambient temperature of 5 °C, whereas these values are even higher (4 and 7 °C respectively) for evaporation pressure of 5 bar. Therefore, both boundary conditions can be satisfied only if the ambient temperature is higher than 5 °C. In a different case the TCM discharging would not be able to produce heat at temperature suitable for charging the hot PCMs and consequently the stored energy would be wasted.

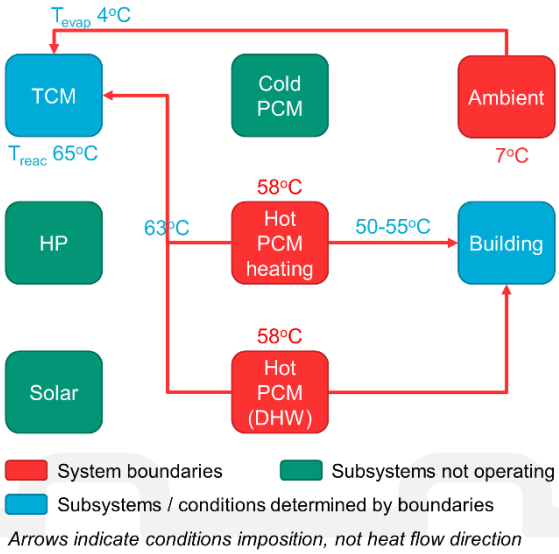

Figure 36: Boundaries of operating temperatures in winter TCM discharge mode

In order to overcome this problem, considering also that the need to utilise the stored energy and confine the heat demand peaks would reasonably coincide with low ambient temperatures, the TCM discharge sub-mode during very cold periods is foreseen. As described in Figure 28 and Figure 29, this sub-mode involves the cold PCM charging utilising low-temperature solar heat. Taking into account the relevant phase change temperature of 11 °C, the heat supply of the solar field should be higher than 16 °C. This is a precondition that can relatively easily be fulfilled even in periods of severe cold. As the TCM evaporator utilises the solar heat stored in the cold PCM as the evaporation heat source, the characteristic cold PCM temperature substitutes the ambient one as the second boundary of the system operating conditions as depicted in Figure 37. This is translated into a heat supplied to the evaporator at a mean temperature of about 7-8 °C, enabling the TCM heat generation at a temperature high enough to charge the hot PCMs. The only limitation in this case is the cold PCM capacity which may not be high enough to provide the necessary energy for a complete TCM discharge.

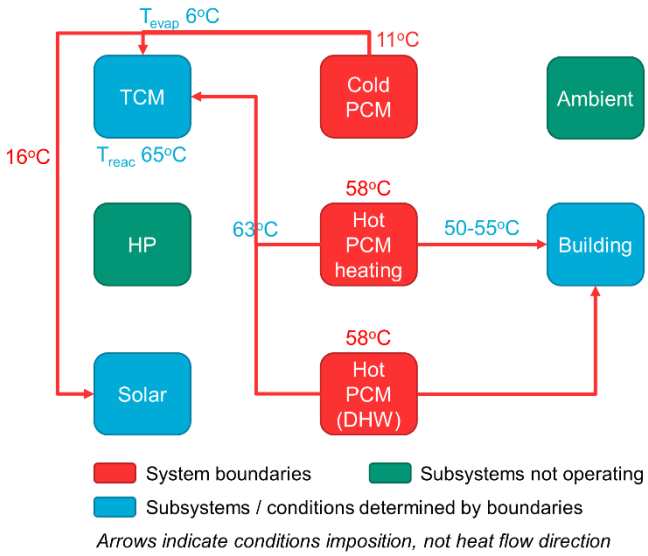

Figure 37: Boundaries of operating temperatures in TCM discharge mode during very cold periods

Similarly, to TCM discharge during very cold periods, in summer the TCM evaporator is connected to the cold PCM vessel. However, in this case the main purpose of this interaction is to produce the necessary cold to charge the cold PCM subsystem. An evaporation temperature of 0 ºC, regarded as sufficient for the implementation of this heat exchange, corresponds to reactor equilibrium conditions of approximately 4 bar and 58 ºC (Figure 38). Since, the latter value is not high enough to enable the hot PCMs charge, the generated heat during this operation mode is rejected to the ambient. This TCM reactor – environment interaction is the other boundary of the system operation, meaning that the evaporation process can be conducted at temperatures as low as -10 ºC, without hindering the TCM heat release to the ambient.

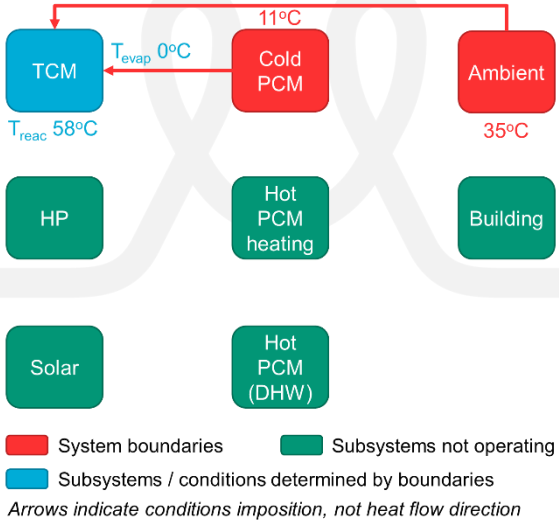

Figure 38: Boundaries of operating temperatures in summer TCM discharge mode

5.2.2.3 Operating conditions in direct supply from solar and demand covered by PCMs modes

As it can be observed in Figure 30 and Figure 31, in direct supply from solar operating mode the only MiniStor thermal subsystems involved are the solar field along with the hot PCMs. Thus, the characteristic temperature of the latter dominates the system operating conditions, as observed also in Figure 39. Interesting is the fact that a solar field heat supply realised at a temperature of 70 ºC, as determined in TCM summer charging mode, can meet the hot PCMs charging requirements too.

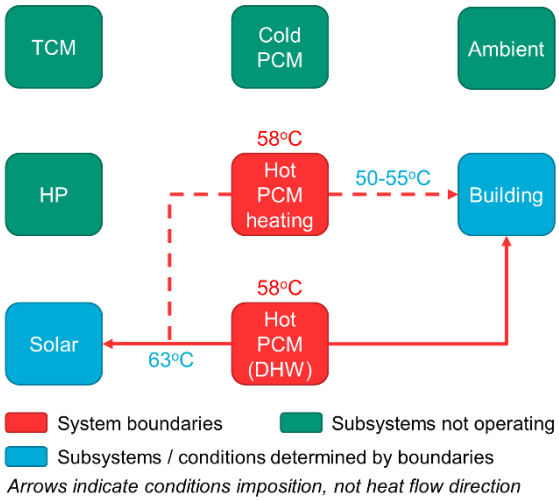

Figure 39: Boundaries of operating temperatures in direct supply form solar mode

Finally, the case where the demand is covered only by the PCMs does not impose any restrictions to the operating conditions of rest MiniStor components. The PCM vessels exchange heat or cold with the building heating and cooling system respectively and only the maximum flow rate and working pressure threshold of the vessels limit the rate of this energy transfer. Obviously, the latter occurs at a temperature defined by the PCM characteristics temperatures (max 50-55 °C for the hot PCMs and min 14-18 °C for the cold one).

5.2.3 System main specifications

From the above analysis it can be deduced that the TCM reactor and evaporator are not expected to experience pressures higher than 5-6 bar under normal operating conditions. On the contrary, in the section between the compressor discharge and the liquid ammonia reservoir pressures ranging from 12 up to 16 bar are considered. Consequently, the specifications of the TCM compressor, condenser and ammonia tank, along with those of the connecting valves and pipes should ensure leak free operation under such high pressures. This is of paramount importance, especially considering the ammonia toxicity as described in Chapter 4.

As far as the developed temperatures in the TCM subsystem is concerned, their normal values would not exceed 65 / 75 °C depending on the occurring reaction. The maximum condensation temperature would be in the range of 28-30 °C, whereas that of evaporation could be as low as -15 °C. However, due to the high temperature of gaseous ammonia exiting the reactor, the corresponding values at the compressor discharge would be as high as 230 °C. The latter value is well beyond the maximum operating temperature of commercially available ammonia compressors, thus necessitating the ammonia vapour subcooling down to around -15 °C at the compressor discharge. This is to be realised by a liquid ammonia injection system, potentially in combination with a gas-cooler as described in D4.3 “Design and development of ancillary equipment for heating/cooling storage”. The smooth and trouble-free operation of these systems is significant in order to avoid a damage of the compressor, which would in turn hinder the implementation of the TCM charge mode.

The HP specifications as shaped by the TCM charge operation mode is winter, as the operation of this subsystem is not foreseen to occur in other system modes. As was mentioned above, HP should combine a heat sink of 63 °C with an evaporation heat source in the range of 22-26 °C. The HP COP under these operating conditions should be as high as possible in order to minimise the system electrical consumption and thus achieve a high overall efficiency. Matching the HP and the TCM subsystems capacities is also important in order to ensure a proper and efficient system operation. On the contrary, the PCMs (cold and hot ones alike) are the MiniStor boundaries towards the building and therefore their specifications are used to estimate those of other internal system components. Similarly, the PCMs specifications regarding their working pressure and allowed flow rate should be taken into consideration when designing MiniStor connection with the building heating and cooling system. Finally, the TCM requirement for heat supply at a specific temperature is a significant constraint that should be taken into account when defining the solar

field layout and choosing the PVTs and the solar collectors' models. However, equipment (air dissipator, pressure relief valves etc.) to keep the heat developed in the solar field temperatures and pressures within the specified thresholds, is necessary to be included in order to avoid damage of the panels or the collectors.

6 Current and future thermal loads estimations for Santiago de Compostela demo site

6.1 Demo site description

The operation of MiniStor thermal energy storage system will be demonstrated in the facilities of University of Santiago de Compostela (USC), which is located in the city of the same name in North-western Spain. More specifically, MiniStor will provide heating, DHW and electricity to an apartment of the Burgo de Las Naciones University Residence (RUBN), a U-shaped building with a South-North orientation, total area of 14686.9 m^2 and constructed in 1991. The dwelling (apartment B) is located in the first floor of the west wing that is marked in circle in Figure 40 below. The RUBN building is used as student residences and the demo apartment, with a heated area of approximately 80.5 m^2 is occupied by a three-person family. Its entrance is on the ground floor and the space below it is a non-heating one as it is occupied by warehouse and boiler rooms. A sketch of the apartment is provided in Figure 41.

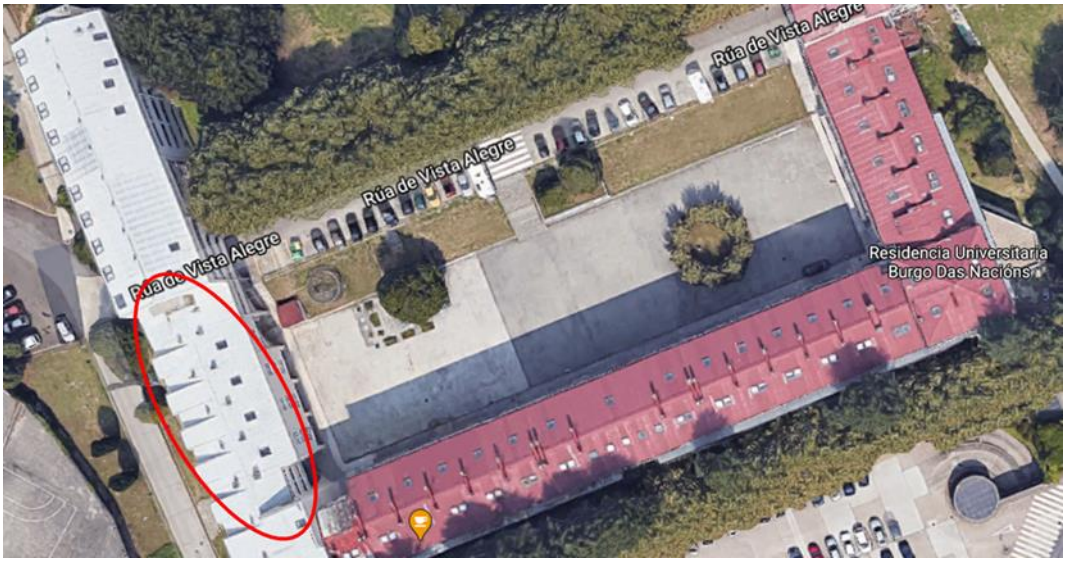

Figure 40: Aerial view of the Burgo de Las Naciones University Residence. The west wing where the demo apartment is located is marked with the red circle.

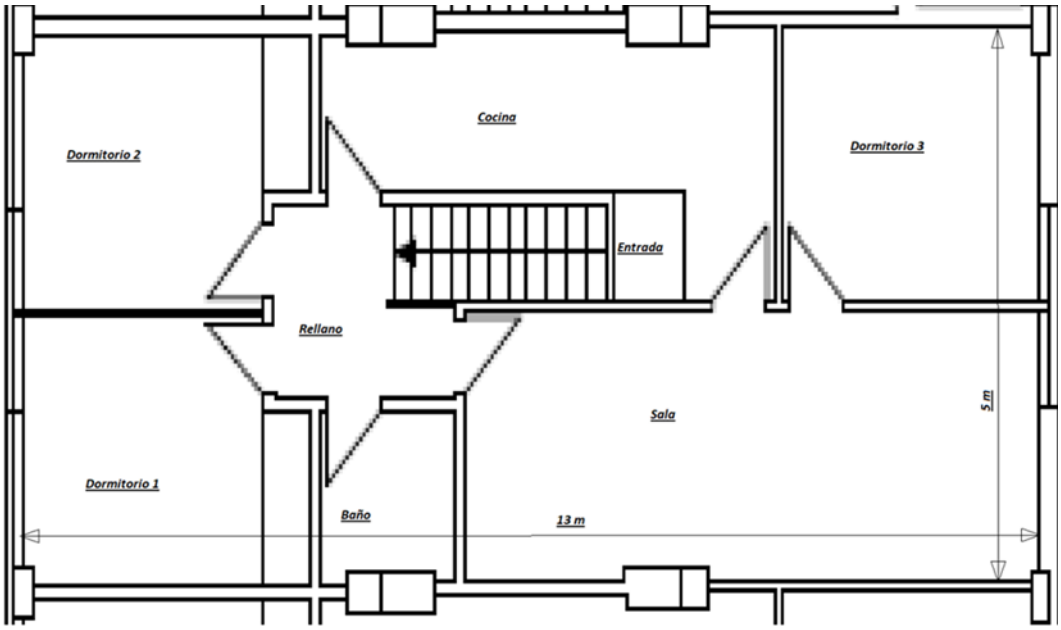

Figure 41: Sketch of the demo Apartment B

This analysis regards the estimations of the current and future thermal loads of USC demo site and follows the same approach as for the rest of the pilot sites presented in Deliverable "D2.2 - Definition of system context and limits of use", incorporating also some aspects of the daily load profiles estimations followed in Deliverable "D3.1 - Initial dimensioning of the system according to general use typologies".

6.2 The Heating and Cooling Degree Days methodology

The first step of the analysis regards the quantification of the building thermal and cooling needs by utilising the heating and cooling degree days (HDD, CDD) methodology, which is a variation of the Heating Degrees Hours concept discussed in paragraph 2.2.1. In general, one HDD expresses a positive difference of 1K between a base temperature, for which heating is not considered necessary, and the daily mean ambient temperature of one day of the year. Monthly or annual values of HDDs are computed by summing up the individual daily degree-days in a month or within a year respectively.

In the current analysis, the base temperatures of Table 6 for Spain are considered (i.e. 17 °C for the HDD and 22 °C for the CDD calculation). Weather data are retrieved from a suitable for the demo site location TMY file from the Meteonorm database (similar to the cases of Sopron, Thessaloniki and Cork), which provides hourly data derived from meteorological stations. Therefore, the daily Heating Degree Day values are defined according to the hourly method, with the use of Equation 3 below:

$$HDD_{daily} = \frac{\sum_{i=1}^{24}(T_b - T_{ext,i})^+}{24} \qquad \text{Equation 3}$$

T_b is the base temperature and $T_{ext,\,i}$ is the ambient temperature at the i^{th} hour of the day. The symbol "+" denotes that only positive differences of the corresponding variables are considered. The resulting annual HDD value is 1795.1, whereas the CDD value is equal to 48.3. It is obvious that the location of the demo site, placed in the north-western Spain and characterized by a temperate oceanic climate (Cfb according to Köppen-Geiger classification), reflects on the very low cooling needs. This trend is very similar to that of Cork demo site (similarly of Cfb classification) as reported in D2.2.

Based on the idea that heat demand can be considered as the product of the building overall Heat Loss Coefficient (*HLC* introduced in paragraph 2.2.1) with the temperature difference between indoor (T_{ind}) and outdoor (T_{ext}) conditions (Equation 4), the HDD and CDD indicators can be used for simplified heat analysis (CIBSE, 2006). By assuming steady state conditions occurring over a period of time, this can lead to a formula combining the building heating demand Q_{ht}, its overall heat loss coefficient and the calculated HDD value (Equation 5). The number of hours of each day ($N_{h,j}$) is also considered in order to derive the energy

in kWh. Similarly, the annual cooling demand can be linked to the CDD value. Thus, by knowing the overall heat loss coefficient and ambient temperature values, estimations of energy demand over different years or approximations of its monthly distribution can be realised.

$$Heat\ losses\ (kW) = HLC\ \cdot (T_{ind} - T_{ext}) \quad \text{Equation 4}$$

$$Q_{ht} = HLC\ \cdot HDD \cdot N_{h,j} \quad \text{Equation 5}$$

6.3 Estimations of the demo site current heat load

6.3.1 Approximation of annual heating demand based on fuel consumption data

In order to calculate the building overall heat loss coefficient, an estimation of the demo site energy demand is necessary. For this purpose, data of fuel (diesel) consumption were provided by the demo site manager. This information regarded measurements of the RUBN building fuel tanks for the periods January 2017 – December 2018 & August 2019 – September 2020, before the renovation of the building heat generation system. It should also be highlighted that the diesel boilers were used for both space heating and DHW generation, however it was not possible to divide the fuel consumption between these two functions. In general, the heating system was due to ensure constant availability of DHW, whereas space heating operation was varying according to weather conditions with 7:00 – 14:00 & 16:00 – 23:00 being a usual schedule for cold days of the year. In addition, a co-generation unit provides heat to three buildings, RUBN building being one of them. Information about the total heat production of this plant were provided for the years 2017 and 2018. Table 35 summarizes the estimated energy content of the consumed diesel for each month for which fuel measurements were available. Because of the latter temporal irregularity, equal daily consumption between two successive measurements was considered in order to approximate the monthly consumptions, whereas for three months (January 2017, December 2018 and August 2019) extrapolation had to be performed due to incomplete consumption data. Table 36 presents the approximated annual heat demand covered by the diesel boilers, considering an average efficiency of 90%, along with the estimated heat supplied to the RUBN building by the co-generation unit.

Table 35: Estimations of consumed diesel energy content per month (USC demo site)

Month	Diesel Energy Content (kWh), 2017	Portion of yearly energy, 2017	Diesel Energy Content (kWh), 2018	Portion of yearly energy, 2018	Diesel Energy Content (kWh), 2019-20	Portion of yearly energy, 2019-20
January	294,817.87	24.86%	203,889.87	15.36%	188,377.62	16.31%
February	144,190.99	12.16%	179,010.32	13.49%	125,907.04	10.90%
March	76,804.60	6.48%	227,261.65	17.12%	169,591.52	14.69%
April	99,564.42	8.40%	135,148.36	10.18%	154,696.44	13.40%
May	86,478.20	7.29%	103,001.14	7.76%	76,084.63	6.59%
June	53,291.84	4.49%	49,091.76	3.70%	16,823.66	1.46%
July	47,984.67	4.05%	47,752.38	3.60%	13,191.58	1.14%
August	46,284.62	3.90%	32,278.33	2.43%	57,069.17	4.94%
September	56,953.62	4.80%	31,237.09	2.35%	55,228.23	4.78%
October	68,462.48	5.77%	32,278.33	2.43%	71,836.76	6.22%
November	81,898.67	6.91%	136,923.43	10.32%	96,997.50	8.40%
December	129,085.52	10.89%	149,288.20	11.25%	128,998.68	11.17%
Total	1,185,817.50	100%	1,327,160.85	100%	1,154,802.82	100%

Table 36: Estimations of annual heat demand (space heating and DHW) of RUBN building

	2017	2018	2019-20
Heat delivered by diesel boilers (kWh)	1,067,235.75	1,194,444.76	1,039,322.54

Heat supplied by Co-generation (kWh)	491,333.33	637,333.33	No data available
Total supplied heat (kWh)	1,558,569.08	1,831,778.10	-

Taking into account all the above presented data, the annual and monthly heat supplied to apartment B was approximated. In order to achieve that the specific heat supply per unit area had to be calculated using the total area of RUBN building (i.e. 14686.9 m^2). Due to the lack of data for the co-generation unit heat supply regarding the period August 2019 – September 2020, the average heat supply was calculated taking into account only the values of years 2017 and 2018. Nevertheless, the monthly percentages of annual energy covered by diesel were computed considering all the available data in order to mitigate some discrepancies between the three datasets, especially in months January, March and April. The results of this analysis are presented in the below Table, giving annual energy delivery for both space heating and DHW production equal to 9288 kWh and a specific energy demand of 115.42 kWh / m^2. The energy for DHW can be approximated by the values of Table 27, which for 3 persons yield an annual energy for DHW equal to 3343.6 kWh. Considering all the above along with the annual HDD value (i.e. 1795.1 HDD), the resulting HLC of the apartment is equal to 0.138 kW/K. By considering a HDD reduction proportional to the heating system operating hours during the day, the resulting HLC increases considerably to 0.2365 kW/K.

Table 37: Average monthly heat demand (space heating and DHW) of RUBN building and apartment B

Month	Average portion of annual energy	Average heat supplied by diesel boilers (kWh)	Average total heat delivered to RUBN building (kWh)	Specific heat delivered to RUBN building (kWh/m^2)	Average total heat delivered to apart. B (kWh)
January	18.85%	213,115.851	319,468.96	21.75	1750.38
February	12.18%	137,776.852	206,532.87	14.06	1131.60
March	12.76%	144,320.035	216,341.35	14.73	1185.34
April	10.66%	120,530.441	180,679.83	12.30	989.95
May	7.21%	81,579.7958	122,291.29	8.33	670.04
June	3.22%	36,375.1745	54,527.80	3.71	298.76
July	2.93%	33,122.1442	49,651.38	3.38	272.04
August	3.76%	42,509.0903	63,722.78	4.34	349.14
September	3.98%	45,003.8938	67,462.59	4.59	369.63
October	4.81%	54,379.3581	81,516.78	5.55	446.63
November	8.54%	96,585.1411	144,784.89	9.86	793.28
December	11.10%	125,542.478	188,193.06	12.81	1031.12
Total	100%	1,130,840.25	1,695,173.59	115.42	9287.91

6.3.2 Approximation of heat load based on the EN 12831:2017 Standard

An alternative way to estimate the building overall heat loss coefficient, is to calculate the building thermal losses following the methodology set out at the EN 12831:2017 Standard. Parameters required for the calculation of the heat demand include:

- Outdoor weather conditions.
- Desired indoor temperature. This was set to 21 °C as this is the interior temperature value indicated by the Spanish Regulation on Thermal Installations in Buildings for the dimensioning of heating systems ("Real Decreto 178/2021, de 23 de marzo, por el que se modifica el Real Decreto 1027/2007, de 20 de julio, por el que se aprueba el Reglamento de Instalaciones Térmicas en los Edificios.," 2021).
- Characteristics of the building affecting the transmission heat losses from the building envelope (e.g. floor area, area of the exposed walls, area of windows and doors, thermal transmittance of the building elements etc.)
- Infiltration and ventilation losses (e.g. air permeability of the building envelope, use of mechanical ventilation etc.)

- Operation pattern of the building heating system (constant or intermittent use that may result in additional heating demand due to reheating of the heated area)

Input data for this calculation were taken from the building plans (Figure 41), information obtained from the demo site manager as well as typical values for the thermal transmittance of the building elements for buildings of that region and year of construction included in one of the Spanish official tools for building energy rating assessment in existing buildings called CE3X (IDAE - Instituto para la Diversificación y Ahorro de la Energía, 2012) (e.g. 1.8 W/m^{2}K for walls, 3.8 W/m^{2}K for opaque elements etc.). Following the methodology of the EN 12831:2017 Standard described above, the Heat Transfer Coefficient of the flat accounting for both the transmission (0.1573 kW/K) and infiltration losses (0.0319 kW/K) was determined at 0.1892 kW/K. This value is almost the average of the two values calculated using the monitoring data of fuel consumption and the computed annual HDDs. Therefore, it can be considered a relatively accurate approximation of the HLC value and was used for the calculations described in the subsequent paragraphs.

6.3.3 Estimation of load profiles for thermodynamic simulations

Similar to the other demo sites, the performance of the Ministor system is to be numerically investigated in this case too by conducting dynamic simulations utilising the thermodynamic model developed in the framework of Task 3.1. These simulations, the results of which will be included in an updated version of D3.1, will concern specific periods of time representative of extreme and typical conditions during the heating season (since the system will be used only for providing heating to the selected dwelling). Additionally, since significant heating needs are observed from October until May, an additional average heating scenario of the spring and autumn months will be considered. Furthermore, in order to make easier the investigation of the Ministor system operational strategies over time periods of variable duration, these scenarios include three subsequent days of the extreme (or correspondingly of the typical) heating conditions.

The representative three-day periods were selected considering the main climate parameters that affect the performance of the system, namely external temperature and levels of solar radiation, and following the approach that was set out in D3.1. The main steps of this approach involve:

1. Defining the daily Heating Degree Day values according to the hourly method. This step was already realised in the beginning of the thermal loads calculations of Santiago de Compostela demo sit and is described in paragraph 6.2.
2. Defining the daily total solar radiation on horizontal surface.
3. Identifying the maximum HDD value (HDD_{max}) and the minimum daily total solar radiation on horizontal surface ($G_{h,min}$).
4. Identifying the average daily HDD (HDD_{ave}) and the average daily total solar radiation on horizontal surface ($G_{h,ave}$) for the heating season.
5. For each day the variables *LSE* and *LSA* are calculated according to Equation 6 and Equation 7 respectively. The first one expresses the difference of the daily HDD and total solar radiation values from the daily extreme values identified in step 3. Similarly, *LSA* is representative of the deviation of the daily HDD and solar radiation values from the average ones (calculated in step 4).
6. The daily *LSE* and *LSA* values are summed over periods of three subsequent days.
7. The three-day period with the lowest *LSE* value, is selected. Effectively this is the time period with weather conditions very close to the extreme ones. Accordingly, the three-day period with the lowest *LSA* value presents weather conditions very similar to the average ones.

$$LSE_j = \frac{(HDD_{max} - HDD_j)^2}{HDD_{max}^2} + \frac{(G_{h,min} - G_{h,j})^2}{G_{h,min}^2} \quad \text{Equation 6}$$

$$LSA_j = \frac{(HDD_{ave} - HDD_j)^2}{HDD_{ave}^2} + \frac{(G_{h,ave} - G_{h,j})^2}{G_{h,ave}^2} \quad \text{Equation 7}$$

Where HDD_j and $G_{h,j}$ are the Heating Degree Day and the total solar on horizontal surface on the jth day of the year.

Following the steps described above, the extreme and typical three-day periods of the heating season (considering a duration of the latter from November until March) along with a typical period for spring / autumn months were determined:

- Extreme winter period: 22 – 24 December
- Averaging heating period: 24 – 26 November
- Spring – autumn period: 1 – 3 October

The hourly fluctuation of ambient temperature and solar radiation on horizontal surface for the extreme winter period and the average heating period that will be used as inputs into the MiniStor thermodynamic model are presented in the following graphs.

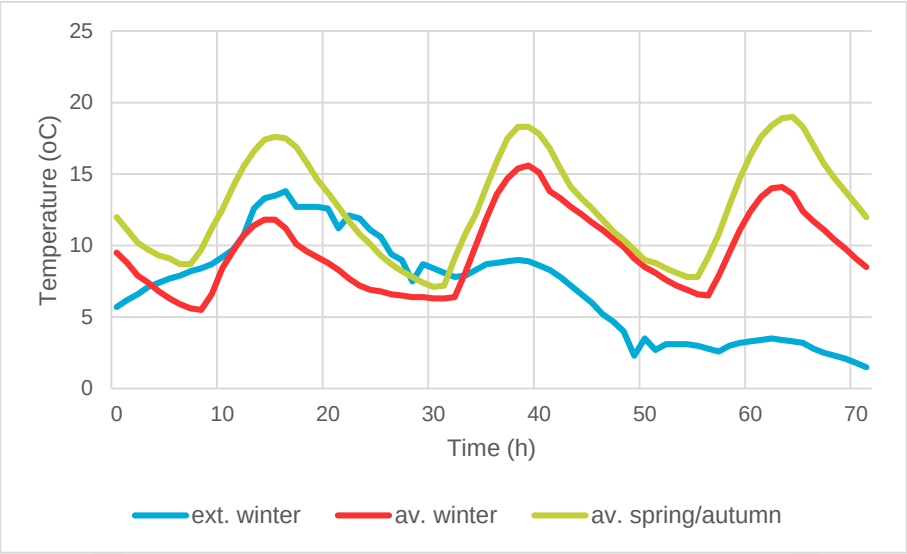

Figure 42: Hourly temperature variation of the extreme and average winter scenarios in Santiago de Compostela

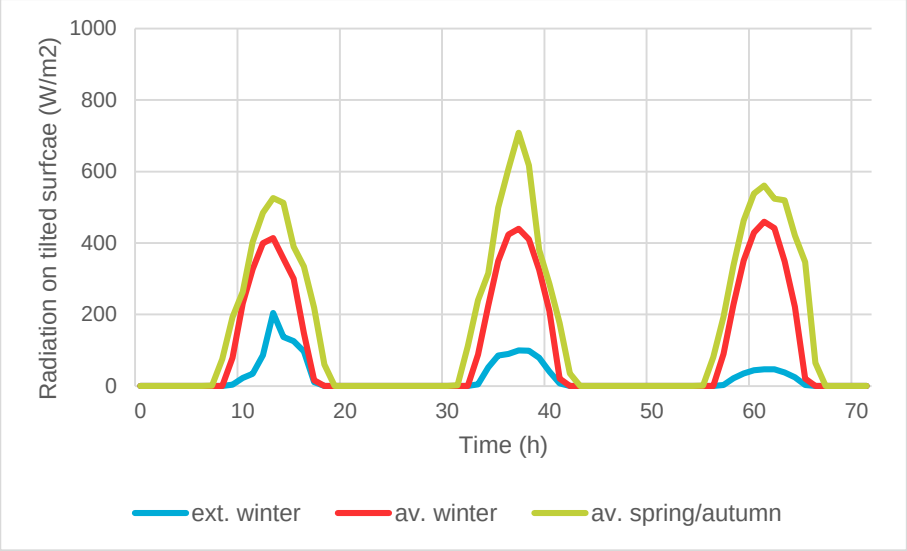

Figure 43: Variation of the hourly radiation on horizontal surface for the extreme and average winter scenarios in Santiago de Compostela

Having determined the outdoor conditions and the relevant time periods for the extreme and average winter scenarios, the heat demand of the demo site was estimated using the overall heat loss coefficient of the apartment as determined by the methodology described in EN 12831:2017 Standard and discussed in paragraph 6.3.2. Finally, a suitable heating operation schedule was set based on feedback from the building manager and the apartment occupants. This involves 9.5 hours of operation during the coldest period of the year (i.e. in the midst of winter) and a 7-hour operation on days with mildly cold weather (i.e. in autumn and at the end of winter). In spring, a 5-hour operation is foreseen, which is very similar to that

of the mildly cold weather with the exception of the function at noon. Both cases are presented in Figure 44 below. Based on these assumptions and data, the maximum heating load for the demo site was estimated at 5.17kW. The hourly variation of heating requirements throughout the 3-day average and extreme winter periods is presented in Figure 45.

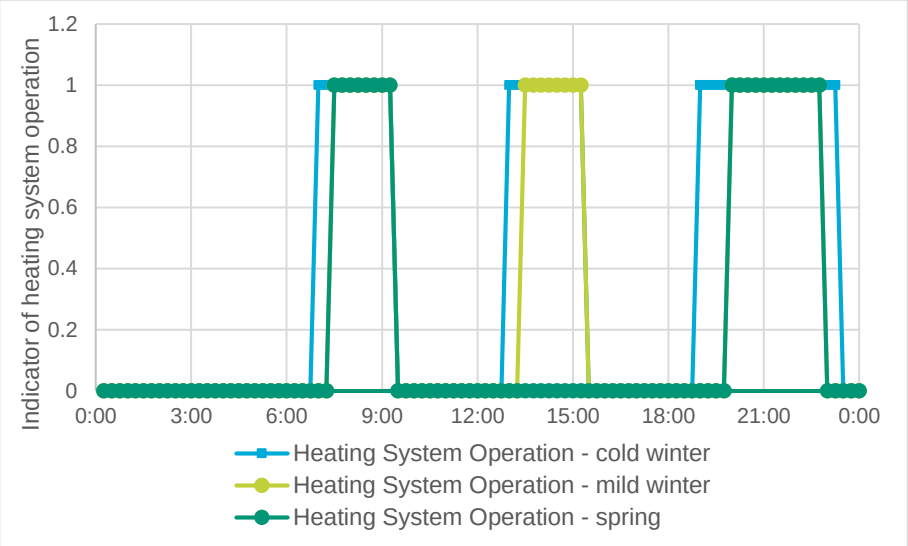

Figure 44: Heating system operation schedule

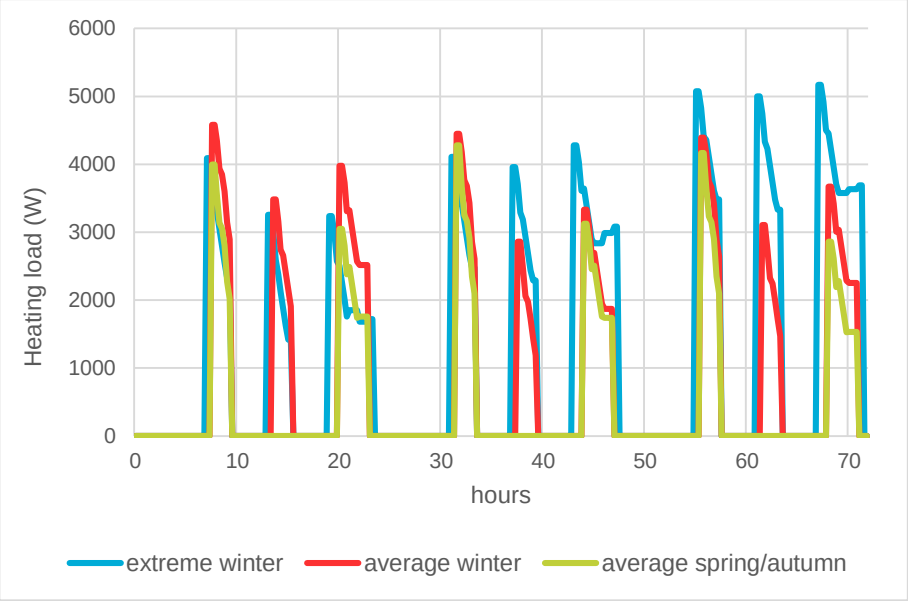

Figure 45: Extreme and Average heating load in Santiago de Compostela demo site

6.4 Estimations of the demo site future loads

6.4.1 Calculation of future Heating and Cooling Degree Days

The future energy needs of the pilot site are also estimated in order to investigate the performance of the system under the future climatic conditions. For this, a short term and a long- term scenario are considered in the analysis where the HDDs for the years 2030 and 2050 are determined. Following the methodology set out in D2.2, projections of the daily mean air temperature for the two selected years were obtained from Coordinated Regional Climate Downscaling Experiment (CORDEX) word climate research program datasets (ECMWF; Horanyi, 2020). More particularly, daily mean temperature data were taken from two separate datasets as shown in table below. It should be noted that similarly to the analysis conducted in

D2.2 for the rest of the demo sites, the Representative Concentration Pathway scenario RCP4.5 was selected for the datasets, i.e. the scenario where radiative forcing is increased by 4.5W/m^2 by 2100 compared to pre-industrial levels (van Vuuren et al., 2011). This is a moderate scenario according to which the equivalent CO_2 concentrations are expected to increase until 2080 and then stabilise from 2080 to 2100 at approximately 650ppm (Thomson et al., 2011). Both datasets regard fine simulation resolution (0.11°), use the same Regional Climatic Model (RCM) and are bias-adjusted, i.e. they use as reference data for the period 1981-2010 the E-OBS high-resolution gridded dataset which results in the mitigation of inaccurate spatial patterns (Jonathan Spinoni et al., 2018). Their main difference is the utilization of a different Global Climate Model (GCM) that provides lateral and lower boundary conditions to the used RCM. For reasons of increased accuracy, the average value of the individual daily temperature obtained from each dataset was considered in the calculation of the HDDs.

Table 38: Characteristics of the used EURO-CORDEX simulations for future temperature estimations

GCM	RCM	GSM members	Resolution
HadGEM2-ES (UK Met Office, UK)	RCA4 (SMHI, Sweden)	r1i1p1	0.11°
IPSL-CM5A-MR (IPSL, France)	RCA4 (SMHI, Sweden)	r1i1p1	0.11°

Using the mean daily temperature data ($T_{ext,\,mean}$) calculated with the above mentioned methodology, the Heating Degree Days for 2030 and 2050 were calculated in order to assess the future thermal loads of the building. In this analysis, the American Society of Heating, Refrigerating and Air-Conditioning (ASHRAE) daily mean temperature method was used described by Equation 8, as it requires only the knowledge of this variable (Mourshed, 2012).

$$HDD_{daily} = \left(T_b - T_{ext,mean}\right)^+ \quad \text{Equation 8}$$

Firstly, in order to account for the relative error introduced by the use of the different sources of data, i.e. the Meteonorm TMY file for the estimation of the current building load and the simulation datasets used for the projected building loads in 2030 and 2050, a comparison was made between the two sources for the reference year[7]. The Degree Days for the reference year using the average daily mean temperature from the two simulation datasets (ISPL and UK Met Office models) were calculated at 1832.4 HDDs and 30.3 CDDs. This was a relative difference of 2.08% for HDDs compared to the results obtained using the Meteonorm TMY file, suggesting very good agreement between the two sources of data and increasing confidence on the results of the future building loads analysis. The relative error in the case of CDDs is high (37.24%), but it be considered acceptable due to the very low magnitude of the absolute values.

The resulted future Degree Days are presented in Figure 46 below. As expected the building heating load for the demo site is set to be decreased; the Heating Degree Days are reduced from 1795.1 HDDs in the reference year of the Meteonorm TMY file (2005) to 1732.3 HDDs in 2030 (-3.5%) and further reduced to 1613.2 in 2050 (-10.1% from reference values). Regarding the cooling load, the future CDD values are lower than the reference TMY-based ones (-42.2% in 2030 and -12.2% in 2050), but in comparison with the reference simulation-based values they remain almost stable in the short-term scenario and show an increase (+ 39.9%) in the long-term scenario. In general, the trend of HDDs future projections is in accordance with the conclusions of other studies, but the latter show more intense rises of the cooling loads throughout Europe (Diffenbaugh et al., 2007; Isaac & van Vuuren, 2009; Jonathan Spinoni et al., 2018).

[7] Both the ISPL model and the Met Office models considered simulation data for 2006, as no relevant data for 2005 were available.

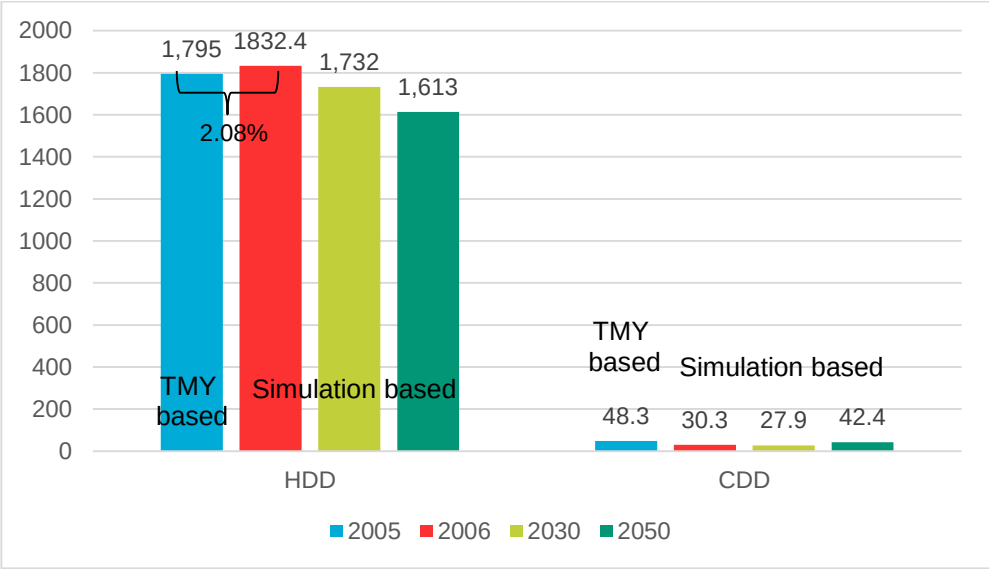

Figure 46: Estimation of the Heating Degree Days in 2030 and 2050 in comparison to the reference year (2005)

Table 39: Average and maximum daily degree day values for USC location

Year	Mean daily HDD	Peak daily HDD	Mean daily CDD	Peak daily CDD
Reference (2005)	6.70	15.28	0.38	5.00
2030	6.96	12.35	0.23	4.59
2050	6.50	14.31	0.34	5.05

In addition, Table 39 summarises the mean and peak daily degree day values for the current and future scenarios. For HDDs these indicators are calculated in the period October – May, whereas for the CDDs in the period June – September. It is very interesting that contrary to the annual sum of HDDs, the short-term scenario presents higher mean daily HDD value than the reference scenario. This denotes that in the latter case the period between June and September presents a not negligible number of HDDs. Mean daily CDDs present a similar variation pattern with their annually summed amounts. Maximum daily degree days show higher values in the long-term scenario than the short-term one. In addition, their relative change from the reference values is quite lower than the corresponding variation of annual values. All the above denote an increased tension of extreme weather conditions in the future, which is in accordance with the conclusion of other relevant studies (Diffenbaugh et al., 2007) and the outcome of D2.2 analysis as well.

6.4.2 Estimation of future heating and cooling loads

By combining the previous Degree Days analysis with the overall heat loss coefficient of the building, estimated to 0.1892 kW/K in paragraph 6.3.2, the future heating and cooling demand can be estimated. By using this HLC value, the annual loads are shaped as following:

Table 40: Estimated heating and cooling loads in reference year, 2030 and 2050 for USC demo site

	Reference year (2005)	2030	2050
Annual heat load (kWh)	8151.2	7866.0	7325.2
Annual cooling load (kWh)	219.3	126.6	192.7

Figure 47 and Figure 48 present the estimated monthly heat and cooling loads respectively. In accordance with the mean daily HDD analysis, in the reference case several non-zero heat loads are spotted during summer months, which are confined in both future cases. January and December are clearly the two

months with the highest thermal loads in the reference scenario (close to 1250 kWh), while February is ranked third (load of 1100 kWh). Short-term future case shows a similar picture, with the notable exception of March presenting comparable heat demand with January and December. In long-term scenario the maximum demand is a bit lower (about 1200 kWh in January), March is the second energy intensive month (about 1100 kWh), followed by February, April and December all presenting loads in the range of 1000 kWh. This distribution pattern is in accordance with the monitoring monthly consumption data, which perhaps denotes a future shift of maximum heat load towards the end of winter that already starts to be experienced. Of further support of this statement, are the higher future heat loads in March and April compared to the reference year. Additionally, autumn heat demand is expected to decrease according to future projections.

Regarding cooling loads projections, reference year presents an arch-shaped distribution from May till October with peaks being spotted in July and August (close to 65 kWh). On the contrary, in the short-term scenario almost all yearly cooling demand is concentrated in August (about 110 kWh). Long-term future case shows a more even cooling load distribution, with peaks of almost equal value (85 kWh) in July and In August. But in this case too, no demand for cooling is observed in May or June.

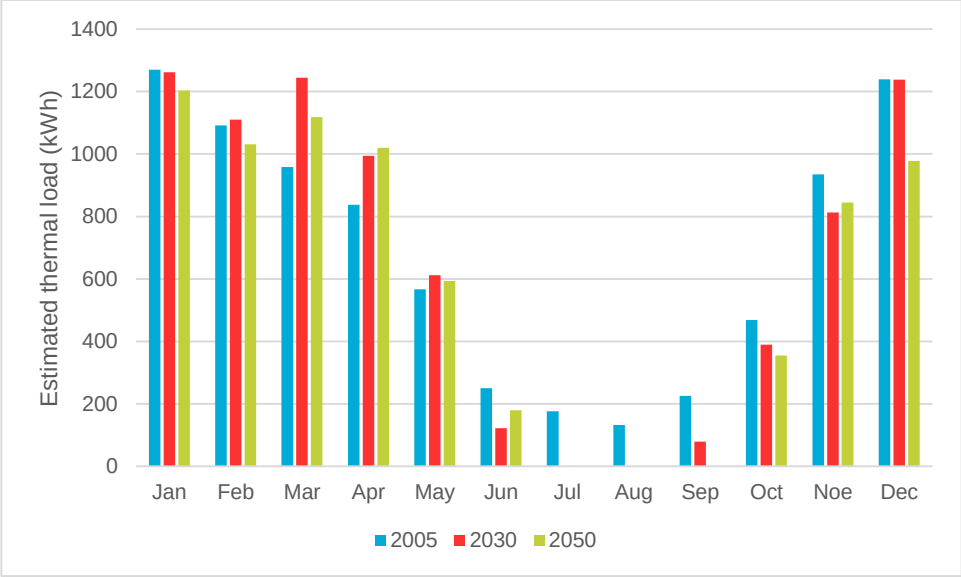

Figure 47: Estimated monthly heating loads in reference year, 2030 and 2050 for USC demo site

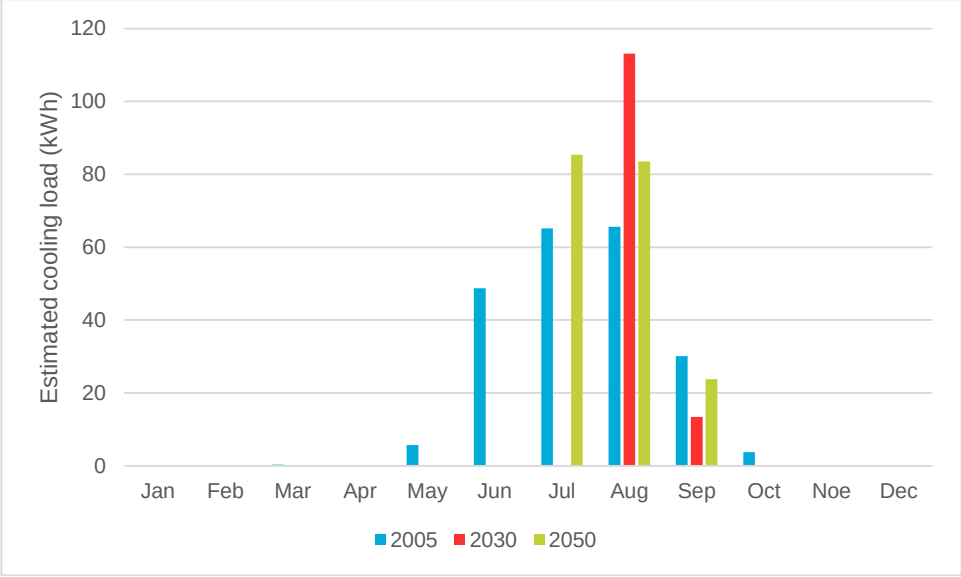

Figure 48: Estimated monthly cooling loads in reference year, 2030 and 2050 for USC demo site

Finally, Table 41 depicts a detailed summary of the estimated mean and peak heating loads for each month of the reference as well as of the future scenarios. In accordance with the previous analysis, the three winter months of reference case present the highest mean daily heat demand (in the range of 39 – 41 kWh), with the highest value being spotted in January (close to 69 kWh). In the short-term future scenario March also presents high mean loads of same magnitude, while the peak values of all months are reduced compared to the 2005 case. Long-term future scenario shows mean daily heating loads higher than 36 kWh for the period January – March and in general peak values higher than 2030 but lower than the reference year. Both future cases present considerably increased average daily heat demand in April, but decreased and negligible in absolute terms daily heating loads from June till September.

Estimated cooling loads of the reference case present mean daily values of 2.10 kWh in both July and August (Table 42), but with a significantly higher peak value of 22.7 kWh in July. Both future cases show maximum loads of comparable magnitude, in August in the short-term scenario and in July in the long-term one. However, the highest mean values are increased and are close to 3.65 kWh in August of 2030 and 2.70 kWh in July and August of 2050. Generally, the latter case presents a pattern close to that of the reference case with the exception of the zero cooling needs in May and June. In general, these two months present in both future scenarios smaller temperature deviations than the reference case. This increase of minimum temperature values leads to a reduction of heating future needs, whereas the decrease of maximum mean daily temperature values below the utilised base temperature for cooling, results in a simultaneous reduction of cooling future needs.

Table 41: Estimated average and maximum daily heating loads in reference year, 2030 and 2050 for USC demo site

	Mean daily heat load (kWh), 2005	Peak daily heat load (kWh), 2005	Mean daily heat load (kWh), 2030	Peak daily heat load (kWh), 2030	Mean daily heat load (kWh), 2050	Peak daily heat load (kWh), 2050
January	40.97	69.36	40.71	54.06	38.83	64.97
February	39.01	63.93	39.66	49.41	36.84	51.26
March	30.93	55.38	40.13	49.94	36.09	46.17
April	27.91	49.40	33.16	43.35	34.00	48.85
May	18.27	37.40	19.73	31.69	19.15	34.04
June	8.34	19.60	4.08	16.71	5.99	21.11
July	5.67	15.84	0.05	0.75	0.00	0.00
August	4.28	12.51	0.00	0.00	0.00	0.00
September	7.52	17.58	2.62	13.77	0.00	0.00
October	15.12	33.79	12.57	24.10	11.44	30.17
November	31.15	54.21	27.09	45.24	28.16	50.85
December	39.98	66.92	39.96	56.10	31.56	50.13

Table 42: Estimated average and maximum daily cooling loads in reference year, 2030 and 2050 for USC demo site

	Mean daily cooling load (kWh), 2005	Peak daily cooling load (kWh), 2005	Mean daily cooling load (kWh), 2030	Peak daily cooling load (kWh), 2030	Mean daily cooling load (kWh), 2050	Peak daily cooling load (kWh), 2050
May	0.18	2.55	0.00	0.00	0.00	0.00
June	1.62	17.69	0.00	0.00	0.00	0.00
July	2.10	22.70	0.00	0.00	2.75	22.92
August	2.12	13.47	3.65	20.84	2.69	15.84
September	1.00	7.45	0.45	5.51	0.79	5.42
October	0.12	1.65	0.00	0.00	0.00	0.00

From the above presented results, it can be deduced that due to the overall decrease of future heating loads in the USC location, the values of the reference scenario can be safely used for the dimensioning of MiniStor system. The mean cooling loads are expected to increase in the future, but the peak values will not face major changes. Nevertheless, this is of minor importance since cooling load coverage is not expected to be realized in this demo site.

7 Conclusions

This deliverable has presented the currently available thermal energy storage technologies, namely sensible heat storage, latent heat-based systems and thermochemical storage systems. The latter are characterised by low maturity, nevertheless they present higher energy storage densities compared to latent and sensible heat storage systems. MiniStor is based on a TCM system, utilising also PCMs for increased flexibility. Despite the system complexity, the utilisation of ammoniated CaCl2 salts as thermochemical materials offers high exergetic efficiency and enables the storage of both heat and cold. Moreover, MiniStor's main operating principle is already used in cold storage commercial applications, thus mitigating the main disadvantage of other thermochemical energy storage solutions.

An important factor that can influence the applicability of the MiniStor system, is the energy demand of residential buildings. Following the building typologies introduced in D2.2 and using online available tools and databases, the peak heating and cooling loads for representative buildings in several European countries were presented. The well-established methodology of heating and cooling degree days was used and apart from the classification of dwellings into detached, semi-detached and flats, distinct calculations were performed for buildings of different age of construction and (when applicable) of different location within each examined country. Additionally, estimations of the monthly DHW-related energy demand in each country were also provided. The general trend regards a decrease of thermal loads in buildings of newer construction throughout Europe. On top of that, detached dwellings tend to have the higher energy demand (in the range of 2.8 – 14.4 kW peak for heating and 1.6 – 12.6 kW peak for cooling in constructions after 1980), whereas flats are the less energy intensive typology (peak heating demand of 1 – 6.9 kW and peak cooling demand of 0.3 – 5.8 kW in buildings constructed after 1980). A comparison with the corresponding thermal needs of MiniStor project demo sites, revealed that the peak heating demands of the latter (3.8 – 6.6 kW) are well within the range of the aforementioned values of representative dwellings of relative new construction. The demo sites cooling demands are higher (5.8 – 8.1 kW) than the statistically obtained values, but this difference can at least in part be attributed to the inability of the utilised methodology to take into account heat gains due to human activity, solar irradiance and operation of appliances. Thus, the evaluation of MiniStor system performance within the framework of the project activities, would yield very useful results and applicable to a high number of European dwellings.

Moreover, RES systems suitable for integration with MiniStor were defined, as this factor would also affect the replication potential of the system. Hybrid PVTs potentially combined with solar thermal collectors is one option that can adequately provide the necessary heat input to the TCM reactor and at the required temperature level (60 ^{o}C if an energy density of 200 kWh/m^{3} is to be achieved). In addition to its renewable and free of emissions nature, this solution offers also the potential of electrical energy generation and storage, covering a wide aspect of the dwelling energy needs. Consequently, this combination will be implemented in the majority of the project demo sites. An alternative solution, similarly based on solar energy harvesting, is the utilisation of conventional PVs (or even PVTs optimised for increased electrical output) providing renewable energy to a HP, that in turn supplies the necessary heat input to the system. This configuration involves increased flexibility as the HP can also be fed from the grid utilising DR schemes and will be tested in Santiago de Compostela demo site. A third solution, a variation of which will be tested in Kimmeria demo site, is the usage of a biomass boiler, which can be very attractive if such heating system is already used by the dwelling. Major advantages of this option compared to the other two, are the limited space requirements and the ability to operate independently from the solar irradiance availability. However, it requires a constant fuel supply and it involves particle, NOx and SOx emissions. The analysis of the RES systems was combined with a brief presentation of recent advances in the fields of PVs, PVTs and HPs. In order to present a complete overview of suitable RES technologies, a survey regarding the renewable generation of electricity, heating and cooling in Europe was also conducted. It was revealed that PVs have a significant share in the makeup of renewable electricity generation in several countries of Southern and Central Europe, whereas significant increase of residential PV installations is forecasted. Biomass has a dominant share in renewable heating generation and only in Southern European countries solar energy is used for relevant purposes. Moreover, HPs are wide spread in many countries of Central and Southern Europe as they are used not only for heating but also for cooling generation. This fact renders the currently under research concept of SAHPs, as a very promising solution for integration with MiniStor. Finally, the use of geothermal energy for supplying heat to MiniStor system is another option worthy of

future consideration, as medium-temperature basins are quite common in Central Europe, but at present not widely exploited.

An assessment of the impact of ammonia-related restrictions on the system installation has also been included in the deliverable, based on the main findings of D2.3. Because of the toxicity of this substance, the ammonia containing components should be placed either in an open shelter or in a closed box, with the latter being the most attractive solution that ensures high levels of safety. A distance of 2m between openings of this “closed machinery room” and building exterior openings must be foreseen. Additionally, this closed space should be equipped with necessary safety instrumentation (i.e. for ventilation, drainage, firing control, ammonia scrubbing etc.) that will mitigate the effects of a potential ammonia leakage. However, all these restrictions impose difficulties and challenges in the system installation in existing machinery rooms or generally in dwellings with open space limitations, such as individual flats.

Another objective of the current document is the conceptual definition of the system operation modes along with the corresponding operating conditions. More particularly, four main operation modes were identified, namely “TCM charge”, “TCM discharge”, “Direct supply from solar” and “Demand covered by PCM units only”. Main and detailed steps of each mode were described in this deliverable, with further details on operating conditions being included in D5.1. “TCM charge” mode involves the highest number of steps, but “TCM discharge” appears to be the most challenging one from control perspective as it involves three different variations depending on the season and the ambient conditions. On the other hand, “Direct supply from solar” and “Demand covered by PCM units only” are simpler modes since their realization involves a limited number of operating components. The corresponding operational conditions are mainly shaped by the system boundaries, i.e. the characteristic temperatures of the storage systems (TCM, PMCs) and the ambient conditions. Noteworthy is the fact that contrary to the control perspective, the operational one involves different conditions for “TCM charge” between winter and summer. In general, hot PCMs’ specifications impose the system operating pressures and temperatures in almost all cases except from summer “TCM charge” and “TCM discharge”, whereas TCM reactor acts as a system boundary only in “TCM charge” mode in winter. Ambient plays an important role when it acts as a heat sink or a heat source for the system, i.e. during regular winter and summer system discharge as well as in summer charge. The proposed utilisation of cold PCM for regulating the ammonia evaporating conditions, enables the smooth system discharge on days with very low temperatures.

Finally, the deliverable has included thermal load estimations for Santiago de Compostela demo site, as this information was not possible to be included in D2.2, due to the late admission of USC into the MiniStor consortium. Due to the lack of heat demand data of the demo site (i.e. the apartment), this is approximated on annual and monthly basis using fuel consumption data of the whole building and after making the necessary assumptions. By combining this information with the HDD methodology, two values of the apartment heat loss coefficient were reached. Heat loads were also approximated by using the methodology described in standard EN 12831:2017 along with building plans and statistical data of heat loss coefficient values for the various building elements. As a consequence, a third overall HLC value was calculated and finally selected for defining the heat load profiles that will feed the thermodynamic simulations for this demo site. Moreover, estimations of future short (2030) and long-term (2050) heating and cooling needs of the apartment were presented.

The outcomes of this deliverable regarding the characteristics of competing thermal storage technologies, the dwellings’ heating and cooling needs, the utilisation of RES in Europe and the integration of such systems with MiniStor and the restrictions imposed by the use of ammonia will be used as input, along with relevant findings of Deliverables 2.1, 2.2 and 2.3, for the market analysis and the investigation of impact maximization to be performed in WP7. The conceptual definition of system operation modes, along with the defined corresponding operational conditions will feed the activities of WP5, in which a detailed assessment of the system control parameters will be conducted and the design of MiniStor control will be realised. Demonstration activities (WP6) will also benefit from this information as well as from the assessment of ammonia related restrictions. The estimated heat loads of Santiago de Compostela demo site will be used for conducting the necessary simulations that will result in the dimensioning of the system components in the framework of WP3.

References

Aguilar, F. J., Aledo, S., & Quiles, P. V. (2016). Experimental study of the solar photovoltaic contribution for the domestic hot water production with heat pumps in dwellings. *Applied Thermal Engineering, 101*, 379-389. doi:https://doi.org/10.1016/j.applthermaleng.2016.01.127

Arpagaus, C., Bless, F., Uhlmann, M., Schiffmann, J., & Bertsch, S. S. (2018). High temperature heat pumps: Market overview, state of the art, research status, refrigerants, and application potentials. *Energy, 152*, 985-1010. doi:https://doi.org/10.1016/j.energy.2018.03.166

Beck, T., Kondziella, H., Huard, G., & Bruckner, T. (2017). Optimal operation, configuration and sizing of generation and storage technologies for residential heat pump systems in the spotlight of self-consumption of photovoltaic electricity. *Applied Energy, 188*, 604-619. doi:https://doi.org/10.1016/j.apenergy.2016.12.041

Bellos, E., Tzivanidis, C., Moschos, K., & Antonopoulos, K. A. (2016). Energetic and financial evaluation of solar assisted heat pump space heating systems. *Energy Conversion and Management, 120*, 306-319. doi:https://doi.org/10.1016/j.enconman.2016.05.004

Bergene, T., & Løvvik, O. M. (1995). Model calculations on a flat-plate solar heat collector with integrated solar cells. *Solar Energy, 55*(6), 453-462. doi:https://doi.org/10.1016/0038-092X(95)00072-Y

Bertsch, S. S., & Groll, E. A. (2008). Two-stage air-source heat pump for residential heating and cooling applications in northern U.S. climates. *International Journal of Refrigeration, 31*(7), 1282-1292. doi:https://doi.org/10.1016/j.ijrefrig.2008.01.006

Buker, Mahmut S., & Riffat, S. B. (2016). Solar assisted heat pump systems for low temperature water heating applications: A systematic review. *Renewable and Sustainable Energy Reviews, 55*, 399-413. doi:https://doi.org/10.1016/j.rser.2015.10.157

Cabeza, L. F. (2019). Latent Thermal Energy Storage. In A. Frazzica & L. F. Cabeza (Eds.), Recent Advancements in Materials and Systems for Thermal Energy Storage. Green Energy and Technology: Springer, Cham. doi:https://doi.org/10.1007/978-3-319-96640-3_2

Cabeza, L. F., Castell, A., Barreneche, C., de Gracia, A., & Fernández, A. I. (2011). Materials used as PCM in thermal energy storage in buildings: A review. *Renewable and Sustainable Energy Reviews, 15*(3), 1675-1695. doi:https://doi.org/10.1016/j.rser.2010.11.018

Chen, Q., Finney, K., Li, H., Zhang, X., Zhou, J., Sharifi, V., & Swithenbank, J. (2012). Condensing boiler applications in the process industry. *Applied Energy, 89*(1), 30-36. doi:https://doi.org/10.1016/j.apenergy.2010.11.020

Chow, T. T. (2003). Performance analysis of photovoltaic-thermal collector by explicit dynamic model. *Solar Energy, 75*(2), 143-152. doi:https://doi.org/10.1016/j.solener.2003.07.001

Chow, T. T., Pei, G., Fong, K. F., Lin, Z., Chan, A. L. S., & He, M. (2010). Modeling and application of direct-expansion solar-assisted heat pump for water heating in subtropical Hong Kong. *Applied Energy, 87*(2), 643-649. doi:https://doi.org/10.1016/j.apenergy.2009.05.036

Chua, K. J., Chou, S. K., & Yang, W. M. (2010). Advances in heat pump systems: A review. *Applied Energy, 87*(12), 3611-3624. doi:https://doi.org/10.1016/j.apenergy.2010.06.014

CIBSE. (2006). *Degree days: Theory and application* (Vol. Technical Manual 41). London,UK: Chartered Institution of Building Services Engineers.

Climate.OneBuilding. Retrieved from http://climate.onebuilding.org/

Cornette, J. F. P., Coppieters, T., Lepaumier, H., Blondeau, J., & Bram, S. (2021). Particulate matter emission reduction in small- and medium-scale biomass boilers equipped with flue gas condensers: Field measurements. *Biomass and Bioenergy, 148*, 106056. doi:https://doi.org/10.1016/j.biombioe.2021.106056

Cuypers, R., Maraz, N., Eversdijk, J., Finck, C., Henquet, E., Oversloot, H., . . . de Geus, A. (2012). Development of a Seasonal Thermochemical Storage System. *Energy Procedia, 30*, 207-214. doi:https://doi.org/10.1016/j.egypro.2012.11.025

da Cunha, J. P., & Eames, P. (2018). Compact latent heat storage decarbonisation potential for domestic hot water and space heating applications in the UK. *Applied Thermal Engineering, 134*, 396-406. doi:https://doi.org/10.1016/j.applthermaleng.2018.01.120

de Gracia, A., & Cabeza, L. F. (2015). Phase change materials and thermal energy storage for buildings. *Energy and Buildings, 103*, 414-419. doi:https://doi.org/10.1016/j.enbuild.2015.06.007

Diffenbaugh, N. S., Pal, J. S., Giorgi, F., & Gao, X. (2007). Heat stress intensification in the Mediterranean climate change hotspot. *Geophysical Research Letters, 34*(11). doi:https://doi.org/10.1029/2007GL030000

Dincer, I., & Rosen, M. A. (2010). *Thermal Energy Storage: Systems and Applications* (Second ed.). Chichester, UK: John Wiley & Sons, Ltd. doi:10.1002/9780470970751

Duffie, J. A., & Beckman, W. A. (2013). *Solar Engineering of Thermal Processes* (Fourth ed.). Hoboken, New Jersey, United States of America: John Wiley & Sons, Inc.

ECMWF. CORDEX regional climate model data on single levels for Europe (Deprecated 2020-11-12). Retrieved March 2021 https://cds.climate.copernicus.eu/cdsapp#!/dataset/projections-cordex-single-levels?tab=overview

Energy: new target of 32% from renewables by 2030 agreed by MEPs and ministers. (2018). Retrieved from European Parliament website: https://www.europarl.europa.eu/news/en/press-room/20180614IPR05810/energy-new-target-of-32-from-renewables-by-2030-agreed-by-meps-and-ministers

EurObserv'ER. (2020). *Heat Pumps Barometer* Retrieved from https://www.eurobserv-er.org/heat-pumps-barometer-2020/

European Standard EN 378-1:2016 - Refrigerating systems and heat pumps - Safety and environmental requirements. (2016). *Part 1: Basic requirements, definitions, classification and selection criteria*. Brussels: Europen Committee for Standardization.

Eurostat. (2019). SHARES (Renewables). Retrieved April 2021 https://ec.europa.eu/eurostat/web/energy/data/shares

Finck, C., Spijker, H., Jong, A.-J., Henquet, E., Oversloot, H., & Cuypers, R. (2013). *Design of a modular 3 kWh thermochemical heat storage system for space heating application*. Paper presented at the IC-SES 2, Sustainable Energy Storage in Buildings Conference, Dublin, Ireland.

Franco, A., & Fantozzi, F. (2016). Experimental analysis of a self consumption strategy for residential building: The integration of PV system and geothermal heat pump. *Renewable Energy, 86*, 1075-1085. doi:https://doi.org/10.1016/j.renene.2015.09.030

Frazzica, A., Brancato, V., Palomba, V., & Vasta, S. (2019). Sorption Thermal Energy Storage. In A. Frazzica & L. F. Cabeza (Eds.), Recent Advancements in Materials and Systems for Thermal Energy Storage. Green Energy and Technology: Springer, Cham. doi:https://doi.org/10.1007/978-3-319-96640-3_4

Freitas Gomes, I. S., Perez, Y., & Suomalainen, E. (2020). Coupling small batteries and PV generation: A review. *Renewable and Sustainable Energy Reviews, 126*, 109835. doi:https://doi.org/10.1016/j.rser.2020.109835

Gautam, A., & Saini, R. P. (2020). A review on technical, applications and economic aspect of packed bed solar thermal energy storage system. *Journal of Energy Storage, 27*, 101046. doi:https://doi.org/10.1016/j.est.2019.101046

Gröhn, A., Suonmaa, V., Auvinen, A., Lehtinen, K. E. J., & Jokiniemi, J. (2009). Reduction of Fine Particle Emissions from Wood Combustion with Optimized Condensing Heat Exchangers. *Environmental Science & Technology, 43*(16), 6269-6274. doi:10.1021/es8035225

Große, R., Binder, C., Wöll, S., Geyer, R., & Robbi, S. (2017). *Long term (2050) projections of techno-economic performance of large-scale heating and cooling in the EU*. Luxembourg: Publications Office of the European Union, EUR 28859 EN. doi:10.2760/24422, JRC109006

Hasan, M. A., & Sumathy, K. (2010). Photovoltaic thermal module concepts and their performance analysis: A review. *Renewable and Sustainable Energy Reviews, 14*(7), 1845-1859. doi:https://doi.org/10.1016/j.rser.2010.03.011

Hauer, A. (2007). Evaluation of adsorbent materials for heat pump and thermal energy storage applications in open systems. *Adsorption, 13*(3), 399-405. doi:10.1007/s10450-007-9054-0

Hawlader, M. N. A., Rahman, S. M. A., & Jahangeer, K. A. (2008). Performance of evaporator-collector and air collector in solar assisted heat pump dryer. *Energy Conversion and Management, 49*(6), 1612-1619. doi:https://doi.org/10.1016/j.enconman.2007.12.001

Hebenstreit, B., Riepl, R., Ohnmacht, R., Höftberger, E., & Haslinger, W. (2011). *Efficiency Optimization of Biomass Boilers by a Combined Condensation - Heat Pump - System*.

Heitkoetter, W., Medjroubi, W., Vogt, T., & Agert, C. (2020). Regionalised heat demand and power-to-heat capacities in Germany – An open dataset for assessing renewable energy integration. *Applied Energy, 259*, 114161. doi:https://doi.org/10.1016/j.apenergy.2019.114161

High energy density sorption heat storage for solar space heating. (1998). Retrieved from https://cordis.europa.eu/project/id/JOR3980199

Horanyi, A. (2020). Overview of regional climate projections. Retrieved from https://confluence.ecmwf.int/display/COPSRV/Overview+of+regional+climate+projections

IDAE - Instituto para la Diversificación y Ahorro de la Energía. (2012). *Manual de usuario de calificación energética de edificios existentes CE3X* Retrieved from http://www6.mityc.es/aplicaciones/CE3X/Manual_usuario%20CE3X_05.pdf

IEA-ETSAP, & IRENA. (2013). *Thermal Energy Storage, Technology Brief E17*.

IEA. (2014). *Technology Roadmap - Energy Storage* Retrieved from https://www.iea.org/reports/technology-roadmap-energy-storage

IEA. (2020). Renewables 2020 Data Explorer. Retrieved April 2021, from IEA https://www.iea.org/articles/renewables-2020-data-explore

IEA Bioenergy, IRENA, & FAO. (2017). Bioenergy for Sustainable Development. Retrieved from https://www.ieabioenergy.com/blog/publications/bioenergy-for-sustainable-development/

Isaac, M., & van Vuuren, D. P. (2009). Modeling global residential sector energy demand for heating and air conditioning in the context of climate change. *Energy Policy, 37*(2), 507-521. doi:https://doi.org/10.1016/j.enpol.2008.09.051

Jakubcionis, M., & Carlsson, J. (2017). Estimation of European Union residential sector space cooling potential. *Energy Policy, 101*, 225-235. doi:https://doi.org/10.1016/j.enpol.2016.11.047

Ji, J., He, H., Chow, T., Pei, G., He, W., & Liu, K. (2009). Distributed dynamic modeling and experimental study of PV evaporator in a PV/T solar-assisted heat pump. *International Journal of Heat and Mass Transfer, 52*(5), 1365-1373. doi:https://doi.org/10.1016/j.ijheatmasstransfer.2008.08.017

Ji, J., Pei, G., Chow, T.-t., Liu, K., He, H., Lu, J., & Han, C. (2008). Experimental study of photovoltaic solar assisted heat pump system. *Solar Energy, 82*(1), 43-52. doi:https://doi.org/10.1016/j.solener.2007.04.006

Johannes, K., Kuznik, F., Hubert, J.-L., Durier, F., & Obrecht, C. (2015). Design and characterisation of a high powered energy dense zeolite thermal energy storage system for buildings. *Applied Energy, 159*, 80-86. doi:https://doi.org/10.1016/j.apenergy.2015.08.109

Kadioğlu, M., Şen, Z., & Gültekin, L. (2001). Variations and Trends in Turkish Seasonal Heating and Cooling Degree-Days. *Climatic Change, 49*(1), 209-223. doi:10.1023/A:1010637209766

Kampouris, K. P., Drosou, V., Karytsas, C., & Karagiorgas, M. (2020). Energy storage systems review and case study in the residential sector. *IOP Conference Series: Earth and Environmental Science, 410*, 012033. doi:10.1088/1755-1315/410/1/012033

Kerskes, H., Heidemann, W., & Müller-Steinhagen, H. (2004). *MonoSorp - Ein weiterer Schritt auf dem Weg zur vollständig solarthermischen Gebäudeheizung.* Paper presented at the 14 Symposium Thermische Solarenergie, OTTI Energie-Kolleg, Regensburg, Germany.

Kerskes, H., Mette, B., Bertsch, F., Asenbeck, S., & Drück, H. (2012). Chemical energy storage using reversible solid/gas-reactions (CWS) – results of the research project. *Energy Procedia, 30*, 294-304. doi:https://doi.org/10.1016/j.egypro.2012.11.035

Krese, G., Koželj, R., Butala, V., & Stritih, U. (2018). Thermochemical seasonal solar energy storage for heating and cooling of buildings. *Energy and Buildings, 164*, 239-253. doi:https://doi.org/10.1016/j.enbuild.2017.12.057

Kuang, Y. H., & Wang, R. Z. (2006). Performance of a multi-functional direct-expansion solar assisted heat pump system. *Solar Energy, 80*(7), 795-803. doi:https://doi.org/10.1016/j.solener.2005.06.003

Lass-Seyoum, A., Blicker, M., Borozdenko, D., Friedrich, T., & Langhof, T. (2012). Transfer of laboratory results on closed sorption thermo- chemical energy storage to a large-scale technical system. *Energy Procedia, 30*, 310-320. doi:https://doi.org/10.1016/j.egypro.2012.11.037

Lass-Seyoum, A., Borozdenko, D., Friedrich, T., Langhof, T., & Mack, S. (2016). Practical Test on a Closed Sorption Thermochemical Storage System with Solar Thermal Energy. *Energy Procedia, 91*, 182-189. doi:https://doi.org/10.1016/j.egypro.2016.06.200

Litjens, G. B. M. A., Worrell, E., & van Sark, W. G. J. H. M. (2018). Lowering greenhouse gas emissions in the built environment by combining ground source heat pumps, photovoltaics and battery storage. *Energy and Buildings, 180*, 51-71. doi:https://doi.org/10.1016/j.enbuild.2018.09.026

Lu, Y. Z., Wang, R. Z., Zhang, M., & Jiangzhou, S. (2003). Adsorption cold storage system with zeolite–water working pair used for locomotive air conditioning. *Energy Conversion and Management, 44*(10), 1733-1743. doi:https://doi.org/10.1016/S0196-8904(02)00169-3

Milone, C., Kato, Y., & Mastronardo, E. (2019). Thermal Energy Storage with Chemical Reactions. In A. Frazzica & L. F. Cabeza (Eds.), Recent Advancements in Materials and Systems for Thermal Energy Storage. Green Energy and Technology: Springer, Cham. doi:https://doi.org/10.1007/978-3-319-96640-3_3

Modular high energy density sorption heat storage. (2008). Retrieved from https://cordis.europa.eu/project/id/13608

Mourshed, M. (2012). Relationship between annual mean temperature and degree-days. *Energy and Buildings, 54*, 418-425. doi:https://doi.org/10.1016/j.enbuild.2012.07.024

N'Tsoukpoe, K. E., Rammelberg, H. U., Lele, A. F., Korhammer, K., Watts, B. A., Schmidt, T., & Ruck, W. K. L. (2015). A review on the use of calcium chloride in applied thermal engineering. *Applied Thermal Engineering, 75*, 513-531. doi:https://doi.org/10.1016/j.applthermaleng.2014.09.047

Nemś, M., Nemś, A., Kasperski, J., & Pomorski, M. (2017). Thermo-Hydraulic Analysis of Heat Storage Filled with the Ceramic Bricks Dedicated to the Solar Air Heating System. *Materials, 10*(8). doi:10.3390/ma10080940

Olonscheck, M., Holsten, A., & Kropp, J. P. (2011). Heating and cooling energy demand and related emissions of the German residential building stock under climate change. *Energy Policy, 39*(9), 4795-4806. doi:https://doi.org/10.1016/j.enpol.2011.06.041

Ould Amrouche, S., Rekioua, D., Rekioua, T., & Bacha, S. (2016). Overview of energy storage in renewable energy systems. *International Journal of Hydrogen Energy, 41*(45), 20914-20927. doi:https://doi.org/10.1016/j.ijhydene.2016.06.243

Papakostas, K., Mavromatis, T., & Kyriakis, N. (2010). Impact of the ambient temperature rise on the energy consumption for heating and cooling in residential buildings of Greece. *Renewable Energy, 35*(7), 1376-1379. doi:https://doi.org/10.1016/j.renene.2009.11.012

Perea-Moreno, M.-A., Manzano-Agugliaro, F., & Perea-Moreno, A.-J. (2018). Sustainable Energy Based on Sunflower Seed Husk Boiler for Residential Buildings. *Sustainability, 10*(10). doi:10.3390/su10103407

Petralli, M., Massetti, L., & Orlandini, S. (2011). Five years of thermal intra-urban monitoring in Florence (Italy) and application of climatological indices. *Theoretical and Applied Climatology, 104*(3), 349-356. doi:10.1007/s00704-010-0349-9

Petri, Y., & Caldeira, K. (2015). Impacts of global warming on residential heating and cooling degree-days in the United States. *Scientific Reports, 5*(1), 12427. doi:10.1038/srep12427

Real Decreto 178/2021, de 23 de marzo, por el que se modifica el Real Decreto 1027/2007, de 20 de julio, por el que se aprueba el Reglamento de Instalaciones Térmicas en los Edificios. (2021). BOLETÍN OFICIAL DEL ESTADO.

Renaldi, R. (2018). *Modelling and optimisation of energy systems with thermal energy storage.* (PhD Thesis), University of Edinburgh, Edinburgh. Retrieved from http://hdl.handle.net/1842/31214

Robles-Ocampo, B., Ruíz-Vasquez, E., Canseco-Sánchez, H., Cornejo-Meza, R. C., Trápaga-Martínez, G., García-Rodriguez, F. J., . . . Vorobiev, Y. V. (2007). Photovoltaic/thermal solar hybrid system with bifacial PV module and transparent plane collector. *Solar Energy Materials and Solar Cells, 91*(20), 1966-1971. doi:https://doi.org/10.1016/j.solmat.2007.08.005

Safijahanshahi, E., & Salmanzadeh, M. (2019). Performance simulation of combined heat pump with unglazed transpired solar collector. *Solar Energy, 180*, 575-593. doi:https://doi.org/10.1016/j.solener.2019.01.038

Sarbu, I., & Sebarchievici, C. (2017). Chapter 6 - Heat Distribution Systems in Buildings. In I. Sarbu & C. Sebarchievici (Eds.), *Solar Heating and Cooling Systems* (pp. 207-239): Academic Press.

Sarbu, I., & Sebarchievici, C. (2018). A Comprehensive Review of Thermal Energy Storage. *Sustainability, 10*(1). doi:10.3390/su10010191

Scapino, L., Zondag, H. A., Van Bael, J., Diriken, J., & Rindt, C. C. M. (2017). Sorption heat storage for long-term low-temperature applications: A review on the advancements at material and prototype scale. *Applied Energy, 190*, 920-948. doi:https://doi.org/10.1016/j.apenergy.2016.12.148

Scarlat, N., Dallemand, J., Taylor, N., & Banja, M. (2019). *Brief on biomass for energy in the European Union* (J. Sanchez Lopez & M. Avraamides Eds.). Luxembourg: Publications Office of the European Union. doi:doi:10.2760/546943, JRC109354

Schreiber, H., Graf, S., Lanzerath, F., & Bardow, A. (2015). Adsorption thermal energy storage for cogeneration in industrial batch processes: Experiment, dynamic modeling and system analysis. *Applied Thermal Engineering, 89*, 485-493. doi:https://doi.org/10.1016/j.applthermaleng.2015.06.016

Shubbak, M. H. (2019). Advances in solar photovoltaics: Technology review and patent trends. *Renewable and Sustainable Energy Reviews, 115*, 109383. doi:https://doi.org/10.1016/j.rser.2019.109383

Skarbit, N., Stewart, I. D., Unger, J., & Gál, T. (2017). Employing an urban meteorological network to monitor air temperature conditions in the 'local climate zones' of Szeged, Hungary. *International Journal of Climatology, 37*(S1), 582-596. doi:https://doi.org/10.1002/joc.5023

Sögütoglu, L. C., Donkers, P. A. J., Fischer, H. R., Huinink, H. P., & Adan, O. C. G. (2018). In-depth investigation of thermochemical performance in a heat battery: Cyclic analysis of K2CO3, MgCl2 and Na2S. *Applied Energy, 215*, 159-173. doi:https://doi.org/10.1016/j.apenergy.2018.01.083

Spinoni, J., Vogt, J., & Barbosa, P. (2015). European degree-day climatologies and trends for the period 1951–2011. *International Journal of Climatology, 35*(1), 25-36. doi:https://doi.org/10.1002/joc.3959

Spinoni, J., Vogt, J. V., Barbosa, P., Dosio, A., McCormick, N., Bigano, A., & Füssel, H.-M. (2018). Changes of heating and cooling degree-days in Europe from 1981 to 2100. *International Journal of Climatology, 38*(S1), e191-e208. doi:https://doi.org/10.1002/joc.5362

Team E3P - DG JRC, D. C.-E., Transport and Climate. Typical Meteorological Year (TMY). Retrieved from https://e3p.jrc.ec.europa.eu/articles/typical-meteorological-year-tmy

Thomson, A. M., Calvin, K. V., Smith, S. J., Kyle, G. P., Volke, A., Patel, P., . . . Edmonds, J. A. (2011). RCP4.5: a pathway for stabilization of radiative forcing by 2100. *Climatic Change, 109*(1), 77. doi:10.1007/s10584-011-0151-4

Tyagi, V. V., Kaushik, S. C., & Tyagi, S. K. (2012). Advancement in solar photovoltaic/thermal (PV/T) hybrid collector technology. *Renewable and Sustainable Energy Reviews, 16*(3), 1383-1398. doi:https://doi.org/10.1016/j.rser.2011.12.013

van Helden, W., Yamaha, M., Rathgeber, C., Hauer, A., Huaylla, F., Le Pierrès, N., . . . Kuznik, F. (2016). IEA SHC Task 42 / ECES Annex 29 – Working Group B: Applications of Compact Thermal Energy Storage. *Energy Procedia, 91*, 231-245. doi:https://doi.org/10.1016/j.egypro.2016.06.210

van Vuuren, D. P., Edmonds, J., Kainuma, M., Riahi, K., Thomson, A., Hibbard, K., . . . Rose, S. K. (2011). The representative concentration pathways: an overview. *Climatic Change, 109*(1), 5. doi:10.1007/s10584-011-0148-z

Weber, R., Asenbeck, S., Kerskes, H., & Drück, H. (2016). SolSpaces – Testing and Performance Analysis of a Segmented Sorption Store for Solar Thermal Space Heating. *Energy Procedia, 91*, 250-258. doi:https://doi.org/10.1016/j.egypro.2016.06.214

Zalba, B., Marín, J. M., Cabeza, L. F., & Mehling, H. (2003). Review on thermal energy storage with phase change: materials, heat transfer analysis and applications. *Applied Thermal Engineering, 23*(3), 251-283. doi:https://doi.org/10.1016/S1359-4311(02)00192-8

Zettl, B., Englmair, G., & Steinmaurer, G. (2014). Development of a revolving drum reactor for open-sorption heat storage processes. *Applied Thermal Engineering, 70*(1), 42-49. doi:https://doi.org/10.1016/j.applthermaleng.2014.04.069

Zhang, J., Zhang, H.-H., He, Y.-L., & Tao, W.-Q. (2016). A comprehensive review on advances and applications of industrial heat pumps based on the practices in China. *Applied Energy, 178*, 800-825. doi:https://doi.org/10.1016/j.apenergy.2016.06.049

Zondag, H. A., de Vries, D. W., van Helden, W. G. J., van Zolingen, R. J. C., & van Steenhoven, A. A. (2002). The thermal and electrical yield of a PV-thermal collector. *Solar Energy, 72*(2), 113-128. doi:https://doi.org/10.1016/S0038-092X(01)00094-9

Annex

The annual heating and cooling demands calculated for each building type in each country/region is presented in this section. Additionally, the values of water supply temperature that were used in the DHW energy demand calculations (considered equivalent to the average monthly ground temperature at 0.5m) are given for each zone and country.

Greece

Table 43: Total annual heating requirements of the most common building types in Greece

Total Annual Heating Demand (kWh)				
Detached				
Year	Zone A	Zone B	Zone C	Zone D
Pre - 1980	8114	17253	24067	27690
1981 - 2000	8101	19807	20041	22428
2001 - 2010	6901	7452	12512	13176
2011 - 2020	2982	7854	7206	8825
Flats				
Year	Zone A	Zone B	Zone C	Zone D
Pre - 1980	2528	3422	5102	9387
1981 - 2000	3785	8628	7890	14532
2001 - 2010	1374	2522	6867	5043
2011 - 2020	1348	1640	3749	4065

Table 44: Total annual cooling requirements of the most common building types in Greece

Total Annual Cooling Demand (kWh)				
Detached				
Year	Zone A	Zone B	Zone C	Zone D
Pre - 1980	7048	12224	5510	2655
1981 - 2000	7037	14033	4588	2150
2001 - 2010	5994	5280	2864	1263
2011 - 2020	2591	5565	1650	846
Flats				
Year	Zone A	Zone B	Zone C	Zone D
Pre - 1980	2196	2424	1168	900
1981 - 2000	3288	6113	1806	1393
2001 - 2010	1194	1787	1572	483
2011 - 2020	1171	1162	858	390

Table 45: Average monthly ground temperature at 0.5m in Greece

Average monthly ground temperature at 0.5m (°C)				
Month	Zone A	Zone B	Zone C	Zone D
January	13.28	6.39	7.23	10.51
February	12.7	7.83	3.86	7.29
March	13.73	10.65	2.94	6.42
April	15.34	13.31	3.73	7.18
May	19.56	18.36	8.28	11.52
June	22.81	21.01	13.38	16.38
July	25	21.75	18.17	20.95

August	25.67	20.4	21.64	24.27
September	24.53	17.29	22.65	25.23
October	22.01	13.41	21.02	23.68
November	18.63	9.59	17.1	19.93
December	15.5	7.07	12.15	15.2

Hungary

Table 46: Total annual heating and cooling requirements of the most common building types in Hungary

	Total Annual Heating Demand (kWh)		Total Annual Cooling Demand (kWh)	
Year	Detached	Flats	Detached	Flats
Prior WWII	14861	7443	3000	1502
1945 – 1979	17354	5248	3503	1059
1980 – 1989	13071	6576	2638	1327
1990 – 2005	9735	4369	1965	882
2006 – 2020	8765	3984	1769	804

Table 47: Average monthly ground temperature at 0.5m in Hungary

Average monthly ground temperature at 0.5m (°C)				
January	1.53		July	20.53
February	0.59		August	21.61
March	2.26		September	19.77
April	4.87		October	15.68
May	11.7		November	10.21
June	16.98		December	5.13

Germany

Table 48: Total annual heating and cooling requirements of the typical detached dwellings in Germany

Detached								
Total Annual Heating Demand (kWh)								
Year	CR1	CR2	CR3	CR4	CR5	CR6	CR7	CR8
Pre – WWII	29242	30322	30298	30748	28772	32482	30743	33659
1945 – 1970	18453	19179	19166	19457	18211	20522	19445	20969
1971 –1980	22196	23078	23078	23666	21815	25725	23493	27092
1981 – 1990	21125	22334	22291	22896	20671	25315	22831	26935
1991 – 2000	16380	17190	17205	17610	16065	19305	17595	20340
2001 - 2010	11217	11849	11977	12287	10982	13921	12287	14930
2011 - 2020	13969	14792	14941	15465	13801	17746	15484	19130
Total Annual Heating Demand (kWh)								
Year	CR9	CR10	CR11	CR12	CR13	CR14	CR15	
Pre – WWII	31543	32923	44049	27895	31959	24687	32807	
1945 – 1970	19941	20776	27866	17606	20171	15589	20727	
1971 –1980	24393	26434	29981	20968	24912	18951	26192	
1981 – 1990	25596	26158	32119	19764	24430	18590	25942	
1991 – 2000	18255	19845	24015	15285	18690	14172	19635	
2001 - 2010	12818	14492	18568	10235	13329	10007	14163	
2011 - 2020	16213	18569	24086	12641	16961	12644	18083	
Total Annual Cooling Demand (kWh)								
Year	CR1	CR2	CR3	CR4	CR5	CR6	CR7	CR8
Pre – WWII	214	536	387	480	220	143	484	141

1945 – 1970	135	338	244	303	139	91	306	89
1971 –1980	164	411	297	368	169	110	372	108
1981 – 1990	161	403	291	361	165	108	365	106
1991 – 2000	123	307	222	275	126	82	278	81
2001 - 2010	87	217	157	194	89	58	196	57
2011 - 2020	109	274	198	246	112	73	248	72
Total Annual Cooling Demand (kWh)								
Year	CR9	CR10	CR11	CR12	CR13	CR14	CR15	
Pre – WWII	351	547	11	1434	584	1174	348	
1945 – 1970	222	346	7	906	369	741	220	
1971 –1980	270	420	9	1101	448	901	267	
1981 – 1990	264	412	9	1080	440	884	262	
1991 – 2000	202	314	7	823	335	674	200	
2001 - 2010	142	222	5	581	237	476	141	
2011 - 2020	180	280	6	734	299	601	178	

Table 49: Total annual heating and cooling requirements of the typical semi-detached dwellings in Germany

Semi-Detached								
Total Annual Heating Demand (kWh)								
Year	CR1	CR2	CR3	CR4	CR5	CR6	CR7	CR8
Pre – WWII	14695	15321	15325	15648	14432	17100	15461	18018
1945 – 1970	9828	10401	10401	10706	9606	11957	10682	12847
1971 –1980	10780	11363	11363	11660	10568	12837	11628	13579
1981 – 1990	10984	11567	11578	11869	10757	13100	11848	13889
1991 – 2000	9818	10419	10432	10854	9600	12019	10714	12890
2001 - 2010	9752	10339	10430	10798	9587	12386	10798	13372
2011 - 2020	12426	13367	13367	13955	12074	15896	13798	17385
Total Annual Heating Demand (kWh)								
Year	CR9	CR10	CR11	CR12	CR13	CR14	CR15	
Pre – WWII	16203	17563	20299	13833	16566	12575	17388	
1945 – 1970	11162	12425	15514	9114	11489	8682	12262	
1971 –1980	12148	13229	16080	10091	12413	9397	13112	
1981 – 1990	12323	13522	16524	10217	12647	9574	13349	
1991 – 2000	11264	12467	15757	9126	11558	8725	12352	
2001 - 2010	11280	12973	16984	8804	11822	8824	12574	
2011 - 2020	14680	16738	22305	11407	15190	11378	16464	
Total Annual Cooling Demand (kWh)								
Year	CR1	CR2	CR3	CR4	CR5	CR6	CR7	CR8
Pre – WWII	109	273	197	244	112	73	247	72
1945 – 1970	75	188	136	169	77	50	170	49
1971 –1980	81	204	147	183	84	55	184	54
1981 – 1990	83	208	150	186	85	56	188	55
1991 – 2000	76	189	137	170	78	51	171	50
2001 - 2010	76	191	138	171	78	51	173	50
2011 - 2020	99	247	178	221	101	66	223	65
Total Annual Cooling Demand (kWh)								
Year	CR9	CR10	CR11	CR12	CR13	CR14	CR15	
Pre – WWII	179	279	6	731	298	598	177	
1945 – 1970	124	192	4	504	205	413	122	
1971 –1980	134	208	4	546	222	447	133	
1981 – 1990	136	212	4	556	227	455	135	
1991 – 2000	124	193	4	507	206	415	123	

2001 - 2010	126	196	4	513	209	420	124	
2011 - 2020	162	252	5	661	269	541	160	

Table 50: Total annual heating and cooling requirements of the typical flats in Germany

Flats								
Total Annual Heating Demand (kWh)								
Year	CR1	CR2	CR3	CR4	CR5	CR6	CR7	CR8
Pre – WWII	12143	12688	12675	12926	11926	13950	12909	14632
1945 – 1970	9178	9678	9678	9932	8976	10954	9901	11620
1971 –1980	6810	7189	7186	7379	6668	8154	7359	8665
1981 – 1990	2155	2276	2274	2341	2107	2602	2334	2779
1991 – 2000	7523	7936	7951	8169	7375	9095	8153	9678
2001 - 2010	6328	6743	6767	7026	6177	8016	6997	8675
2011 - 2020	8502	9056	9108	9469	8283	10860	9443	11762
Total Annual Heating Demand (kWh)								
Year	CR9	CR10	CR11	CR12	CR13	CR14	CR15	
Pre – WWII	13357	14273	17774	11488	13578	10393	14198	
1945 – 1970	10335	11296	13843	8568	10572	8010	11199	
1971 –1980	7700	8418	10320	6370	7870	5959	8350	
1981 – 1990	2448	2694	3323	2012	2506	1895	2671	
1991 – 2000	8496	9414	11584	6979	8753	6607	9266	
2001 - 2010	7362	8392	10983	5782	7665	5732	8221	
2011 - 2020	9984	11375	14879	7794	10383	7742	11195	
Total Annual Cooling Demand (kWh)								
Year	CR1	CR2	CR3	CR4	CR5	CR6	CR7	CR8
Pre – WWII	90	225.5	163	201.9	92.4	60.4	203.8	59.2
1945 – 1970	69.4	173.8	125.6	155.6	71.2	46.5	157.1	45.7
1971 –1980	51.6	129.3	93.4	115.8	53	34.6	116.8	34
1981 – 1990	16.4	41.1	29.7	36.8	16.9	11	37.2	10.8
1991 – 2000	57.2	143.4	103.6	128.4	58.8	38.4	129.6	37.7
2001 - 2010	49.6	124.4	89.9	111.4	51	33.3	112.4	32.7
2011 - 2020	67	168	121.4	150.4	68.9	45	151.8	44.1
Total Annual Cooling Demand (kWh)								
Year	CR9	CR10	CR11	CR12	CR13	CR14	CR15	
Pre – WWII	147.9	230.4	4.8	603.8	245.9	494.2	146.6	
1945 – 1970	114	177.5	3.7	465.3	189.5	380.9	112.9	
1971 –1980	84.8	132.1	2.8	346.2	141	283.3	84	
1981 – 1990	27	42	0.9	110.1	44.8	90.1	26.7	
1991 – 2000	94	146.4	3.1	383.8	156.3	314.2	93.2	
2001 - 2010	81.5	127	2.7	333	135.6	272.5	80.8	
2011 - 2020	110.1	171.6	3.6	449.7	183.2	368.1	109.2	

Table 51: Average monthly ground temperature at 0.5m in Germany

Average monthly ground temperature at 0.5m (°C)								
Month	CR1	CR2	CR3	CR4	CR5	CR6	CR7	CR8
January	4.91	4.95	9.01	4.39	5.57	2.46	2.03	8.02
February	2.42	2.26	5.07	1.63	3.16	-0.12	1.31	4.22
March	1.74	1.53	2.65	0.88	2.5	-0.82	2.59	1.26
April	2.33	2.16	1.92	1.53	3.07	-0.21	4.61	-0.24
May	5.69	5.79	3.37	5.25	6.33	3.27	9.87	-0.69
June	9.45	9.86	6.64	9.42	9.97	7.16	13.93	1.19

July	12.99	13.68	10.7	13.35	13.41	10.83	16.67	4.37
August	15.56	16.45	14.68	16.19	15.89	13.49	17.5	8.17
September	16.3	17.26	17.35	17.02	16.62	14.26	16.08	11.44
October	15.1	15.96	17.98	15.68	15.45	13.02	12.93	13.25
November	12.2	12.83	16.43	12.47	12.64	10.01	8.72	13.21
December	8.54	8.87	13.21	8.41	9.09	6.22	4.81	11.33
Average monthly ground temperature at 0.5m (°C)								
Month	CR9	CR10	CR11	CR12	CR13	CR14	CR15	
January	0.85	-0.87	-1.05	3.56	3.28	2.45	-0.93	
February	0.14	0.77	-3.63	2.78	0.33	1.67	-1.69	
March	1.4	3.96	-4.33	4.16	-0.48	3.06	-0.35	
April	3.38	6.98	-3.72	6.32	0.22	5.23	1.75	
May	8.54	12.69	-0.24	11.99	4.2	10.91	7.22	
June	12.53	15.7	3.67	16.36	8.67	15.3	11.45	
July	15.22	16.53	7.35	19.31	12.86	18.25	14.3	
August	16.04	15.01	10.01	20.2	15.9	19.15	15.17	
September	14.64	11.48	10.78	18.67	16.79	17.62	13.69	
October	11.55	7.09	9.53	15.28	15.36	14.22	10.41	
November	7.41	2.76	6.52	10.75	11.92	9.67	6.02	
December	3.57	-0.09	2.73	6.54	7.59	5.44	1.95	

France

Table 52: Total annual heating requirements of the most common building types in France

Total Annual Heating Demand (kWh)			
Detached			
Year	H1	H2	H3
Pre – WWII	18575	15499	11071
1945 – 1969	15247	13035	9891
1970 –1979	19251	16450	12023
1980 – 1989	12912	11535	8542
1990 – 1999	9876	8710	6431
2000 - 2009	9492	8125	5771
2010 – 2020	6427	5346	3461
Semi-Detached			
Year	H1	H2	H3
Pre – WWII	15846	14178	12096
1945 – 1969	14616	12476	10283
1970 –1979	15590	14477	12389
1980 – 1989	9451	8643	7018
1990 – 1999	8242	6960	4737
2000 - 2009	4789	4043	2719
2010 – 2020	5189	4297	2753
Flats			
Year	H1	H2	H3
Pre – WWII	7196	6586	5578
1945 – 1969	8513	7548	6383
1970 –1979	9522	8673	6902
1980 – 1989	7213	6335	4676
1990 – 1999	4631	3976	2768
2000 - 2009	3770	3187	2215
2010 – 2020	2174	1762	1085

Table 53: Total annual cooling requirements of the most common building types in France

Total Annual Cooling Demand (kWh)			
Detached			
Year	H1	H2	H3
Pre – WWII	1090	2321	3539
1945 – 1969	927	1974	3010
1970 –1979	1155	2461	3753
1980 – 1989	802	1708	2605
1990 – 1999	607	1294	1973
2000 - 2009	565	1204	1836
2010 – 2020	365	778	1187
Semi-Detached			
Year	H1	H2	H3
Pre – WWII	1034	2202	3359
1945 – 1969	912	1943	2964
1970 –1979	1045	2226	3394
1980 – 1989	615	1310	1998
1990 – 1999	480	1023	1560
2000 - 2009	278	592	903
2010 – 2020	293	624	952
Flats			
Year	H1	H2	H3
Pre – WWII	476	1013	1545
1945 – 1969	550	1172	1787
1970 –1979	614	1307	1994
1980 – 1989	442	942	1437
1990 – 1999	275	585	892
2000 - 2009	221	471	718
2010 – 2020	120	255	389

Table 54: Average monthly ground temperature at 0.5m in France

Average monthly ground temperature at 0.5m (°C)			
Month	H1	H2	H3
January	11.61	6.39	11.18
February	8.32	7.83	8.43
March	6.3	10.65	7.68
April	5.69	13.31	8.33
May	6.9	18.36	12.05
June	9.64	21.01	16.21
July	13.03	21.75	20.12
August	16.36	20.4	22.95
September	18.59	17.29	23.78
October	19.11	13.41	22.45
November	17.82	9.59	19.24
December	15.13	7.07	15.2

Italy

Table 55: Total annual heating and cooling requirements of the most common building types in Italy

	Total Annual Heating Demand (kWh)			Total Annual Cooling Demand (kWh)		
Year	Detach	Semi Detach	Flats	Detach	Semi Detach	Flats
Pre-WWII	17466	13572	6344	4515	3495	1634
1945 – 1960	21935	12177	7956	5649	3136	2049
1961 – 1975	22043	10609	4795	5676	2732	1235
1976 – 1990	19323	11238	5409	4976	2894	1393
1991 – 2005	14018	8980	6302	3610	2313	1623
2006 - 2020	11554	8458	5270	2975	2178	1357

Table 56: Average monthly ground temperature at 0.5m in Italy

Average monthly ground temperature at 0.5m (°C)				
January	8.97		July	23.58
February	10.35		August	22.3
March	13.02		September	19.34
April	15.56		October	15.65
May	20.35		November	12.02
June	22.88		December	9.62

Spain

Table 57: Total annual heating and cooling requirements of the most common building types in Spain

	Total Annual Heating Demand (kWh)			Total Annual Cooling Demand (kWh)		
Year	Detach	Semi Detach	Flats	Detach	Semi Detach	Flats
Pre – 1936	12709	22568	7613	3916	6954	2346
1937 – 1959	46410	10567	6585	14300	3256	2029
1960 – 1979	16194	14709	5905	4990	4532	1819
1980 – 2006	7319	6982	3291	2255	2151	1014
2007 – 2020	5200	3232	2357	1602	996	726

Table 58: Average monthly ground temperature at 0.5m in Spain

Average monthly ground temperature at 0.5m (°C)				
January	5.47		July	25.02
February	7.31		August	23.31
March	10.89		September	19.35
April	14.29		October	14.41
May	20.71		November	9.55
June	24.09		December	6.34